To the Graduate Council:

I am submitting herewith a dissertation written by Adam N. Mullenix entitled "Electrochemical Investigation of Anthraquinone tagged Oligonucleotides and Electrodes." I have examined the final electronic copy of this dissertation for form and content and recommend that it be accepted in partial fulfillment of the requirements for the degree of Doctor of Philosophy, with a major in Chemistry.

James Q. Chambers

Major Professor

We have read this dissertation
and recommend its acceptance:

David C. Baker

M. W. Guidry

S. D. Gilman

Accepted for the Council:

Anne Mayhew

Vice Provost and Dean of Graduate Studies

(Original signatures are on file with official student records.)

Electrochemical Investigations of Anthraquinone tagged Oligonucleotides and Electrodes

A Dissertation
Presented for the
Doctor of Philosophy Degree
The University of Tennessee, Knoxville

Adam N. Mullenix

December 2004

DEDICATION

This dissertation is dedicated to my parents and brother:

Nathan and Judy Mullenix
Brandon Mullenix

And in memory of my grandparents:

Kendall “Shug” and Eula Mullenix
Homer and Evelyn Light

whose love and sacrifice have made it all possible.

ACKNOWLEDGEMENTS

I would like to thank all my mentors for their wisdom and guidance bestowed upon me through the years,

Prof. Chris McGowan
Prof. Edward C. Lisic
Prof. James Q. Chambers

those whose work provided many of the materials used for this research,

Neil Whittemore
Matthew McKinney
Dr. David C. Baker

and to those people whose friendship have made the hard times a little easier to bear.

Dr. Kristian Scaboo
Dr. Vilmos Kertesz
Dr. Tim Gibson
Jason Stephens
Joseph Kennedy
“Tall Paul”and Kristie Bobal
Mr. And Mrs. James C. McCoy
Dr. And Mrs. Tim Perry
Wes and Mary Dykes

This work was supported in part by a grant from the National Science Foundation and the University of Tennessee.

ABSTRACT

The DNA double helix is one of the most studied structures in modern science. These molecules provide the basic blueprint for all life as it is presently known to exist. Continuing studies of this structure, and the implications that come with them, currently yield a constantly growing base of knowledge for the study of drug interactions, specifics in the role of the sequence of bases in the DNA chain, and an understanding of the small structural abnormalities and the resulting benefits and problems in the human genome. The research presented herein attempts to examine such interactions using anthraquinone-based modifications for the development of sensor systems for detection of the hybridization event. The anthraquinone modifications described were applied using modified electrodes and modified nucleotides included in the DNA sequences.

The first study examines the use of an anthraquinone-modified uridine nucleotide. This nucleotide was included in the synthesis of a DNA pentamer and a set of 20mers varying in the positioning and number of the anthraquione moiety. The free adsorption of these compounds at a hanging mercury drop electrode obeyed the Langmuir adsorption isotherm. The molecular footprint and adsorption parameters scaled with the size of the molecule. These adsorbed layers were examined by cyclic voltammetry to determine the effects of competitive adsorption and hybridization upon the measured signal. Results in these studies indicated a detectable change in the standard potential and signal size with hybridization. This study was limited, however, with the use of a mercury electrode making it impracticable in mass use sensor systems.

The other two studies involved the application of thiol modifications for the formation of self-assembled monolayers on gold electrodes. The first approach used a molecular beacon type system to examine the effect electrode positioning played in the measured signal. Here oligodeoxynucleotides (ODNs) were modified on one end with a thiol group for electrode attachment. The other end

of the ODN was substituted with the anti-cancer drug, daunomycin, for its electrochemical activity. Addition of a complementary DNA strand changed the position of this drug in relation to the electrode surface and in turn affected the kinetics of the electrode reaction under study. The preliminary results indicated a disappearance in the detectable signal resulting from the hybridization event prompting future examination.

The final study applied an anthraquinone to a gold electrode using a thiol modification. Interaction of DNA with this immobilized layer was examined for any effects in the reduction/oxidation kinetics of the anthraquinone redox couple in the presence of DNA. The kinetics were measured by two methods: potential step chronoamperometry and AC voltammetry. The chronoamperometric data were fit to a two-stepped EE reduction mechanism. While no effect of DNA on the AC voltammetry data was seen, a slight decrease in the rate constants derived from the anodic chronoamperometric data was seen.

TABLE OF CONTENTS

Chapter Page

1 DNA SENSOR BACKGROUND..... 1

DNA Structure..... 1

Non-Electrochemical Methods..... 3

Electrochemical Methods..... 5

Present Studies..... 11

2 ANTHRAQUINONE-MODIFIED DNA..... 13

Introduction..... 13

Langmuir Isotherm Model..... 14

Experimental..... 16

Chemicals..... 16

UV Spectrometric Methods..... 17

Electrochemical Studies..... 18

Results and Discussion..... 19

Concentration Dependence..... 25

(1) Adsorption Isotherms..... 25

(2) Competitive Adsorption..... 27

(3) Effect of Hybridization on CV Signal..... 34

Conclusions..... 44

3 ELECTROCHEMICAL DAUNOMYCIN-BASED STEM-AND-LOOP DNA SENSOR..... 46

Introduction..... 46

Molecular Beacons..... 46

Daunomycin Interaction..... 49

Experimental..... 53

Materials..... 53

Synthesis..... 54
Electrochemical Studies..... 54
Results and Discussion..... 55
Alkylation..... 55
Electrochemical Characterization..... 56
Conclusions..... 60

4 AQ-MODIFIED GOLD ELECTRODES..... 62
Introduction..... 62
SAM Formation..... 63
AQ Kinetics..... 64
CA Theory..... 67
ACV theory..... 69
Experimental..... 70
Materials..... 70
Electrode Preparation..... 72
Electrochemical Experimental..... 72
Results and Discussion..... 73
Effect of Electrode Modification..... 73
Effects of pH..... 75
DNA Sensor System..... 80
Conclusions..... 89

5 SPECULATIONS FOR FURTHER WORK..... 90

WORKS CITED..... 93

VITA..... 98

LIST OF TABLES

Table Page

2.1 Sequences and molar absorptivities of AQ-modified ODNs..... 18

2.2 Langmuir adsorption isotherm parameters for AQ conjugates on HDME in pH 7.1 buffer solution..... 33

2.3 20mer melting temperatures..... 38

4.1 Effects of pH on individual $E_{1/2}$ potentials..... 78

4.2 Standard rate constants (s^{-1}) for 6AQ-modified electrodes at various pH's..... 81

4.3 Standard rate constants (s^{-1}) for 6AQ-modified electrodes in the presence of 10 ppm calf thymus DNA at various pH's..... 81

4.4 Transfer coefficients for 6AQ-modified electrodes at various pH's..... 82

4.5 Transfer coefficients for 6AQ-modified electrodes in the presence of 10ppm calf thymus DNA at various pH's..... 82

4.6 Kinetic data for the 6AQ electrode and the 6AQ- and 2ME-modified electrode in pH 7.1 phosphate buffer measured by CA and ACV..... 88

LIST OF FIGURES

Figure Page

2.1 AQ-modified nucleotide (U*)..... 13

2.2 Typical cyclic voltammogram of the monomer nucleotide in pH 7.15 buffer at 100 mV/s..... 20

2.3 Typical cyclic voltammogram of the AQ-modified pentamer in pH 7.77 buffer at 100 mV/s..... 21

2.4 Typical cyclic voltammogram of the 2AQ-modified 20mer in pH 7.15 buffer at 100 mV/s..... 22

2.5 Pourbaix diagram for AQ-modified nucleotide..... 23

2.6 Typical Laviron volcano plot for the monomer species in a pH 7.15 buffer..... 24

2.7 Formation of the 2AQ 20mer monolayer versus time on HDME..... 26

2.8 Adsorption isotherm of monomer species on HDME in pH 7.15 Britton–Robinson buffer with 0.25 M NaCl..... 28

2.9 Adsorption isotherm of pentamer species on HDME in pH 7.15 Britton–Robinson buffer with 0.25 M NaCl..... 29

2.10 Adsorption isotherm of 2AQ 20mer species on HDME in pH 7.15 Britton–Robinson buffer with 0.25 M NaCl..... 30

2.11 Adsorption isotherm of 9AQ 20mer species on HDME in pH 7.15 Britton–Robinson buffer with 0.25 M NaCl..... 31

2.12 Adsorption isotherm of 2,9AQ 20mer species on HDME in pH 7.15 Britton–Robinson buffer with 0.25 M NaCl..... 32

2.13 Competitive adsorption study of 2AQ 20mer on its untagged model.... 35

2.14 Linear competitive adsorption model..... 36

2.15 Typical 2AQ/complement 20mer melting profile..... 37

2.16 Voltammetry on 2AQ 20mer (A), upon addition of untagged DNA (B), and after thermal cycling (C)..... 39

2.17 Voltammetry on 2AQ 20mer (A), with complement addition (B), and

Annealing (C)..... 40
2.18 Illustration of the adsorption of an AQ monolayer..... 41
2.19 Effect upon current by sweep rate..... 43
2.20 Volcano plot for 2AQ 20mer with and without complement..... 45
3.1 Typical stem-and-loop configurations..... 48
3.2 Daunomycin..... 49
3.3 Alkylation of guanine nucleotide by daunomycin and formaldehyde..... 52
3.4 CV measurements of daunomycin on mercury electrodes before and after the addition of DNA..... 57
3.5 CV response of DM modified DNA before and after the addition of the complementary sequence..... 59
4.1 AQ used to modify gold electrodes..... 62
4.2 Typical nine-membered square scheme..... 65
4.3 Randles circuit..... 66
4.4 Typical ACV frequency response curve..... 71
4.5 Overlayed measurements of various gold modifications..... 74
4.6 Background subtracted chronoamperometric measurement..... 76
4.7 CV measurement of 6AQ layer at 50 μV/s in pH 5.2 buffer..... 77
4.8 CV measurements taken in various phosphate buffers at 100 mV/s... 79
4.9 Typical modifications to gold electrodes by thiol-modified 6AQ..... 83
4.10 Typical ACV measurement of a 6AQ-modified electrodes measured at a frequency of 1 Hz..... 85
4.11 Rate constant versus overpotential for typical 6AQ electrode..... 86
4.12 Plot of ACV current ratio data used for determination of k_{et} value..... 87

ABBREVIATIONS

AC	Alternating current
ACV	Alternaring current voltammetry
AFM	Atomic force microscopy
Ag/AgCl	Silver/silver chloride reference electrode
AQ	Anthraquinone
CA	Chronoamperometry
CV	Cyclic Voltammettry
DM	Daunomycin
DNA	Deoxyribonuleic acid
HMDE	Hanging mercury drop electrode
ITO	Indium-tin oxide electrode
2ME	2-Mercaptoethanol
MB	Molecular beacons
6MH	6-Mercaptohexanol
ODN	Oligodeoxynucleotides
PNA	Protein nucleic acid
QCM	Quartz crystal microbalance
SAM	Self-assembled monolayer
SPR	Surface plasmon resonance
XPS	X-ray photoelectron spectroscopy

SYMBOLS

A	Electorde area
β	Adsorption coefficient
cm	Centimeters
E°	Standard reodx potential
$E_{1/2}$	Half-wave potential

E_p	Peak potential
F	Faraday's constant
ΔG_{ads}	Free enery of adsorption
Γ	Surface coverage (moles/cm^2)
I	Electrical current
kJ	kilijoules
k	Electron transfer rate constant
k_{et}	Electron transfer rate constant used in AC voltammetric method
M	Molar concentration
mL	milliliters
mol	mole
mV/s	sweep rate millivolts per second
ppm	concentration in parts per million
N_A	Avogadro's number
Q	Integrated peak charge
R	Molar gas Constant
s	Time in seconds
σ	Molecular footprint (nm^2/molecule)
T_m	DNA melting temperature
V	Electrical voltage
ν	Voltammetry sweep rate in Volts per second

CHAPTER 1
DNA SENSOR BACKGROUND

DNA Structure

The DNA double helix is one of the most studied structures in modern science. These molecules provide the basic blueprint for all life as it is presently known to exist. Continuing studies of this structure, and the implications that come with them, are yielding a constantly growing base of knowledge for the study of drug interactions, specifics in the role of the sequence of the bases in the DNA chain, and an understanding of small structural abnormalities and their resulting benefits or problems in the human genome.

DNA structure at the simplest level begins with the nucleotides, which consist of a phosphate, a deoxyribose sugar, and an attached base. The base is one of a group of four: adenine, cytosine, guanine, and thymine. The adenine and guanine units are nine-membered purine ring structures, and the thymine and cytosine units are six-membered pyrimidine rings. The nucleotides are joined through alternating phosphate and sugar groups that form a "backbone," leaving the base groups free to form complementary base pairs via hydrogen bonding between adenine and thymine groups and cytosine and guanine groups. Each complementary sequence serves as a template for the production of the next generation of DNA strands with a sequence pair forming the double helix first described by Watson and Crick.[1]

Double helix hybridization, the joining of two strands by hydrogen bonding between complementary purine and pyrimidine bases, can be considered the most important interaction the DNA molecule undergoes. DNA hybridization, by its nature, is in itself an indirect method of DNA sequencing. Two non-complementary strands have little effect upon each other. However, complementary strands, if provided stable conditions, will form the double helix, which has been shown to be one of the most stable complexes formed in the biochemical world. Detection of this helix formation has been done by several

methods described below.

As large projects, such as the human genome project, see their completion, and the ability to directly link specific genes to given diseases increase, the need for detection of specific sequences has increased the desire for fast detection of the hybridization event. The means to measure these interactions have been developed with various methods of analyses. Such measurements must take into account the interactions between the strands themselves in the helix structure and other interacting molecules. These interactions all play important roles in DNA sensor systems. In these systems, the term “probe” is given to the molecule or DNA strand sensitive to, or complementary to, the sequence that is to be detected, otherwise known as the “target”.

On a similar thought, the hybridization event is the basis for the detection of point mutations. These mutations occur when one base pair is deleted or shifted as a result of one of many effects, like intercalation, in the transcription or translation of the original DNA strand. The point mutations can have a vast range of effects upon the system involved in the sequence in question. The mutation carried through the transcription process causes changes in the corresponding protein. The changes result in variations in amino acid sequences and in turn differences in protein shapes for the enzyme lock-and-key models of interaction.

Also of recent interest has been the direct characterization of the DNA double helix itself. One of the controversial arguments being pursued in the research world is the behavior of DNA as a wire or as an insulator. Some groups argue that the stacked nature of the bases in the double helix and the corresponding pi bonds lend themselves to the natural wire-like conduction of electrical charge through the twisted ladder.[2, 3] Others thinking this not possible, make the case for the insulation argument.[4, 5] Results of various groups discussed later have not indicated a clear winner to this argument. Either way, the need to clearly understand the Watson and Crick model is just as important

and continues to be one of the hottest areas of research being pursued via various techniques.

Non-Electrochemical Methods

One of the simplest means of detecting oligonucleotide hybridization of the double helix is UV-visible spectroscopy. The inherent chemical structure of DNA provides for the measurement of absorption of light at an ultraviolet wavelength of 260 nm. In their single-stranded form, the bases absorb more light than their complexed, double-stranded counterpart. This characteristic has been utilized to monitor the hybridization of the double helix. Every oligonucleotide strand has an inherent temperature at which it "melts", or separates, into its two individual component strands. This temperature can serve as an indication of the stability of the double helix being measured, which in turn can indicate the degree of mutation of the double helix.

In a similar manner, the quartz crystal microbalance (QCM) system can be used to detect the hybridization event.[6, 7] Gold layers deposited on a quartz crystal enable measurements of the piezoelectric fields that respond to changes in mass attached to their surfaces. In the most common approach, the oligonucleotides are attached directly to the gold surface. A change in mass is detected during this step and again with the hybridization of DNA double helix. This can also be done in several serial steps to apply multiple layers to enhance the measured signal.

Studies done by Tarlov et. al examined the hybridization of a thiol derivative of DNA immobilized on a gold substrate.[8] Confirmation of hybridization of immobilized DNA was performed via measurements of a ^{32}P-labeled strand. These layers were also studied via means of X-ray photoelectron spectroscopy (XPS) in order to determine the density of probes attached to the surface in question. Tarlov's studies illustrated that their DNA sensor system was able to hybridize with its complementary strand from the immobilized condition.

Fluorescence has received a great deal of attention in the study and development of DNA sensor systems. This is a result of the ready availability of inexpensive dyes and the good levels of detection of most fluorescence systems. In the simplest of these studies, a fluorescent compound is placed in a solution containing DNA. Chemical structures inherent with many organic fluorescent compounds can make them suitable for DNA binding. One of the more common dyes used in such manner is ethidium bromide. Results presented from various groups have demonstrated the use of the anti-cancer drug daunomycin in DNA measurements.[9, 10]

One of the more promising means of fluorescence detection, called molecular beacons (MB), first reported by Kramer et al. in 1996, has stirred a great deal of interest. [11] In this method an oligonucleotide with self-complementary ends forms a hairpin, or stem-and-loop, structure. To one end of the oligonucleotide is attached a fluorescent species, and to the other, its quenching counterpart. The hairpin conformation places the two moieties in proximity to the other so that the fluorophore emission is quenched. Upon addition of the complement to the loop sequence, the loop opens to form the more stable double helix in which the two compounds are separated so that a fluorescent signal can be measured. MBs have gained enough popularity that many commercial DNA synthesizers offer their production.

Results reported from the R.D. Smith group and others illustrated the ability to use the electrospray ionization technique for oligonucleotide analyses through means of mass spectrometry.[12-14] Their method was able to distinguish hybridization of the complementary strand from any of the strand's possible self-complementary interactions. This technique offers the advantage of simultaneously distinguishing types of interactions between different DNA strands. However, the negatively ionized gas-phase samples make the sample more dependant upon other ions from the solution for stability in the gas phase than other means of detection.

The surface plasmon resonance (SPR) technique has been used by Lloyd

Smith and co-workers to detect the DNA hybridization event.[15] SPR measures the refractive index of a system. This in turn is related to the mass of an immobilized analyte. Smith and co-workers illustrated the ability to distinguish the hybridization event and some related kinetics for their system. Work from the Burgener group has presented SPR results monitoring the hybridization of a complementary peptide nucleic acid (PNA) sensor strand with sequences from the polio virus.[16] SPR measurements offer the advantage of direct measurement of the oligonucleotide and no need for "tagged" species synthesis.

Electrochemical Methods

Electrochemical DNA-based sensor systems have shown great promise in nucleic acid structure and sequence analyses. These methods offer the advantage of detection in turbid and optically opaque media not suited for spectroscopic measurements. Greater freedom in the design of electrochemical sensors allows for better adaptability to *in situ* measurements. This means less sample preparation and in turn less sample loss than is seen with other methods. Other methods like XPS and SPR are not suited for this freedom in their sensor designs. Electrochemical analysis is also readily adapted for system miniaturization and array style methods of measurement, meaning signal enhancement or simultaneous analysis of multiple samples. The nature of the information obtained through electrochemical analysis provides an added degree of determination through simultaneous quantitative and system kinetic determinations with the same measurement. Each of these properties provide justification for its use in nucleic acid sensor design. Perhaps the most important advantage electrochemical analysis provides to the study of such systems is its relatively inexpensive cost.

The first look into the electrochemical behavior of nucleic acids was reported in the 1950s by Emil Palacek.[17] These studies found that the potentials required for direct nucleic acid oxidation and reduction required either mercury or carbon electrodes. The only portion of a DNA molecule to exhibit

electroactive behavior arises from three of the four of the base portions. Guanine and adenine were able to be oxidized at nitrogen-carbon-nitrogen double bonds located in the pyrimidine structures. Guanine, adenine, and cytosine each have a double bond that is reducible. Later studies showed that the sites capable of oxidation/reduction reactions correspond to bonds accessible through the groove of the DNA double helix. Each of these reactions are mechanistically complex and non-reversible in nature. This work and its succeeding studies laid the foundation for the investigation of DNA via electrochemical means and measurement of compounds other than the nucleic acids.

Work presented by Allen Bard *et.al* immobilized DNA onto gold substrates through the use of an aluminum carboxylate film.[18] Carboxylate groups were attached via adsorption of mercaptopropanoic acid and then reacted with aluminum(III) nitrate. These films were able to attract the negative charge in the DNA phosphate groups. After soaking these electrodes in DNA solutions, atomic force microscopy (AFM) measurements were able to distinguish differences in single and double stranded DNA layers through extra repulsive forces of complexed $Ru(phen)_3^{2+}$ in the immobilized DNA. The signal differences were likely distinguishable due to the propensity for the $Ru(phen)_3^{2+}$ to complex with the negatively charged phosphate backbone in ds-DNA systems.

Another of the early systems utilizing electrochemical detection for sequence determination was described by Susan Mikkelson and co-workers.[19] Their work measured the interaction between cobalt and ferrocene complexes with DNA immobilized in both single- and double-stranded states on a glassy carbon electrode. Electroactive metal complexes were pre-concentrated by intercalation into the double helix structure at the electrode surface before performing stripping voltammetric measurements. Diffusion parameters of these complexes were determined from this measurement. Those complexes, bound or intercalated into the DNA double helix, showed the expected slowing or hindrance as compared to the single stranded molecules.

Similar studies reported by Tarlov and co-workers measured the effect that various immobilized monolayers had upon the capacitance of a DNA-modified gold electrode.[20] System capacitance was determined through cyclic voltammetry and chronocoulometry measurements of hexaaminеruthenium(III) chloride, potassium ferricyanide, and tris(2,2-bipyridyl)cobalt(III) perchlorate salts. Measurements showed an observable effect on the system capacitance related to the probe density. This density relates to the availability of negative phosphate groups available for interaction with the cationic marker salts mentioned above. Even though the interactions between probe and target are non-specific, this system showed a possible ability to distinguish between single- and double-stranded DNA, which is directly related to sequence.

A similar thiol-attached sensing system from Itamar Willner et al. performed DNA sequence analysis by Faradaic impedance spectroscopy, and quartz crystal microgravimetry.[21] The basic strategy of the Willner design entails the attachment of attached a 6-mercaptohexyl-functionalized ODN through chemisorption onto a gold support for use in sequence-specific measurements. The sequences in their sensors were chosen such that the desired target sequence serves as a bridge via hybridization on the 3'- and 5'-ends simultaneously between the thiol-immobilized DNA sequence and a sensor strand modified with an enzyme-based amplifying unit. The amplifying unit enzymes included horseradish peroxidase and others that were monitored through various methods including QCM, AC impedance, and chronocoulometry.

Initial Willner systems measured the response with enzyme enhancement of their electrochemical system. Other Willner systems studied the result of precipitation of an insoluble product onto to the electrode surface. This was accomplished with various enzyme/precipitate systems including the peroxidase-mediated oxidation of 4-chloro-1-napthol. This electrode system was used for AC impedance measurements of the oxidation/reduction of an $Fe(CN)_6^{3-/4-}$ indicator. The formation of the precipitate enhanced the impedance inherent

from the natural repulsion of this redox couple for the negatively charged backbone of the DNA double helix. Other work with the Willner system included an additional step attaching the enzyme through biotin–avidin complexation or through liposome formation. The dendritic nature of the liposome yielded an even greater enhancement to the detection capabilities of their system.

A method designed by Holden Thorpe and associates incorporated the DNA as part of the electrochemical pathway.[22, 23] Thorpe and co-workers measured the oxidation current of $Ru(bpy)_3^{2+/3+}$ and similar complexes at indium–tin oxide (ITO) electrodes modified with immobilized DNA. Guanine nucleotides in the immobilized DNA act to reduce the $Ru(bpy)_3^{3+}$ species generated at the ITO surface. The reduced form is then available for repetitive oxidation at the ITO electrode. Oxidation currents at the DNA electrode show an enhanced current compared to the same electrode without the DNA. Further work on their sensor designs were applied toward making multichannel sensor systems for sequence detection.

Electrochemical nucleic acid sensors using peptide nucleic acids, or PNA's, have been described in promising studies by Wang et al.[24] In PNA-based sensor systems the sugar-phosphate backbone is replaced with *N*-(2-aminoethyl)-modified glycine molecules that are joined linearly using normal protein synthesis chemistry. This compound has shown a greatly enhanced binding affinity between complementary DNA and RNA sequences as compared to that of natural ODN's. PNA's also offer the advantages of stronger electrode adsorption at more negative potentials and lower electrolyte concentrations, conditions that hampered adsorption with regular ODN's. Changes in the chronopotentiometric signals of immobilized ODNs were monitored in response to the addition of complementary PNA probes.

Another system studied by Joseph Wang and co-workers examined the use of conducting polymer-based electrodes.[25] The Wang system used a polypyrrole-doped interface based on a system described by Garnier and others that applied a DNA-modified polypyrrole layer to the electrode.[26] Oxidation of

the free forms of the uncomplexed polymer layers can easily be achieved due to the freedom of movement in these layers. However, several degrees of movement for the layer are lost with the attachment of double-stranded DNA sequences, thus shifting the oxidation to a more positive electrode potential. The greater flexibility inherent with the single-stranded DNA molecule allows movement of the polymer strands, and with it, the oxidation of the layers at lower potentials.

Work from the Heller group in 2002 used a modified version of this process again using acrylimide polymer coatings in the preparation of their electrode.[27] Upon hybridization of the DNA strands, enzyme-catalyzed electroreduction is favored in solution and can be monitored via amperometric detection. Other research with enzyme systems presented by Heller and Caruana utilized soybean peroxidase in detection of single base pair mismatch in the double helix.[28] In Heller's system, the peroxidase enzyme was attached to the desired ODN. An 18mer complement to this sequence was incorporated into a polymer immobilized onto an electrode surface. Enzyme reduction of hydrogen peroxide was then monitored via amperometric measurements.

The systems discussed thus far all are based on the electrochemical measurement of modified electrode systems in which a redox couple is cycled and measured in response to the layer. Another path for the detection of DNA sequences involves the direct modification of the oligonucleotide strands themselves. This includes the chemical attachment of an electrochemically active marker to the DNA strands. This approach allows certain steps in synthesis to be eliminated allowing for better yields and providing easier measurement.

Systems with attached tags have appeared in various forms. One such system reported by Kuhr and associates measured the frequency response with sinusoidal voltammetry (SV) of various tagged nucleotides.[29] Their tags were various substituted ferrocenes covalently attached to modified nucleotides that were incorporated in the ODN synthesis. The design of the tags allowed for

individual standard half-wave potentials for each nucleotide. The SV signal measurement permitted differentiation by frequencies for nucleotide specific signals and offered a low resolution sequencing method. Others have also used the ferrocene complexes in ODN detection.[30]

The Barton group presented many methods for the measurement of various ODN sensor systems. One group of compounds under study consisted of metallic complexes chosen for their known ability for double helix intercalation. Research studying various metallointercalators and the use of intercalation for tag binding has been presented using electrochemical and fluorescence techniques.[31, 32] Barton also reported utilizing other electroactive organic compounds such as daunomycin and ethidium bromide in her sensor designs. Also reported was the ability to orientate chemisorbed DNA strands on gold electrode surfaces. This orientation of the monolayer was controlled with an applied voltage and the thickness measured by AFM.[33]

Combining these systems Barton was able to develop an attached probe sensor system. Using a procedure described by J.B. Chaires group, daunomycin intercalated in the double helix was reacted with formaldehyde for the covalent “cross-linking” of the drug with guanine nucleotides.[34] After thiol attachment to a gold electrode, voltage was used to orient a modified monolayer of 15mers for cyclic voltammetry measurements. Variations in the site of intercalation and point mutations between the tag and electrode were used to show a conductor type behavior for DNA in its double helix form.[3] Electrodes with a base pair mismatch between the tag and the electrode showed little, if any, sign of electrochemical behavior from the attached drugs. This work with others has been argued by many as evidence for the mediation of electrochemical charge by the DNA double helix.

Opponents to the idea of DNA as a “wire” point to researchers like Schuster when making their arguments. In one of Schuster’s system the anthraquinone, *N,N*-Bis(3-aminopropyl)-2-anthraquinonesulfonamide dihydrochloride (AQS2), was used and compared by its similarity in structure to

daunomycin, a known DNA intercalator. This set of experiments induced an electron “hopping” mechanism and led to the cleavage of the DNA strands verified through gel electrophoresis. The Schuster group stated results led to the conclusion that the cleavage will not occur without what they call intimate contact for charge transfer through the helix.[5]

Present Studies

The studies presented herein involve systems similar to those mentioned above that utilize the electrochemical behavior of anthraquinone (AQ) for the monitoring of the DNA hybridization event. Studies were conducted with two styles of sensor design in mind: (1) modification of a nucleotide, and (2) modification of the electrode. The first of these systems examined were those with an AQ-modified nucleotide incorporated in the DNA molecule. The tagged nucleotide and DNA were then electrochemically characterized by examining the adsorption of the compounds on working electrodes with emphasis on ss- versus ds-DNA effects.

Similar studies were done adding a stem-and-loop hairpin DNA system in which daunomycin (DM) was incorporated after DNA synthesis. DM is a known intercalator that has been illustrated as having the ability to bond to guanine residues in given systems. This sensor style modified a gold electrode by applying an the stem-and-loop DNA with thiol modification added during synthesis. Measurements of the thiol-bound DNA modified with DM was then manipulated in order to maximize any effects created with the addition of the complementary sequence.

The third method of examination modified a gold electrode with a thiol-bound AQ group. This sensor was then characterized by AC voltammetric and chronoamperometric measurements for the kinetic data. Comparison between electrodes, with and without the presence of DNA, was hoped to yield a measurable signal difference to determine if the hybridization event could be observed.

Since anthraquinones are easily obtained, and a vast amount of literature is available involving their use in various systems, they are good candidates for redox tags. Furthermore, the AQ unit is not prone to further chemical reactions. The exact specifics for the reduction and oxidation of AQs can vary from system to system. In general, the mechanism involves a two-electron and two-proton reduction to the hydroquinone state. The chemically induced reaction is widely used in industry for forming dyes and similar compounds. Electrochemically induced reduction can vary as standard potential varies for a given set of conditions and with the modifications done to any carbon in the fused three-ring structure.

CHAPTER 2
ANTHRAQUINONE-MODIFIED DNA

Introduction

The work presented in this chapter describes a hybridization detection system based upon a nucleotide unit modified with an attached electrochemical tag. The tag was a uridine nucleotide of Figure 2.1 modified with a 9,10-anthraquinone (AQ) moiety tethered to the 2'-O position of the ribose sugar. Measurements were taken with a modified monomer nucleotide unit, and on various ODNs of five and twenty base pair lengths. Each ODN varied in the number and location of their respective AQ modifications. Synthesis and spectroscopic characterization of these compounds is described in Whittemore et al.[35]

The point of attachment of the uridine ribonucleotide is a 2'-O group not available in deoxyribose nucleotides. This position offers free access for attachment to the sugar group while at the same time providing for minimum hindrance in double-helix formation through the grooves of the double helix . Use of an AQ group as an electrochemical tag for nucleic acid offers the stability necessary for use in normal phosphoramidite ODN synthesis. The AQ group

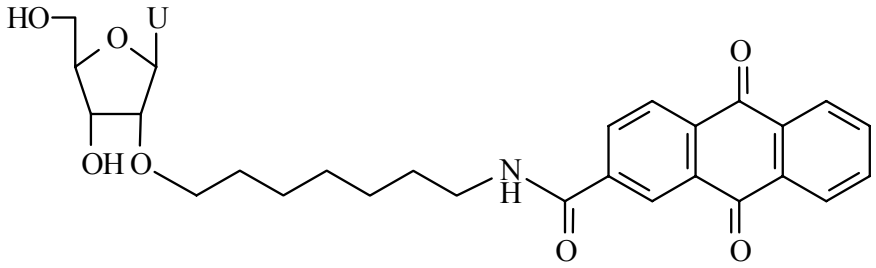


Figure 2.1 AQ-modified nucleotide (U*)

also offers an easily measured potential window for the electrochemical signal. An added bonus arises from the potential of the AQ moiety as an intercalator in the DNA double helix.

Each compound was characterized with cyclic voltammetry (CV) before examination with complementary strands and hybridization where applicable. CV measurements were conducted in various aqueous buffer solutions using a hanging mercury drop electrode (HMDE). Each compound showed the tendency for the diffusion-controlled formation of a self-assembled monolayer (SAM) on the HMDE surface as indicated by the redox waves that had the characteristic shapes associated with the reduction of a surface-confined species. In all cases the concentration dependence was consistent with a simple Langmuir isotherm model.

Langmuir Isotherm Model

The Langmuir adsorption isotherm is the simplest model describing the equilibrium partition of a solute dissolved in a liquid and adsorbed on a solid surface. It has been used in the calculation of band profiles for pure components in liquid chromatography. Derived by Irving Langmuir in 1918, the isotherm is based on three assumptions: [36] (1) a uniform surface with equivalent adsorption sites, (2) only one interaction per site, and (3) adsorption energy at a given site that is independent of its neighbors. Assuming the basic adsorption reaction:

$$AQ(aq) + n\ (H_2O)_{ads} \rightleftharpoons AQ_{ads} + n\ (H_2O)$$

the surface concentration of the adsorbed AQ species is calculated from the coulomb integral (Q)of the voltammetric wave

$$Q = \int_{E-}^{E+} I \frac{dE}{\nu} \qquad (2.1)$$

The compound's surface coverage (Γ in moles/cm^{-2}) and molecular footprint (σ in nm^{-2}/molecule) can then be calculated with equations 2 and 3, respectively;

$$\Gamma = \frac{Q}{2pFA} \qquad (2.2)$$

and

$$\sigma = \frac{10^{16}}{N_A \Gamma} \qquad (2.3)$$

where F is Faraday's constant, ν is the sweep rate in volts per second, A is the electrode area in cm^2, p the number of AQ groups per ODN, and N_A is Avogadro's number.

In a case of single species non-competitive adsorption the Langmuir equilibrium expression is

$$\frac{\Gamma_1}{\Gamma_{max} - \Gamma_1} = \beta C \qquad (2.4)$$

which can be rearranged to the linear form:

$$\frac{C}{\Gamma_1} = \frac{1}{\beta \Gamma_{max}} + \frac{C}{\Gamma_{max}} \qquad (2.5)$$

where C is the concentration of the species, Γ_1 the surface coverage at that concentration, Γ_{max} the saturated surface coverage, and β is the adsorption coefficient for the species in question. The β term is related to the free energy of adsorption for the molecule through equation 2.6.

$$\Delta G_{ads} = RT \ln(\beta) \qquad (2.6)$$

Adsorption of all the compounds studied adhered to this model. In addition, the examination of the 20mers included the use of their complementary strands. The competition of these untagged species for the sites mentioned above must be accounted for in any description of the adsorption event. In the

experiments described below, this competition for adsorption sites was monitored. The Langmuir system equations for competition between two species with identical saturation surface coverages has been described before.[37, 38]

$$\Gamma_1 = \frac{\Gamma_{max} \beta_1 C_1}{1 + \beta_1 C_1 + \beta_2 C_2} \qquad (2.7)$$

Rearrangement to a linear equation in terms of the concentration of species 2 yields:

$$\frac{1}{\theta_1} - 1 = \frac{1}{\beta_1 C_1} + \frac{\beta_2 C_2}{\beta_1 C_1} \qquad (2.8)$$

where θ_1 is the fractional surface coverage (Γ_1/Γ_{max}) for a given compound. The measurement of θ_1, as the concentration of competing species is increased, allows for determination of the adsorption coefficients of both species.

Competition for sites of adsorption in studies involving DNA are further complicated by the hybridization question. The double helix of double-stranded DNA may compete with the single strands for those same sites of adsorption. The difference in the characteristics of single- versus double-stranded DNA molecules could result in great changes of the nature of the adsorption event. Double-stranded DNA could also render a degree of order to what would otherwise be a very random and complex layer on the electrode surface. Each of these provides a possible reason for a variation in the signal measured for double versus single stranded DNA.

Experimental

Chemicals

The AQ-modified nucleotide, pentamer, and 20mers were synthesized in the laboratories at ISIS pharmaceuticals (Carlsbad, CA) and by Neil Whittemore at the University of Tennessee. Non-tagged ODN sequences were received

from ISIS pharmaceuticals or ordered from Operon Technologies, Inc. (Alameda, CA). A master stock solution of each ODN received was diluted with 10 mL of sterile, deionized water. Sequences for the ODNs used in this study are listed in Table 1 where the U* denotes the AQ-modified uridine nucleotide of Figure 1.

Other chemicals were used as received from Fisher Scientific Co.

UV Spectrometric Methods

Spectra were obtained using an HP Model 8452A diode array spectrophotometer equipped with a HP Model 89090A Peltier temperature controller (Hewlett-Packard Co., Palo Alto, CA). The temperature controller provided for temperature cycling of the ODN solution and simultaneous UV absorbance of the solution. Spectral measurements and thermal cycling were performed in the same aqueous media for a given set of CV measurements with appropriate blanks.

Each compound was examined via UV-visible spectrometry for two primary reasons: (1) it served as the primary source for concentration determination in the ODNs, and (2) spectrum monitoring during thermal cycling allows for confirmation and measurement of the hybridization event. Compounds for these studies were received in a manner as to not guarantee moisture content and ran the risk of possible of decomposition upon drying. Absorption values at 260 nm were obtained for all compounds and used to determine concentration with the molar absorptivities in Table 2.1. The molar absorptivity for each ODN was calculated using the nearest neighbor effect methods.[39] Absorption of the AQ moiety itself at a 260 nm wavelength was calculated with assumption of uridine and thymine being approximately equal and determining the AQ absorptivity to be 26,400 $M^{-1}cm^{-1}$ by subtraction of the ε_{260} value from that of the monomer species. This value was then added to the calculated value obtained for each ODN where applicable. Solutions were made for each set of compounds, and standard laboratory methods were employed for concentration of said solutions based upon the sequence provided in the

Table 2.1 Sequences and molar absorptivities of AQ-modified ODNs. The modified nucleotide is noted as U* in each sequence

ODN	Sequence	ε ($M^{-1}cm^{-1}$)
Pentamer	5'-d(GAU*CT)-3'	80,500
2AQ	5'-d(AU*G CAT TCT GCC CCC AAG AG)-3'	214,000
9AQ	5'-d(ATG CAT TCU* GCC CCC AAG AG)-3'	214,000
2,9AQ	5'-d(AU*G CAT TCU* GCC CCC AAG AG)-3'	241,000
Complement	5'-d(CTC TTG GGG GCA GAA TGC AT)-3'	194,000
Blank 20-mer	5'-d(ATG CAT TCT GCC CCC AAG AG)-3'	188,000

multiple nucleotide species compounds.

Electrochemical Studies

The electrochemical studies were performed using a hanging mercury dropping electrode (HMDE) purchased from EG&G, Oak Ridge, TN. The electrode area was 0.0225 cm^2 for most of the voltammetric experiments. The reference electrode was a Ag/AgCl wire immersed directly in the test solution. Two potentiostats, a Cypress Model CS-2Ra (Cypress Systems, Inc., Lawrence, KS) and a CHI 650A (CH Instruments, Inc., Cordova, TN), were used. Simulation of the cyclic voltammograms was done using software supplied by CH Instruments, Inc.

CV was carried out using aqueous buffers containing NaCl at various concentrations. For the pH studies on the monomer and pentamer, 0.125 M phosphate and acetate buffers were used for pH <7, and Britton–Robinson (BR)[40] buffers were used for pH >7. The latter buffer system was also used for the determination of the adsorption isotherms at pH 7.15. Before measurements

were taken, solutions were purged with purified nitrogen that had been passed through a column containing Mn(II) oxide dispersed on a vermiculite support to remove oxygen.

Results and Discussion

Initial electrochemical measurements were performed on each tagged species alone in buffered solution to determine the suitability for SAM formation. CVs presented in Figures 2.2 through 2.4 show readily measurable waves due to SAM formation at dilute concentrations in a matter of minutes. The shape of the waves obtained were indicative of a redox reaction for a surface-confined species. Each voltammogram of 2.2 through 2.4 contains a simulated curve made with the simulation software available through the CH Instruments potentiostat. Simulation using a simple EE model the system is based on two sequential oxidation/reduction reactions. The k_1 and k_2 rate constants determine the rate for their respective reactions.

$$\mathrm{AQ} \underset{\mathrm{E_1^o}}{\overset{k_1}{\rightleftharpoons}} \text{semi-AQ} \underset{\mathrm{E_2^o}}{\overset{k_2}{\rightleftharpoons}} \mathrm{AQH_2}$$

Each reaction also has a potential, E_1° and E_2°, associated with it that determines electrochemical potential where it occurs.

Greater availability of the monomer allowed for measurement of the pH dependence of the redox potential, $E^{\circ'}$ (= $(E_{pk}^{a} + E_{pk}^{c})/2$). The slope of the data over a pH range from approximately 4 to 10 in Figure 2.5 measured 63 mV/pH unit. This is close to the expected 60 mV/pH unit in the case of a typical two-electron, two-proton process. Similar measurements for the 20mer species were prevented due to limited quantities of material. Values obtained from measurements at representative points were consistent with those obtained for the monomer species.

Data comparing the effect of sweep rate on peak potential of the monomer at a pH of 7.15 are shown in Figure 2.6. This shows the expected trend of peak

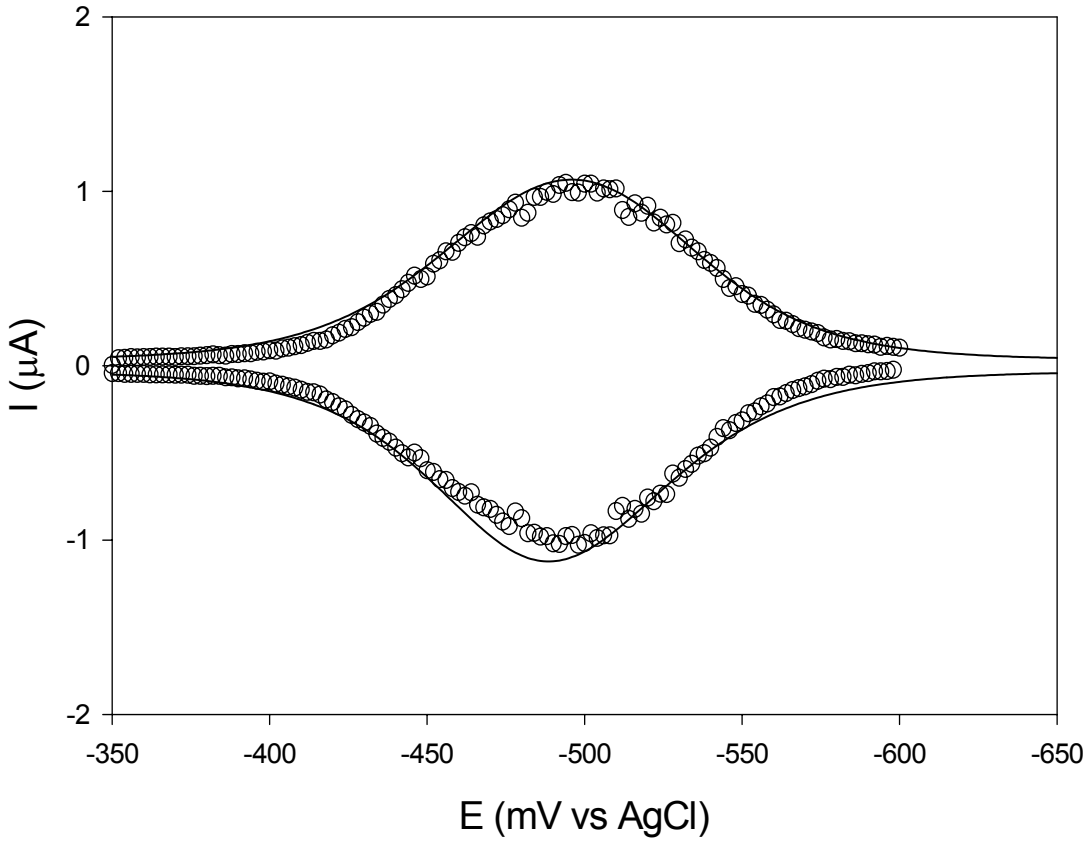


Figure 2.2 Typical cyclic voltammogram (circles) of the monomer nucleotide in pH 7.15 buffer at 100 mV/s. Accompanying EE mechanism simulation (line) parameters: k_{s1} = 100 s^{-1}, k_{s2} = 20 s^{-1}, E°_1 = -0.475 V , E°_2 = -0.510 V.

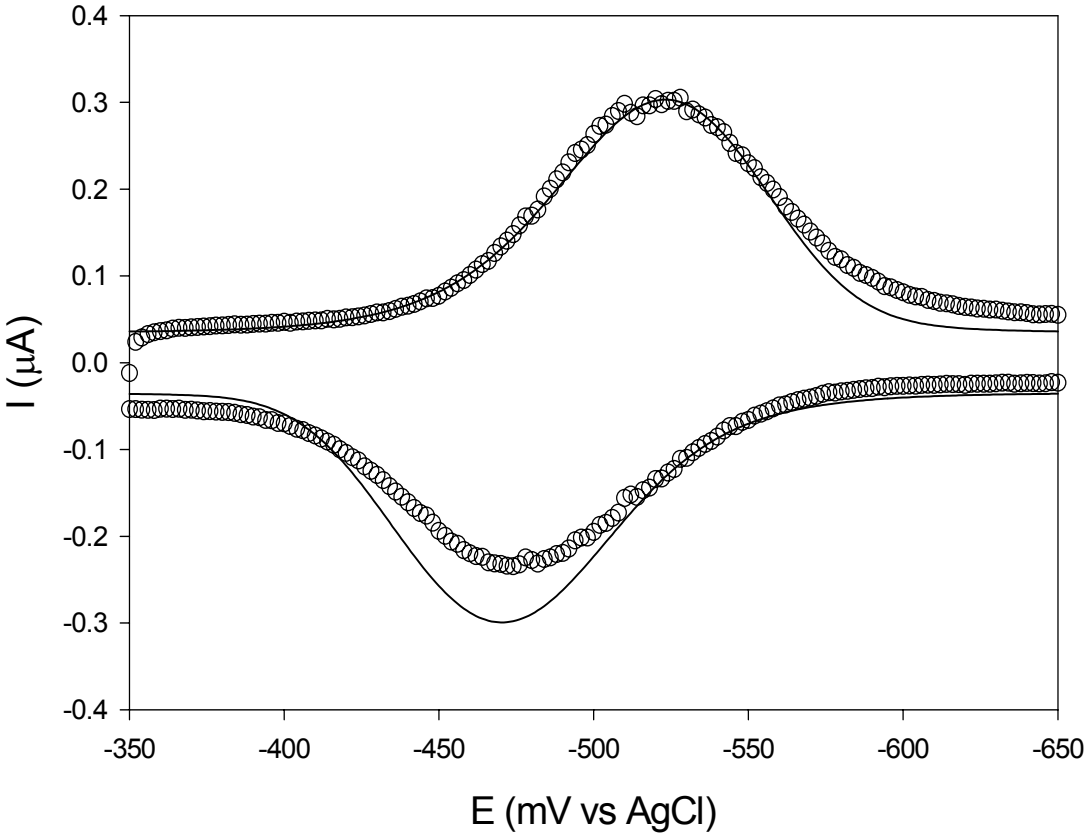


Figure 2.3 Typical cyclic voltammogram (circles) of the AQ-modified pentamer in pH 7.77 buffer at 100 mV/s. Accompanying EE mechanism simulation (line) parameters: k_{s1} = 100 s^{-1}, k_{s2} = 2 s^{-1}, E°_1 = -0.510 V, E°_2 = -0.490 V

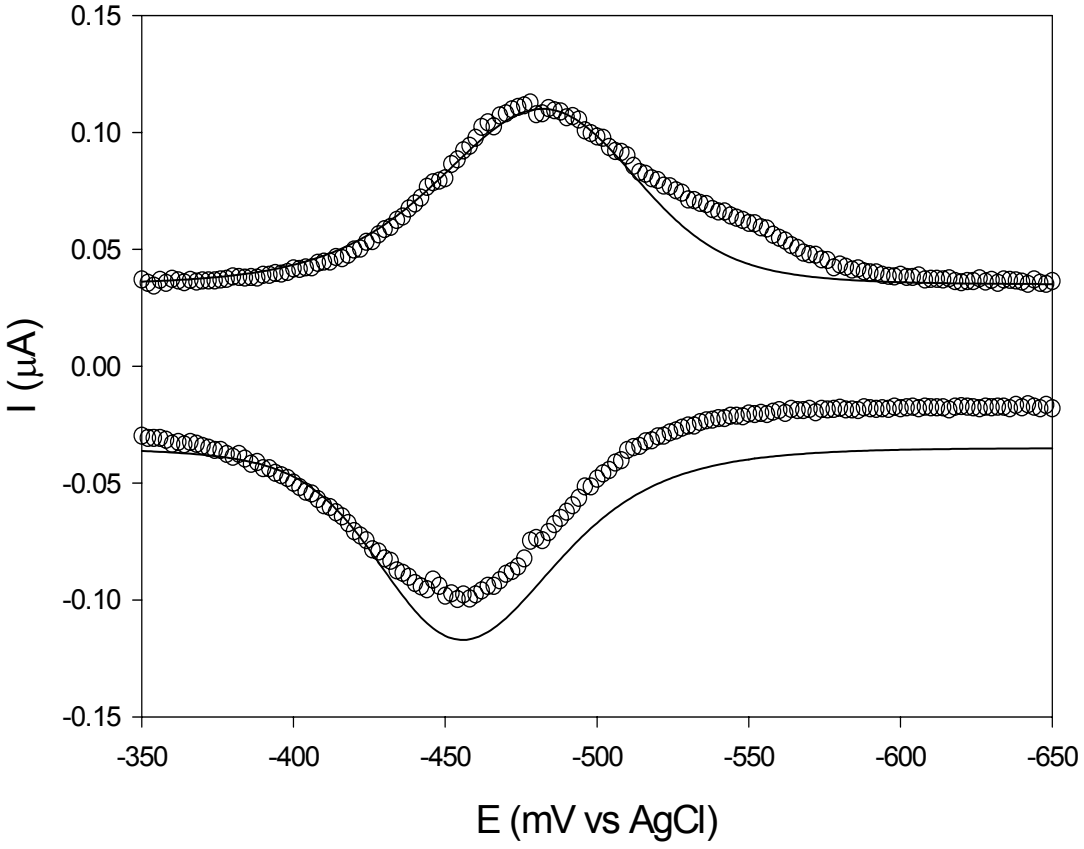


Figure 2.4 Typical cyclic voltammogram (circles) of the 2AQ-modified 20mer in pH 7.15 buffer at 100 mV/s. Accompanying EE simulation (line) parameters: k_{s1} = 100 s^{-1}, k_{s2} = 5 s^{-1}, $E°_1$ = -.470 V, $E°_2$ = -0.470 V

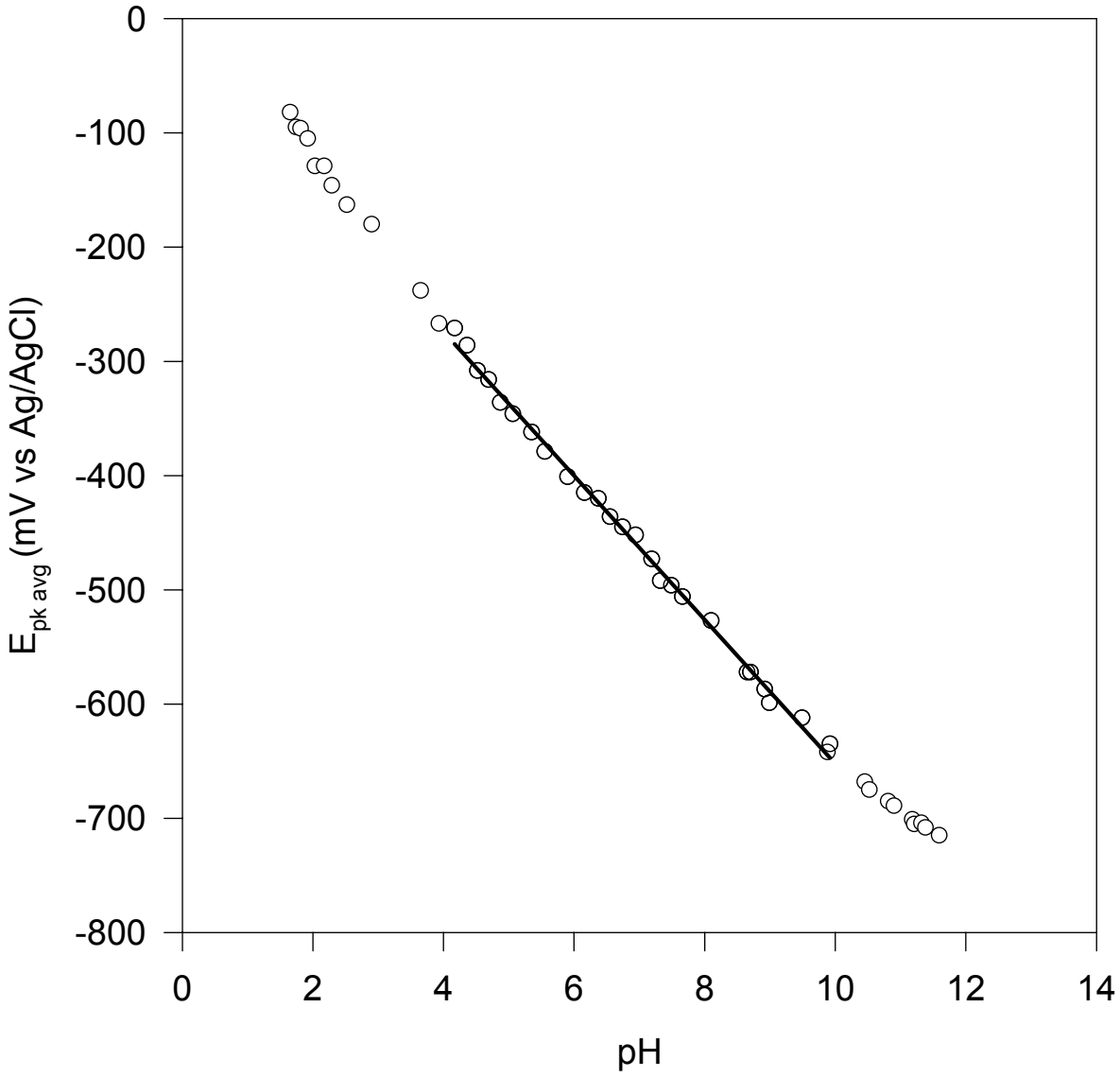


Figure 2.5 Pourbaix diagram for AQ-modified nucleotide. The line is a linear regression of the data between pH 4 and 10 to yield a 63-mV slope

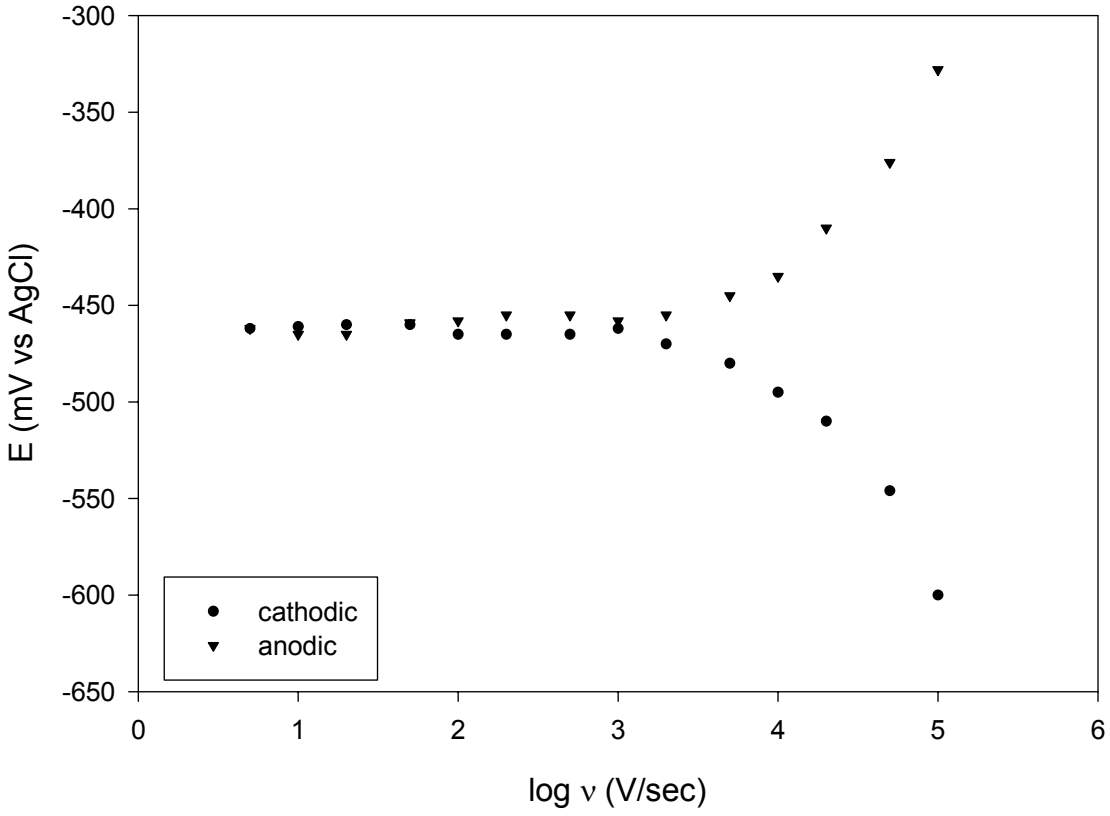


Figure 2.6 Typical Laviron volcano plot for the monomer species in a pH 7.15 buffer

separation with increasing sweep rates as the measurement becomes faster than reactions in the SAM can take place. The uniformity of the measured width and shape of the waves offers two explanations: a well-ordered surface with the AQ group in the similar relative positions yielding a single global E°`, or an unordered layer with various AQ positioning and a wide dispersion of global E°` values. The consistency of peaks over a wide pH range are best explained with the well-ordered layer model. Work presented by Forster yielded similar values in relative potential and wave shape with typical reduction/oxidation of related AQ species.[41]

Some anomalies were seen in the peak shape compared to the theoretical value obtained from the simulation. Where the monomer species matched on both the reduction and oxidation sweeps, pentamer and 20mer measurements did not have as close a match in their oxidation sweeps or in the double-layer capacitance throughout the cycle. The most probable explanation for this arises from a shifting in the monolayer order as that reported by Kelley and Barton.[33] Also apparent in measurements of the 20mer is a shoulder associated with the cathodic wave in Figure 2.4. The explanation for this is unclear, but similar results with these compounds reported by Kertesz et al. show a split peak at early adsorption times that could arise from different orientation of the AQ to the electrode surface as the monolayer forms.[42]

Concentration Dependence

(1) Adsorption Isotherms

Data shown in Figure 2.7. illustrates the formation of the monolayer for the 2AQ 20mer species in a solution stirred by the effect of nitrogen bubbling. Time dependence of the charge calculated from an AQ voltammetric measurement indicated that their adsorption was a diffusion controlled process. Formation of the observed monolayer for all species usually reached a constant level in two to five minutes in a stirred solution.

The dependence of voltammograms on concentration was measured for

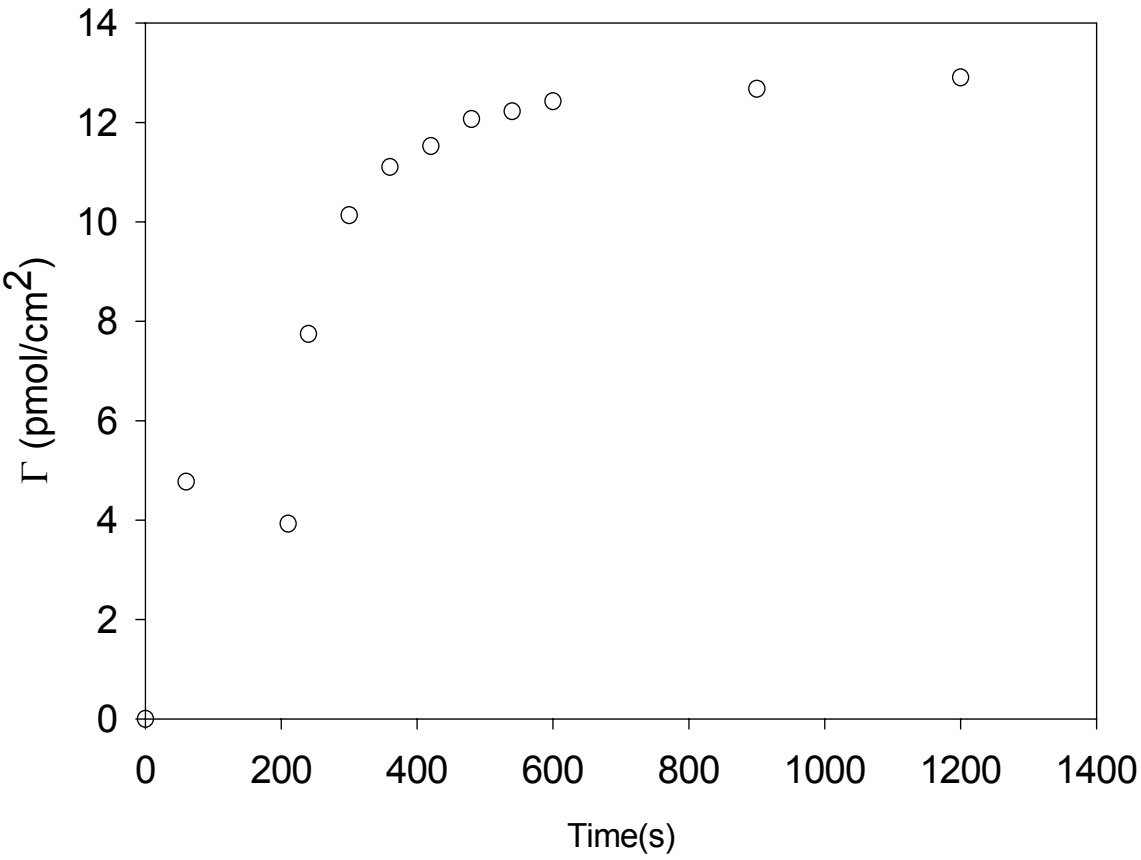


Figure 2.7 Formation of the 2AQ 20mer monolayer versus time on HMDE.

each of the AQ-modified species in neutral pH phosphate buffer solutions. High affinity for the mercury electrode surface seen by the bases, nucleic acids and the AQ moiety meant that saturation coverages were exhibited at micromolar concentrations. Figures 2.8 through 2.13 illustrate the typical dependence of Γ versus concentration for the monomer, pentamer, and each 20mer species respectively. Fits of these data using a simple Langmuir isotherm model are also presented in these plots as lines. Data obtained from these fits are presented in Table 2.2. The fits were done roughly for comparison of the chain length and degree of substitution.

Molecular footprints (σ), which were calculated from the limiting Γ_{max} value from the fitted data, appear to scale with the size of the molecules. Agreement between the footprint of the doubly substituted 20mer species and with the single substitution 20mers was accomplished when calculations used an n value of four, i.e two per AQ group. This assumption indicates the involvement of all the AQ groups in the monolayer electrochemistry. Apparent effects are also seen in the adsorption characteristics versus ODN sizes. The values for β increase with chain length indicating that the adsorption of the DNA nucleotides is primarily dependent on the number of monomer units in the chain. This in turn is seen in the calculated ΔG_{ads} terms and their greater surface affinity.

Adsorption parameters calculated from these fits also varied with the species. Values obtained for the adsorption coefficient of the monomer species were about 100 times lower than those measured for the ODNs. In turn, the ΔG_{ads} was lower than its 20mer counterparts. This most likely arises from the lack of phosphate groups and fewer bases for adsorption to the electrode surface. Comparison of ΔG_{ads} values between the 20mers and the pentamer yield values that are virtually identical values considering experimental error.

(2) Competitive Adsorption

Adsorption studies on the 20mer species were complicated through co-adsorption when measurements involved the use of any non-tagged

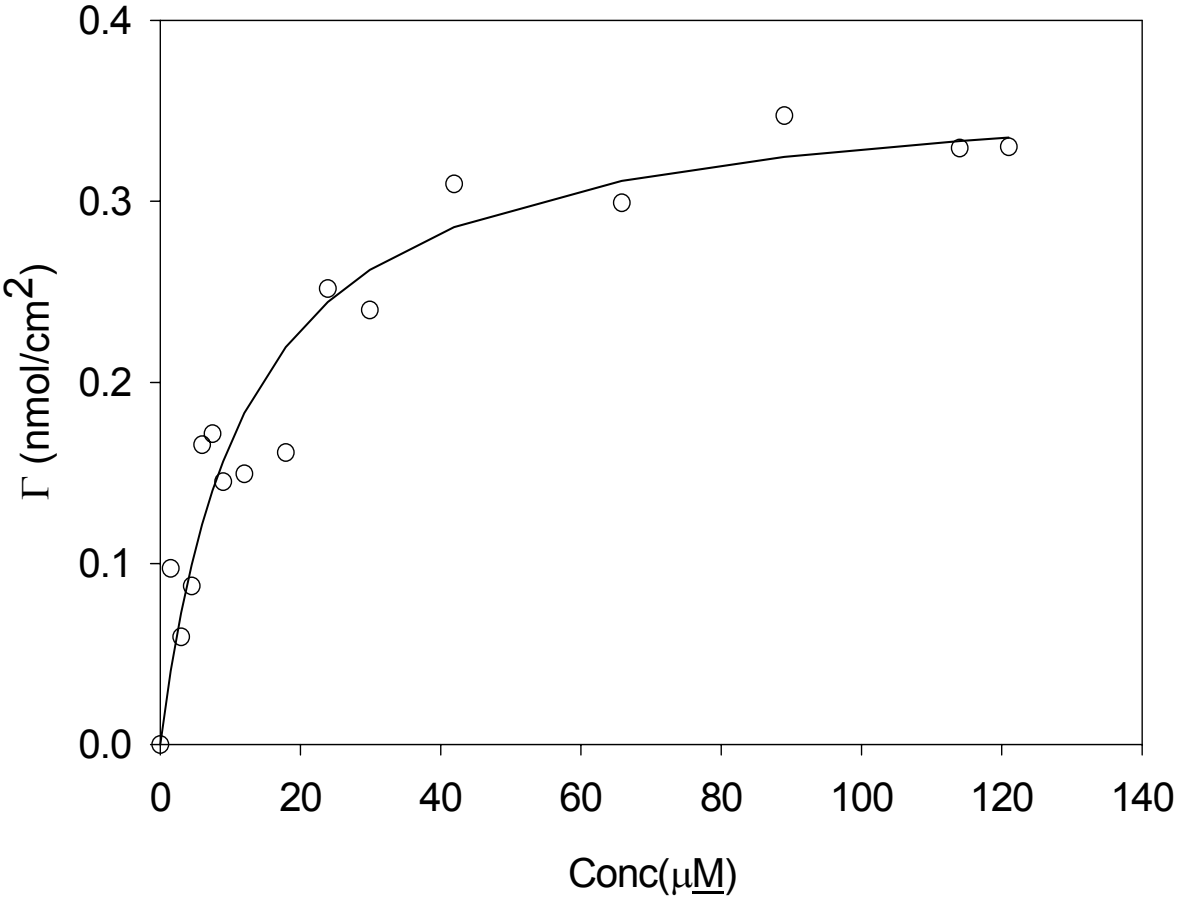


Figure 2.8 Adsorption Isotherm of monomer species on HDME in pH 7.15 Britton–Robinson buffer with 0.25 M NaCl. Line represents fit to a Langmuir model where Γ_{max} = 0.369 nmol cm^{-2} and $\beta = 1.01\times10^{5}$ M^{-1}

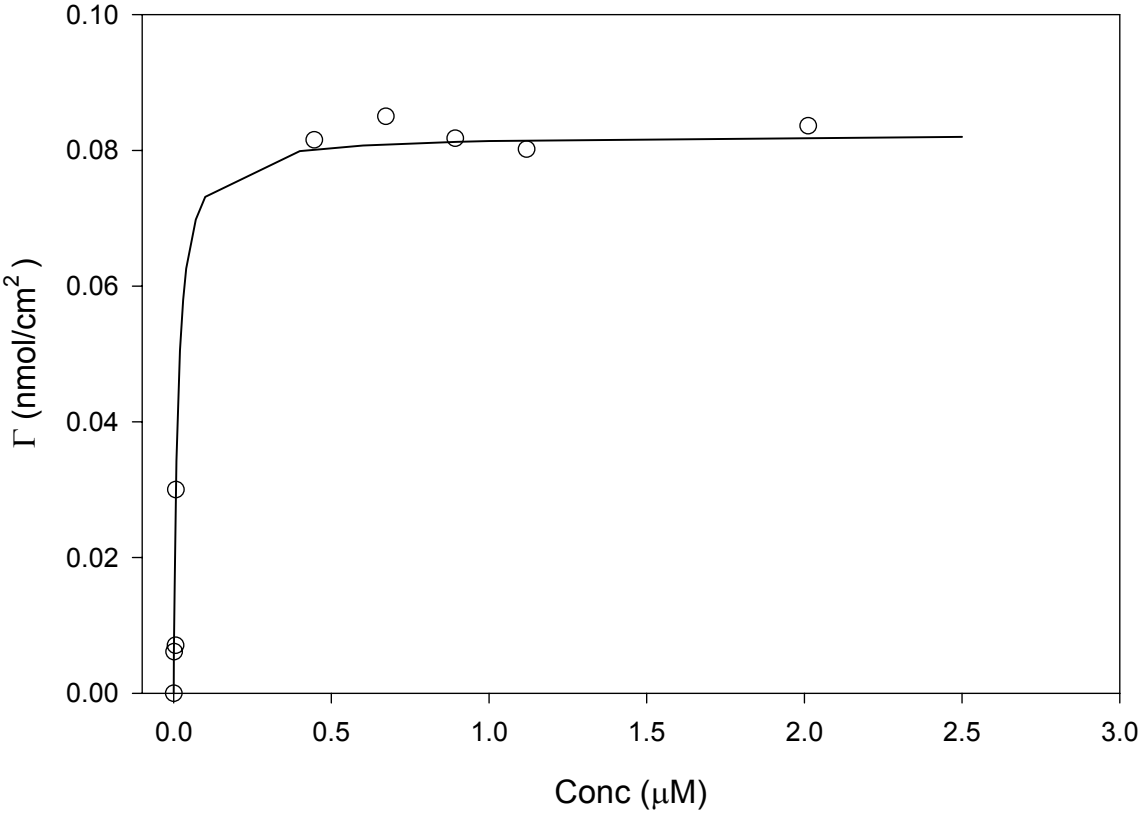


Figure 2.9 Adsorption isotherm of pentamer species on HDME in pH 7.15 Britton–Robinson buffer with 0.25 M NaCl. Line represents fit to the Langmuir isotherm model where Γ_{max} =83.3 pmol/ cm^2 and β = 7.9×10^7 M^{-1}

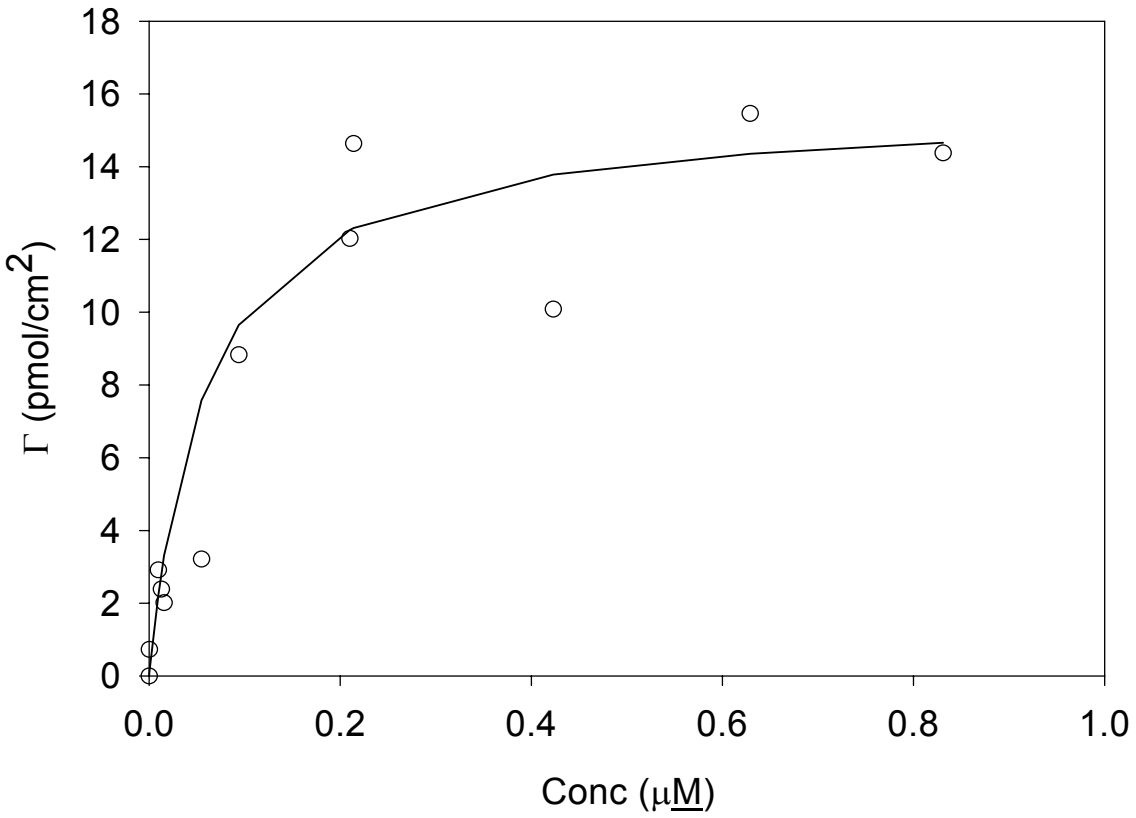


Figure 2.10 Adsorption isotherm of 2AQ 20mer species on HDME in pH 7.15 Britton–Robinson buffer with 0.25 M NaCl. Line is a fit with the Langmuir model where Γ_{max} = 15.7 pmol/cm^2 and $\beta = 1.7\times10^7$ M^{-1}

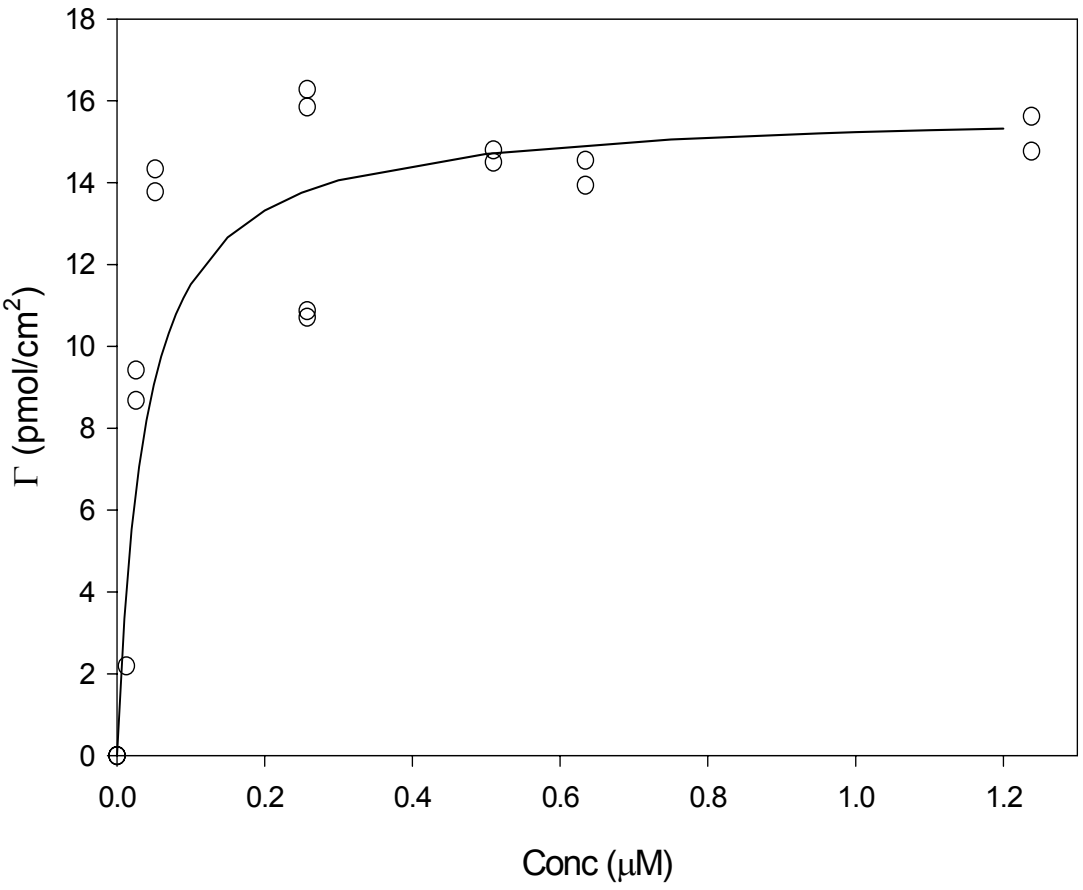


Figure 2.11 Adsorption isotherm of 9AQ 20mer species on HDME in pH 7.15 Britton–Robinson buffer with 0.25 M NaCl. Line represents a fit to the Langmuir isotherm model where Γ_{max}=15.8 pmol/cm^2 and β=7.9×10^{7}M^{-1}

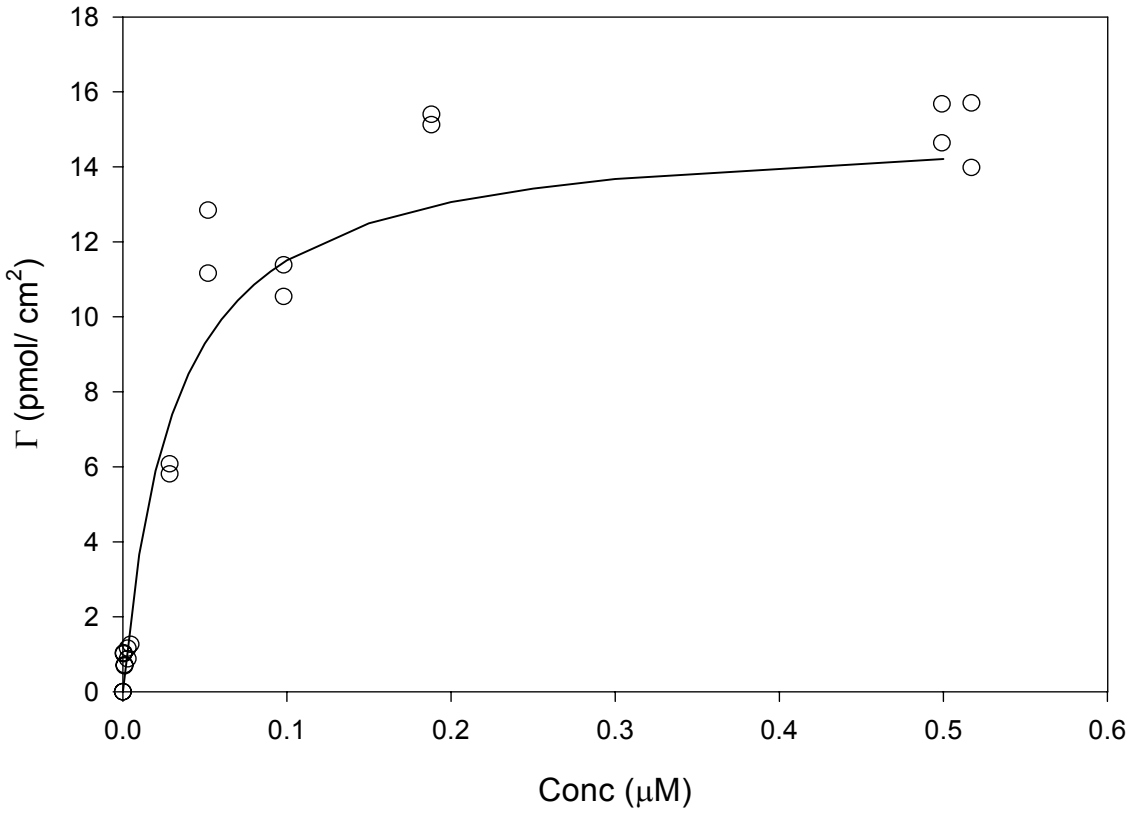


Figure 2.12 Adsorption isotherm of 2,9 AQ 20mer species on HDME in pH 7.15 Britton–Robinson buffer with 0.25 M NaCl. Line represents a fit to the Langmuir isotherm model where Γ_{max}=15.1 pmol/cm^2 and β=7.9×10^7 M^{-1}

Table 2.2 Langmuir adsorption isotherm parameters for AQ conjugates on HDME in pH 7.1 Buffer Solution

	Footprint σ (nm^2/molecule)	β (M^{-1})	ΔG_{ads}(kJ/mol)
Monomer	0.48	1.01×10^5	-28
Pentamer	1.99	7.9×10^7	-45
2AQ 20mer	11.0	8.50×10^6	-40
9AQ 20mer	10.5	2.69×10^7	-42
2,9AQ 20mer	11.1	3.2×10^7	-43

complementary or non-complementary DNA sequences. Similarities between the structures of the tagged and untagged 20mer species allow for the Langmuir competitive adsorption models of equations 2.7 and 2.8. With the characterization of the adsorption characteristics of the single molecules, several experiments were performed to account for the effects of a simple monolayer displacement versus those seen with DNA hybridization effects.

Measurements of tagged species taken in the presence of equal amounts of untagged species showed an attenuation of the signal strength as seen in later in figures. Essentially identical signal attenuations were initially seen whether or not the untagged strand was complementary in nature. Therefore it could not be said with certainty that the cause of attenuation in the signal was a result of double helix formation or a simple competition for sites of adsorption on the electrode surface. The results do offer a process of monitoring the monolayer formed by our tagged 20mer by its displacement from the formed monolayer.

Displacement titrations were carried out involving the 2AQ 20mer and an untagged 20mer of identical sequence. As seen in Figure 2.7, surface coverage

for both species appeared to reach equilibrium status in a matter of minutes. The voltammetric signal decreased as the amount of untagged 20mer added in a phosphate buffer electrolyte solution was increased (Figure2.13). Manipulation of the data favoring the linear equation 2.8 provided for the plot shown in Figure 2.14. These data were fit with the linear regression software available with the SigmaPlot™ program and used to calculate of the adsorption coefficients for both ODNs. The β value from the linear fit for the 2AQ 20mer was 1.3×10^{7} M^{-1} and its untagged counterpart 3.5×10^{6} M^{-1}. The difference between these numbers corresponds to 4 kJ/mol stronger adsorption of the AQ-tagged species. This also indicates that the attached AQ moiety could offer a slight effect in the adsorption process itself.

(3) Effect of Hybridization on CV Signal

This set of experiments utilizes the adsorption differences between double- and single-stranded DNA for the determination of DNA hybridization with cyclic voltammetry. Without hybridization the system would basically be no different than that of competition for the electrode surface described before. Hybridization in itself offers the specificity needed in sensor system. It is hoped that any difference in the double- and single-stranded DNA molecule can provide that detectable difference.

Studies with the complementary strand required a verification of double helix formation. The large free energy of adsorption seen with the 20mers illustrates a tendency described by Palacek where mercury electrodes may cause DNA molecules unzip and adsorb as single-strands as they adsorb.[43] Verification of double helix formation was documented through UV-visible spectroscopy in the free solution beforehand. Thermal profiles similar to Figure 2.15, determined the melting point (T_m) of the all the AQ 20mers and complement to be about 68 ^{0}C, The data in Table 2.3 show T_m values for each 20mer that are about the same as that of the untagged sequence.

Cyclic voltammetry experiments were carried out on the same solutions

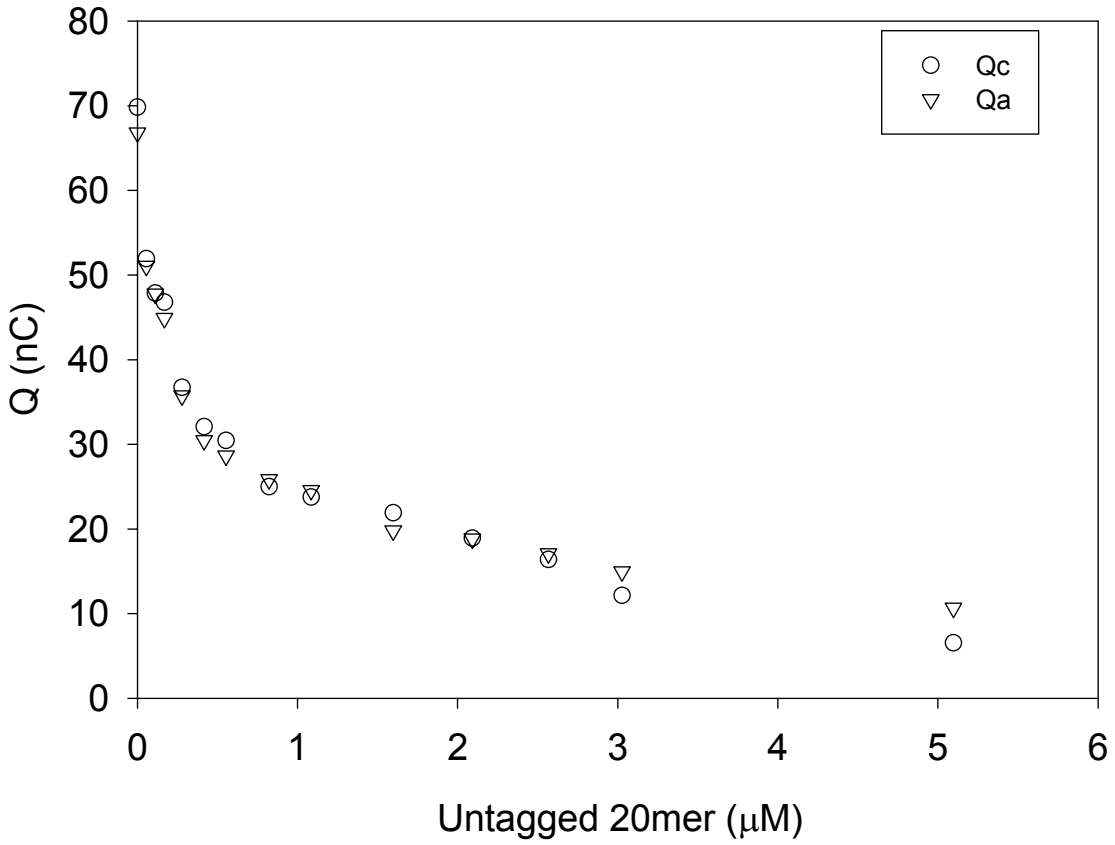


Figure 2.13 Competitive adsorption study of 2AQ 20mer and its untagged model. Q_c and and Q_a represent the respective cathodic and anodic peak charges calculated from CV measurements.

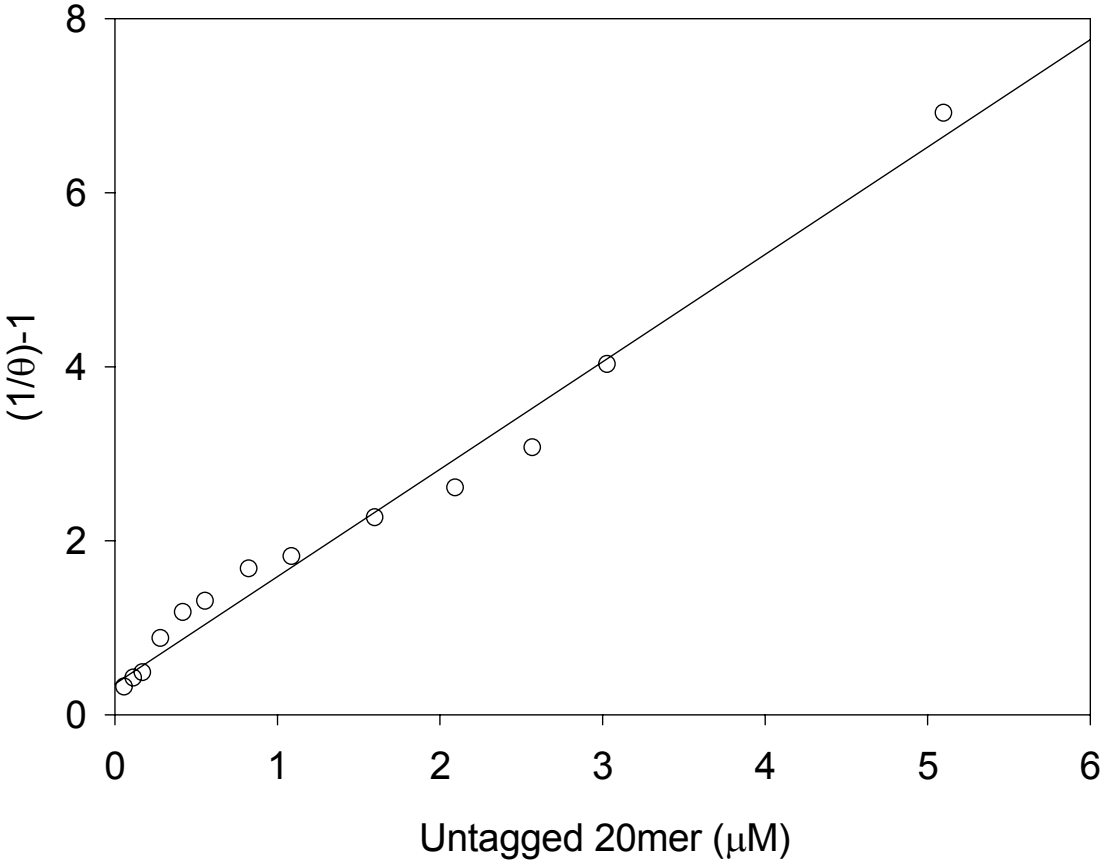


Figure 2.14 Linear competitive adsorption model

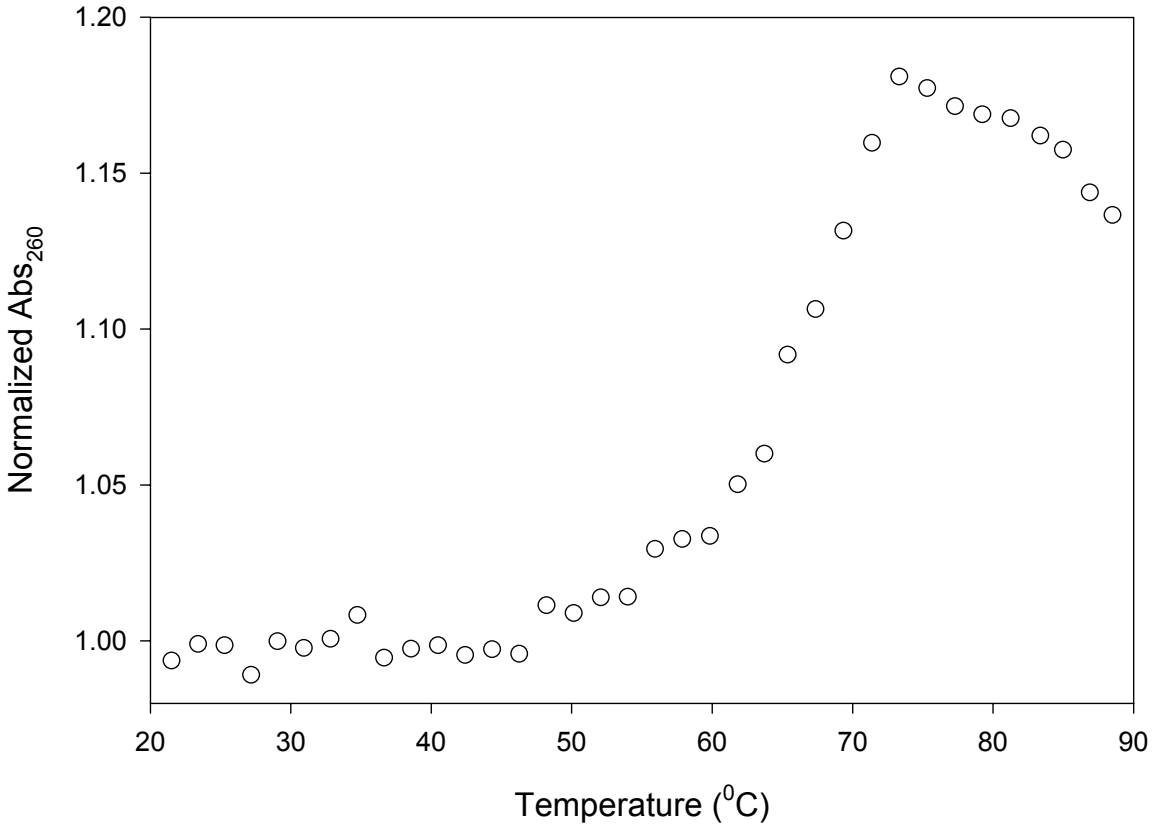


Figure 2.15 Typical 2AQ/complement 20mer melting profile

Table 2.3 20mer melting temperatures

20mer	T_m (°C)
Untagged	66.4
2AQ	68.3
9AQ	68.4
2,9AQ	69.1

used to measure DNA melting temperatures. The solutions were prepared with amounts of the 2AQ 20mer in phosphate buffer to ensure thorough surface coverage. CV measurements marked A in Figures 2.16 and 2.17 indicate formation of the monolayer. At this point, an untagged ODN, either the complementary sequence or a blank probe sequence, was added to the solution. After stirring for approximately 20 minutes, the CV was measured again (see Figure 2.18). The signal determined for the AQ 20mer showed an attenuation by almost fifty percent with addition of an equimolar amount of untagged strand. This appears consistent with the results described before in the competition studies. Thermal cycling was then performed on both solutions to facilitate formation of a double helix. The non-complementary 20mer sequence had little if any further effect on the voltammetry in Figure 2.16, signal B versus C. This system is still a basic two-species competition for the electrode sites of adsorption.

The use of a complementary sequence yielded a further decrease upon the CV signal size. The voltammogram marked C in Figure 2.17 shows the attenuation of almost 50% the competition signal (B) with the formation of the double helix. Also seen is a negative shift of about 30mV in the redox potential for this system.

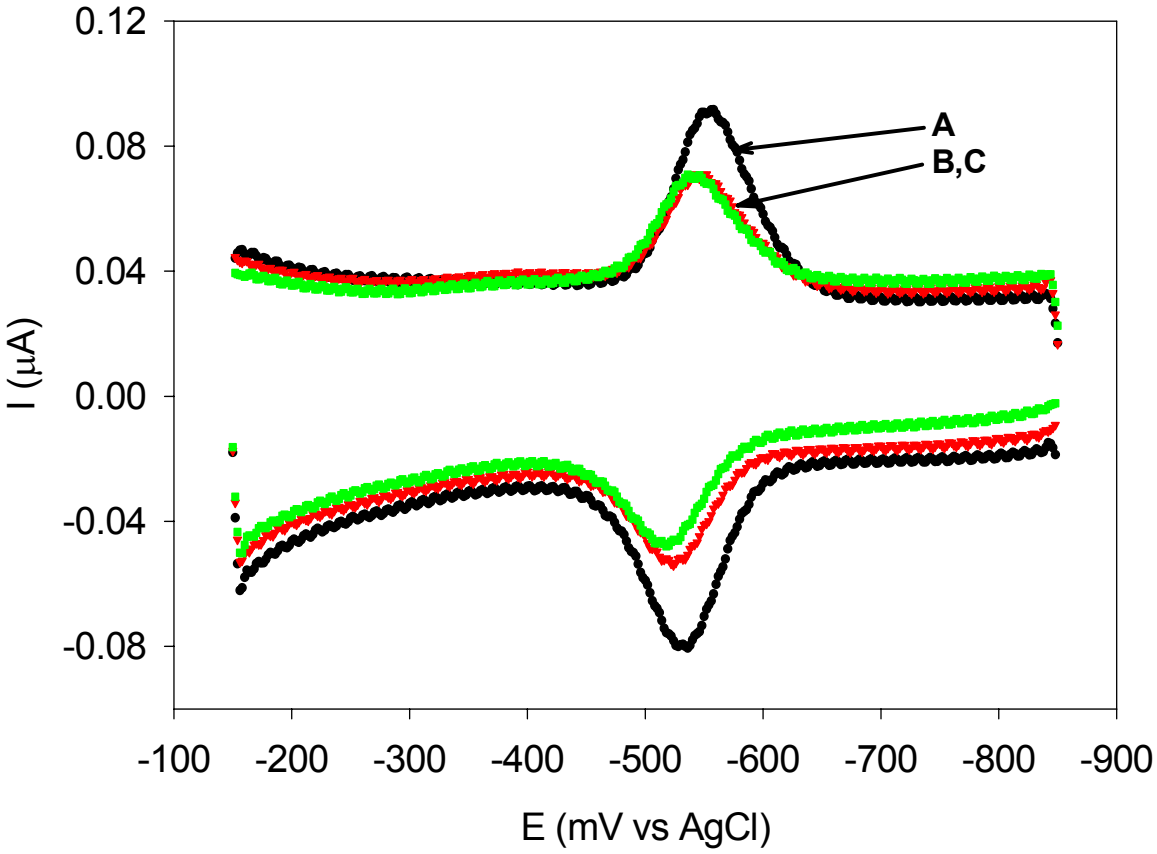


Figure 2.16 Voltammetry on 2AQ 20mer (A), upon addition of untagged DNA (B), and after thermal cycling (C)

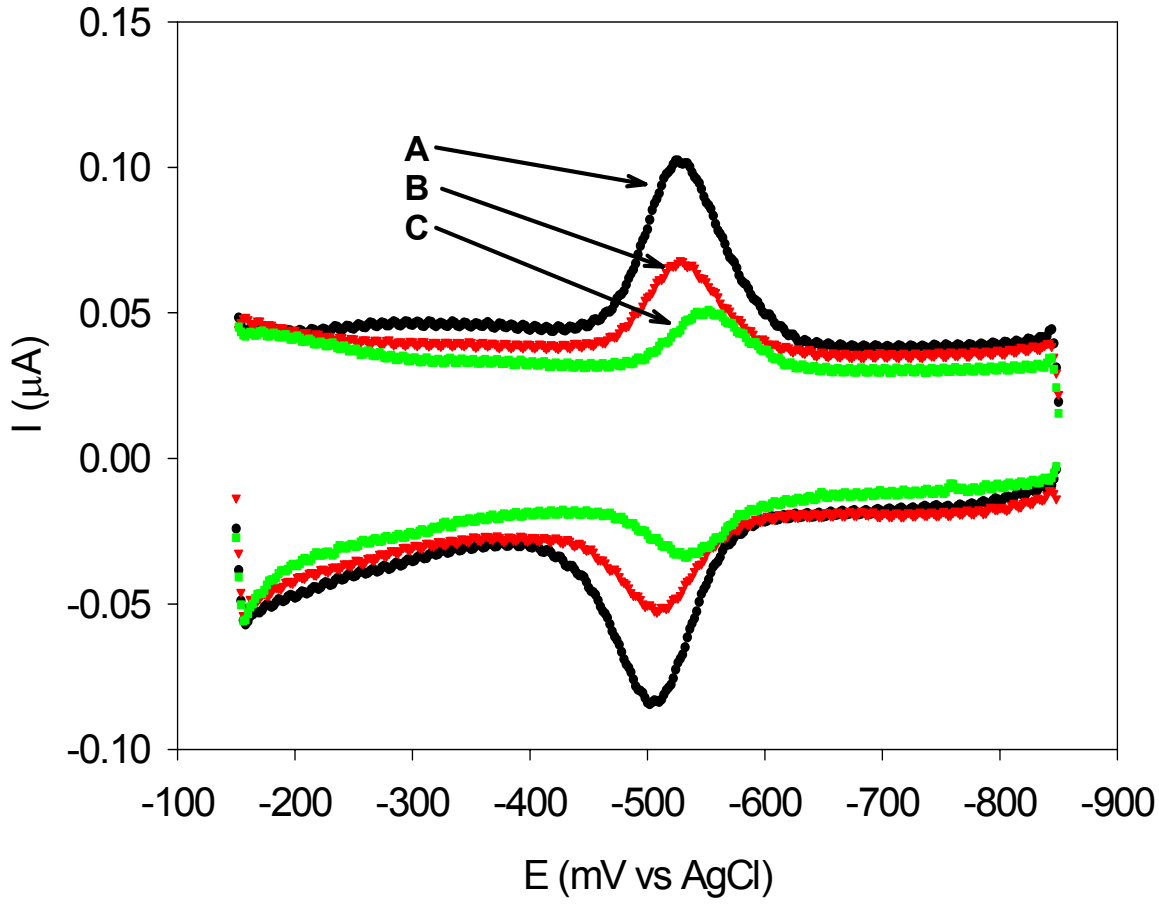


Figure 2.17 Voltammetry on 2AQ 20mer(A) with complement addition (B) and annealing (C). Measured in pH 7.4 0.1 M phosphate buffer with 0.05 M NaCl and 5 mM EDTA

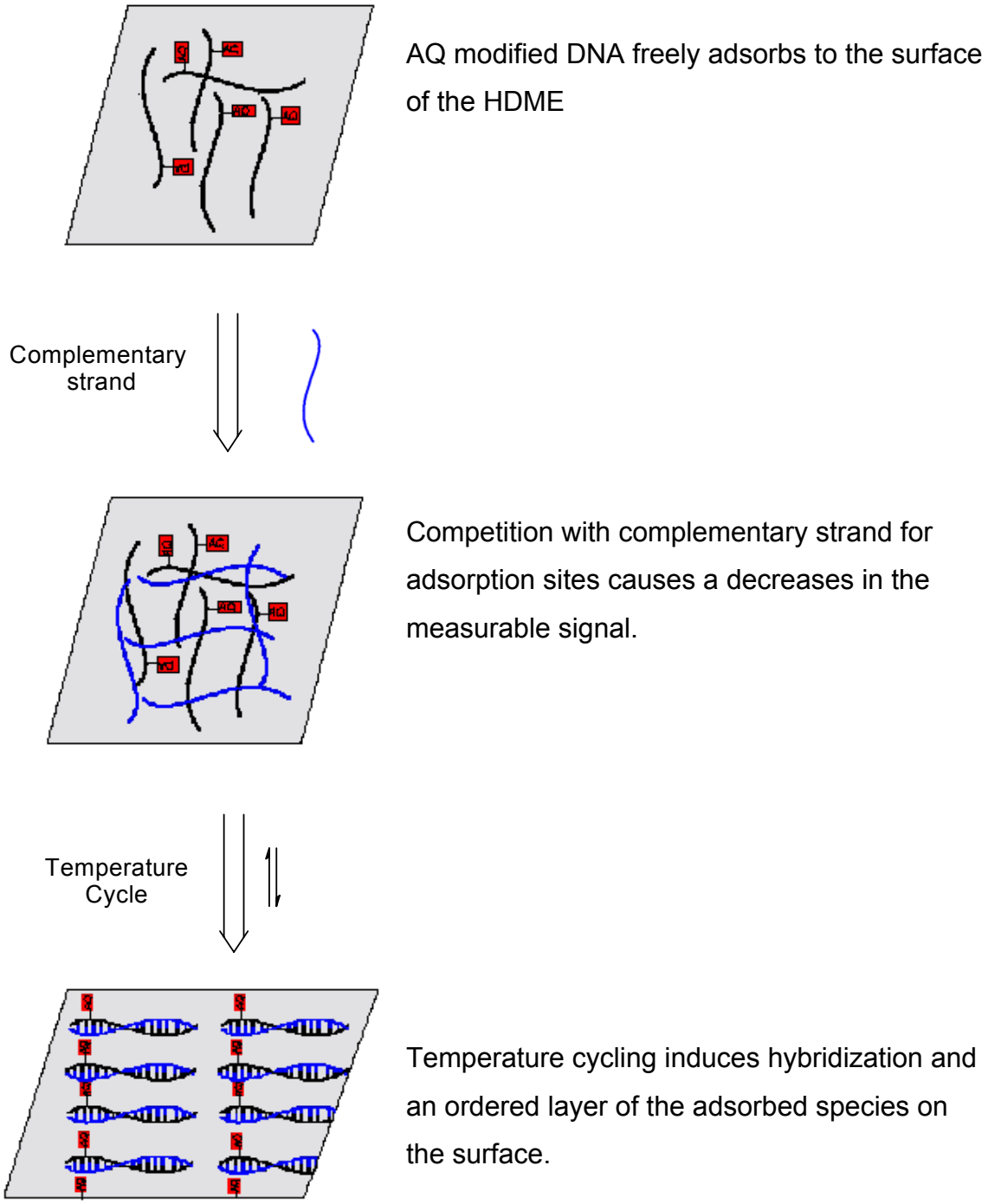


Figure 2.18 Illustration of the adsorption of an AQ monolayer

Various reasons could explain the further attenuation in the signal size. First, the signal measured could decrease due to a larger footprint requirement for the double helix species. Also present is the potential for electro-inactivity of the double helix AQ due to intercalation or its lack of adsorption to the HDME surface. Another probable explanation is that the AQ-tagged double helix is electroactive, but has a smaller adsorption coefficient (β) due to shielding of the bases. This in turn causes the system no longer to be at a saturation coverage point in the isotherm consequently, the surface coverage is decreased.

The potential shift observed offers another point of investigation. The 30 mV shift in potential likely arises as the AQ moiety is positioned differently in the electrode double layer in an adsorbed double stranded DNA state. Similar studies by the Yamana et. al have examined systems in which the AQ moiety is attached to the ODN via with a one carbon, linker arm.[44] Their system sees a similar potential shift (ΔE) upon formation of the double helix at a glassy carbon electrode but in the opposite direction. They report a direct correlation between the amount of DNA and the ΔE signal measured. They report seeing this shift occur up to the point of a 1:1 ratio between the labeled sequence and it complement.

Further work from the Yamana group applied their AQ-modified DNA to a gold electrode through an end-tethered thiol group.[45] Studies of the effects of sweep rate showed a great deal of information on monolayer formation and electrode kinetics in their system. Plots of the log of peak current(I) or the peak potential (E_p) versus changes in sweep rate (ν) indicate that they had a well defined layer on the electrode surface. The E_p versus ν plots for their layer also saw an enhancement on electrode kinetics in the presence of double stranded DNA.

Using the Yamana et al. research as a model, similar treatment of the data reported was done on the 2AQ 20mer described here. Analysis of the log I versus log ν data yielded a linear plot in both cases of single and double stranded DNA. Regression analysis in Figure 2.19 of the slope for both lines

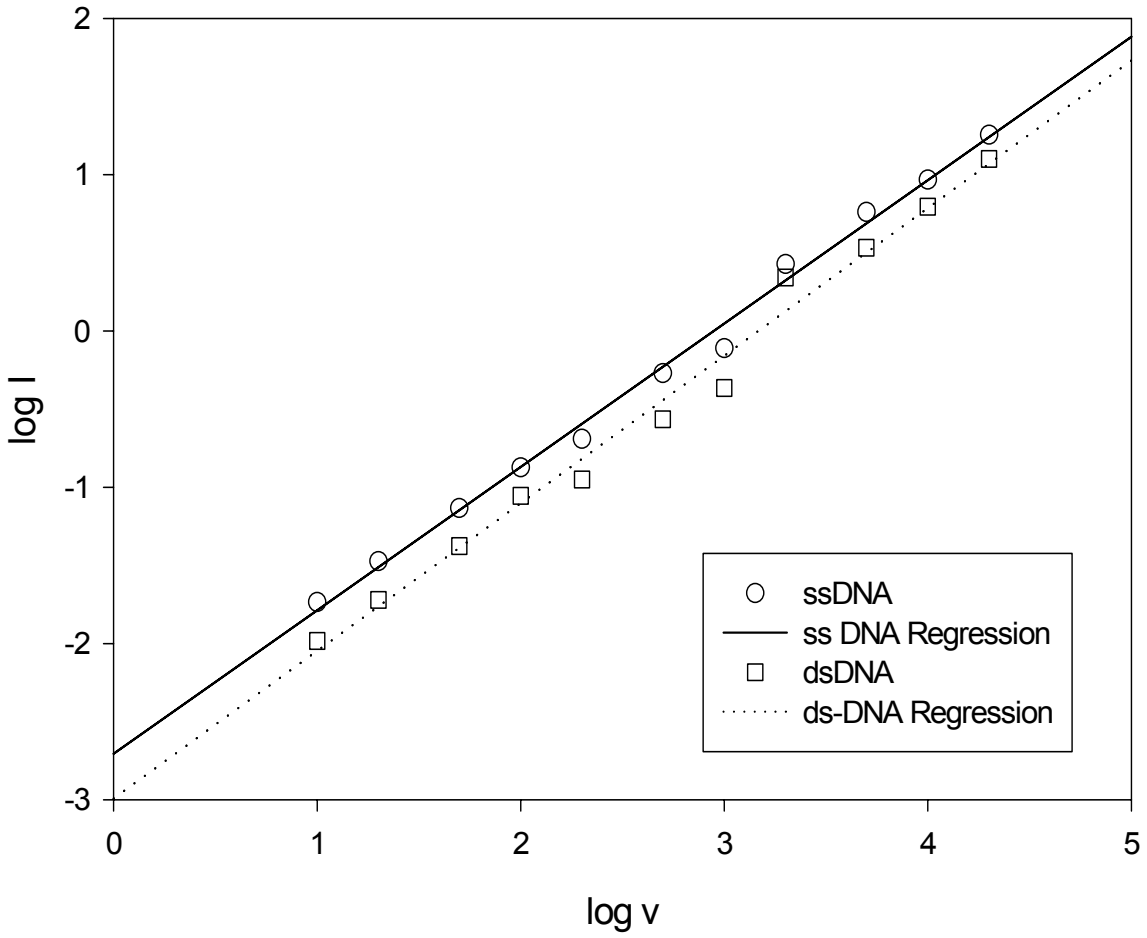


Figure 2.19 Effect upon current by sweep rate

show values of 0.96 and 0.93 respectively. Both values are close to the theoretical slope of unity expected for a surface bound species.

Contrary to the Yamana et al. results, treatment of the E_p versus ν data in Figure 2.20 for the system described here indicates a slowing effect on the electrode kinetics in the double-stranded form. Peak potentials show a greater widening with sweep rate in the double-stranded form compared to the single-stranded counterpart. Explanations likely arise from the biggest difference of the two systems. Yamana's chemisorption of the probe DNA to the electrode via a thiol linker could allow for a greater access of the π stacked base pairs, in the double helix center, to facilitate electron transfer. The system described here most likely is in an orientation with the DNA helix lying flat on the surface. This causes the π stack to be shielded from taking part in this electron transfer as shown in Figure 2.18.

Conclusions

Studies reported here have examined the use of an AQ-modified nucleotide and its incorporation into a set of sensor probes for the determination of the DNA hybridization event. Adsorption of the nucleotide and its corresponding 20mers at mercury electrodes follows a simple Langmuir isotherm model. With the 20mers, competition with complementary and non-complementary untagged sequences for the sites of adsorption attenuates the measurable AQ signal in accordance with a Langmuir model.

Hybridization of the tagged DNA results in an apparent shift in the AQ global $E^{o'}$ redox value to a more negative potential. This most likely results from a repositioning if the AQ group in the diffuse double layer at the electrode surface. While the data shows some potential for the detection of the DNA hybridization event, the magnitude of the effect is small which makes the design of a real sensor somewhat problematic.

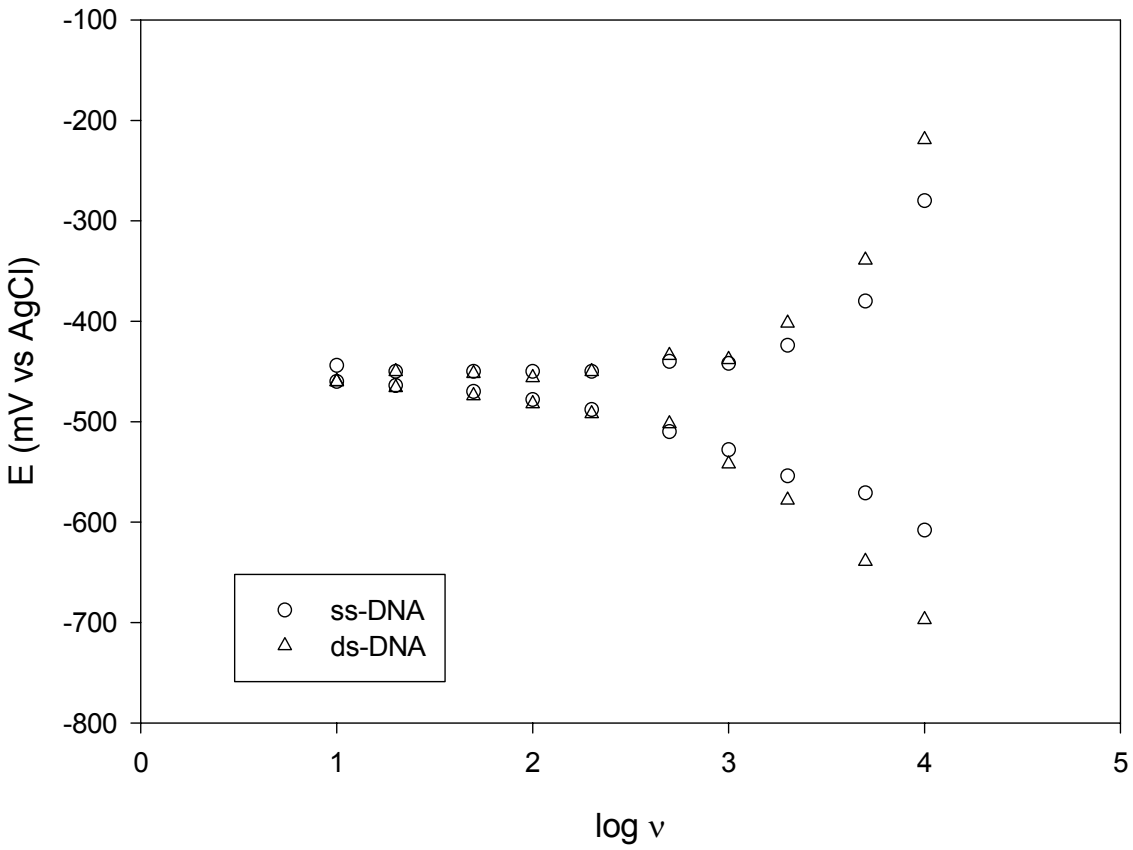


Figure 2.20 Volcano plot for 2AQ 20mer with and without complement

CHAPTER 3
ELECTROCHEMICAL DAUNOMYCIN-BASED STEM-AND-LOOP DNA SENSOR

Introduction

Sequence specific DNA studies have received a great deal of attention in recent years. Of the methods used in these studies, molecular fluorescence has shown some of the greatest promise. Inherent in their design, fluorescence systems lend themselves to quality measurements due to low background signals and in turn a good signal-to-noise ratio. Methods utilizing fluorescence based systems have achieved single molecule detection of certain molecules. Another area of promise has used fluorescence systems in the study of the interaction of small molecules with DNA. Most of this benefit arises from the similarity of structure between fluorophores and the planar structure favored in DNA intercalation interactions. Electroactivity in many of these compounds also allows for their use in electrochemical sensor systems.

The work described in this chapter utilizes the characteristics and system models described below for the detection of the DNA hybridization event. Synthesis of a DNA/daunomycin adduct species was attempted as described below. The goal of the research was to incorporate the adduct into a stem-and-loop structure of a sensor system based on a DNA probe attached to a gold electrode using a thiol group associated with the DNA strand. Electrochemical characterization of these adducts was done using cyclic voltammetry. Upon exposure to the proper complementary sequence, the hairpin should open causing a variation in the tag's position in the electrode double layer and in turn its measured signal.

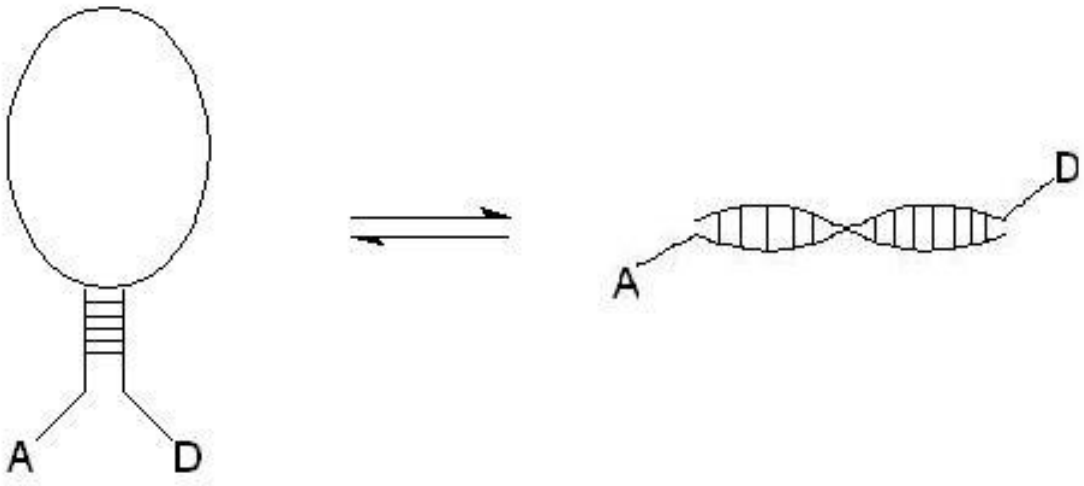
Molecular Beacons

A system first reported by Sanjay Tyagi and Russell Kramer used a DNA stem-and-loop structure as a sequence specific sensor for the detection of the

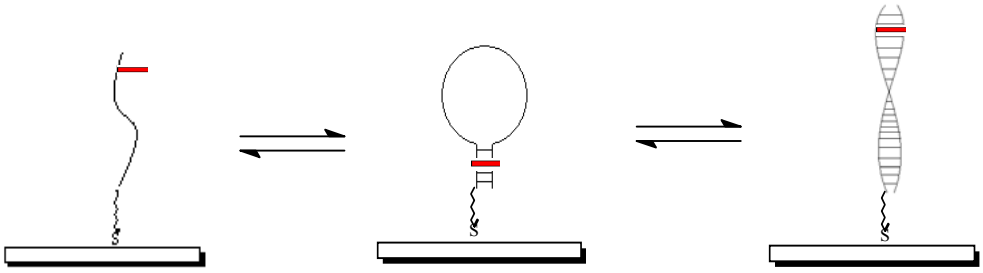
hybridization event.[46] In their approach an oligonucleotide of 25 base pairs in length was synthesized such that the sections of five bases on both the 3'- and 5'-ends were self-complementary. This enabled the DNA strand to fold back upon itself forming the stem-and-loop structure, which was stable under normal *in vivo* conditions. A fluorescent moiety was attached to one end of this sequence and a corresponding non-fluorescent quenching molecule to the other. In the stable hairpin form this places the donor-acceptor pair in close proximity such that the fluorescence event does not occur.

Changes in many conditions, such as temperature or ionic strength, that may cause the stem and loop to open will allow the fluorescence event. Experimental conditions are maximized in a given beacon system to account for these and assure that the only fluorescence comes from the hybridization event. Upon exposure to its complement, the loop is able to hybridize and form a more rigid linear double helix configuration (see Figure 3.1A). In this open linear form, the 3'- and 5'- ends are distant enough apart such that fluorescence can be observed. The simplicity of this system and its degree of sequence specificity has made it a widely used method in sequence determinations. This method has yielded such promise that most commercial DNA synthesizers now offer these pre synthesized molecules for purchase and use with virtually any sequence.

The system described herein relies similarly on a positional dependence for a signal generation. For the molecular beacon model, a single- stranded hairpin configuration places the fluorophore and its corresponding quencher in close proximity, as in Figure 3.1A, which limits the fluorescence signal measured. In a similar configuration, the system described here (Figure 3.1B) should show an increase in the electrochemical signal measured due to a closer proximity of an electrochemical tag to the electrode surface. Upon DNA hybridization, the electroactive group for detection finds itself in a position further extended into the electrode double layer making reduction/oxidation more difficult.



(A)



(B)

Figure 3.1 Typical stem-and-loop configurations. (A) the stages used in a fluorescence MB. (B) thiol 25mer stem-and loop proposed electrode configurations

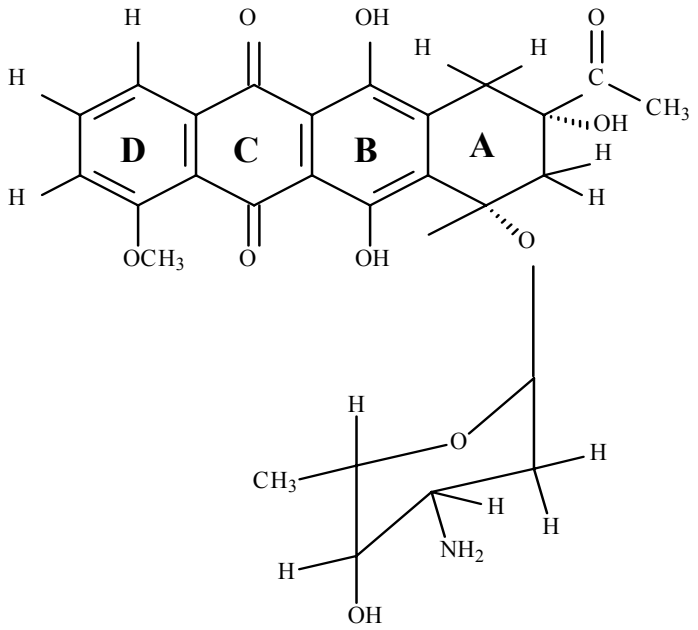


Figure 3.2 Daunomycin

Daunomycin Interaction

Intercalation of the planar ring structure of certain drugs into the base pair stacks of the DNA double helix has been well documented and modeled with various techniques. Daunomycin (DM), shown in Figure 3.2, is an anthracycline based antibiotic similar to adriamycin. It has shown some effectiveness in clinical chemotherapy treatments of leukemia. The primary mechanism of action for the intercalated species is thought to arise from interactions of the A-ring in the structure and the amino sugar groups in the minor groove. This interaction results in topoisomerase-induced DNA strand breaks. High tumor cell uptake allows for the drug's cytotoxic effects that have been linked to oxygen species from reactions catalyzed by the quinone moiety . All of these characteristics have led to a great deal of interest into the site specificity and binding thermodynamics of daunomycin with DNA sequences.

Work presented by the Breslauer group documented daunomycin

intercalation into the DNA double helix through fluorescence measurements.[9] Their studies measured variations in the fluorescence of the drug based on the free and intercalated forms. The Breslauer results indicated an approximately three base pair length for each intercalated molecule. Determination of melting point profiles in their system showed that daunomycin intercalation enhanced the stability of the double helix. DNA melting temperatures were increased by 20 degrees Celsius on average. Fluorescence was also used by Roche et al. to examine the site selectivity for intercalation of the drug.[10]

Daunomycin has been a popular compound of many electrochemical sensor systems due to the electroactivity of the quinone portion of the drug. This has led to its utilization as a reversible redox species in numerous electrochemical studies. The electrochemical response of daunomycin arises from primarily from rings B and C of the anthracycline rings in Figure 3.2. The redox potential associated with the oxidation of ring B generally falls at a higher potential than the range of most common electrodes for general use. The response associated with the reduction of ring C falls in a more accessible range for the examination of redox species.

Palanti, Marrazza, and Mascini illustrated the use of daunomycin for electrochemical hybridization detection in 1996.[47] Their work measured a solution of daunomycin with glassy carbon electrodes modified with oligonucleotides that had been immobilized through different means. Reported results indicated a shift in daunomycin redox potential with hybridization. The direction of the shift appeared to depend on the method of immobilization and the electrode environment created by it.

Daunomycin also exhibits useful characteristic with its nature for forming bonds with the DNA strands upon intercalation. Studies have shown the drug's ability for "cross-linking" with the DNA strand through an alkylation reaction with guanine nucleotides in the sequence. Work from multiple labs have examined the circumstances necessary for such reactions.[9, 10, 48, 49] Initially it was thought that these reactions required iron chelated by the drug, but further work yielded

various other routes for achieving the same adduct. The most examined of these used formaldehyde forming the adduct through a Schiff's base type reaction as seen in Figure 3.3.

Phillips and co-workers attempted to maximize the cross-linking reaction for several adducts in the adriamycin drug class by altering various parameters such as temperature, buffer, etc.[50, 51] This work illustrated the *in vitro* formation of the drug-DNA adduct with a DTT (dithiothreitol)/ Fe (III) reduction system. Their data also indicated a sensitivity of the adducts to temperature. Experiments took the formed adducts and applied a biological temperature of 37 degrees Celsius for various times. The reaction was then stopped with a phenol extraction and the amount free drug was measured by UV-visible absorbance.

J.B. Chaires and co-workers used formaldehyde for the cross-linking reaction.[34] Studies with various anthracycline drugs showed that this system required the 3'- amino group of daunomycin, and the N2 amine of the guanine nucleotide in order for the reaction to occur. Their results indicated that the cross-linked drug, which remained intercalated during and after the reaction, also stabilized the duplex structure as indicated by an increase of melting temperature of the double helix in question. The adduct formed by Chaires and co-workers showed similar sensitivity to temperature and other conditions as in the Phillips study above.

Work presented by Barton and co-workers utilized daunomycin modified ODN's synthesized by the reaction below (Figure 3.3). In this study the intercalated drug was cross linked to their DNA sequence of interest which had been modified with a thiol linker arm for immobilization on gold electrodes.[3] Guanine/Cytosine base-pair preference for intercalation was used to attach the drug at various positions and distances from the electrode in the double helix. Electrochemical measurements of the hybridized ODNs were used to determine the ability of DNA to transfer a charge through the double helix.

The work described in this chapter describes the use of daunomycin

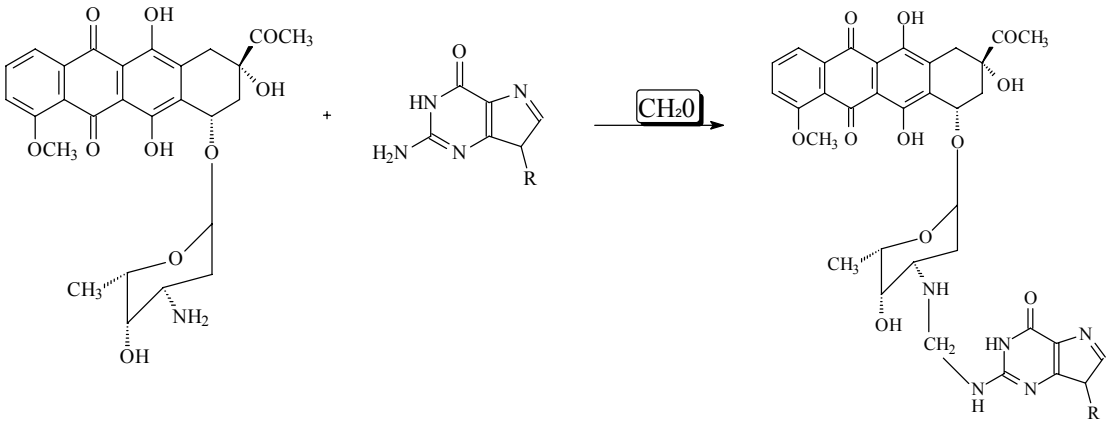


Figure 3.3 Alkylation of guanine nucleotide by daunomycin and formaldehyde

alkylated DNA for creation of a reusable sensor sensitive to the hybridization event. DNA was alkylated under conditions similar to those used by various other groups using the daunomycin adduct. Once immobilized on gold electrodes, measurements of molecular beacon-like DNA were conducted to determine strength and stability of the detectable signal. Upon hybridization, the change in the tag's position relative to the electrode surface resulting in a change in the measurable signal.

As described below these concepts have been validated by two other groups in works published since these studies were conducted.[52, 53] Work from Heeger and co-workers constructed a similar system involving a ferrocene tag for the electroactive component for measurement. The Qi Ouyang group also did work with a similar modeled system using the reduction of thionine tethered to the end of their stem-and-loop sequence. Results reported by both groups saw similar effects to the signal measured upon opening of the attached stem-and-loop ODN.

EXPERIMENTAL

Materials

Daunomycin hydrochloride (MW 564 g/mol) was obtained from ICN Biomedicals in 1-mg samples. Stock solutions were prepared by dilution of each sample with two milliliters nanopure water. Concentration of the stock was determined with UV-Vis absorbance of serial diluted stock samples at a wavelength of 477 nm using a value of 11,500 $M^{-1}cm^{-1}$ for the molar absorptivity.[2] Microliter amounts were used for measurement and synthesis steps.

Oligonucleotides were purchased from IDT synthesis (Ames, Iowa). The 25mer sequence for modification was 5'-CCC CCC CAA AAA AAA AAA CCG GGG G-3' and its corresponding 18mer complement 5'-CCC CCG GTT TTT TTT TTT-3'. Thiol modifications on 25mer stem and loop ODNs with were designed with the thiol group on the 5'- end with cytosine nucleotides fixed for interaction

with guanine nucleotides at the 3'- end. This design was chosen to allow free movement of the alklyated guanine residues upon hybridization.

Other chemicals were obtained from Fisher Scientific Co.

Synthesis.

Adduct synthesis was done under conditions similar to that used in the literature which consist of the combination of ODN, formaldehyde, and daunomycin. Micromolar concentrations of the stem-and-loop DNA sequence were prepared in phosphate buffered water solutions. Alkylation reactions were carried out in 1.5 mL phosphate buffer, 10 μL daunomycin solutions; 20 μL formaldehyde was added to make approximately 2% solutions. These mixtures were allowed to react with either a 25mer DNA modified electrode or solution of the hybridized DNA for a minimum of 12 hours before the reaction was stopped. Reactions done in solution were stopped through standard methods of cold ethanol and phenol precipitation of the modified ODN. The resulting aqueous phase after the precipitation was then used to soak gold electrodes for a minimum of two hours to form a thiol anchored monolayer on gold electrodes for electrochemical measurement.

Electrochemical Studies

All measurements were taken using CH Instruments 650 potentiostat. A gold disk or hanging mercury drop working, a platinum wire counter, and a silver/silver chloride reference electrode were used. Electrochemical measurements were carried out using a 0.1 M phosphate buffer with 50 mM NaCl under nitrogen atmosphere. Working electrodes were prepared by polishing with alumina, rinsed and cleaned in piranha solution (3:1 H_2SO_4:H_2O_2) followed by washing with nanopure distilled water. The area of the gold electrodes was then measured by performing cyclic voltammetry in 1 M H_2SO_4. This consisted of cycling the potential between 0 and 1.6 volts versus Ag/AgCl and measuring the charge associated with the reduction of the oxide layer

formed. This charge was then converted to area using the value of 390 $\mu C\ cm^{-2}$ reported by Trasatti and Petrii.[54] Prepared electrodes were then soaked in a solution of thiol modified DM tagged DNA.

Once the DNA layer was applied, measurements were taken before and after addition of the complementary sequence. Solution temperatures were cycled at certain points to facilitate melting of the DNA helix in an attempt to reclaim the original single stranded stem-and-loop structure. Thermal cycling was carried out with the HP 89909 peltier heating apparatus with an HP 8452A diode array spectrometer.

Result and Discussion

Alkylation

Early studies of the alkylation process were accomplished using the blank and thiol modified complementary 20mer sequences from Table 2.1. Upon completion of the alkylation and precipitation steps, mass spectra were obtained looking for indication of the modified DNA. Spectra for a blank solution, consisting of the original DNA strands with no daunomycin, indicated peaks of 6062 and 6502 amu for each individual 20mer and other peaks at intervals of 22 amu for each of the sodium ions complexed with the two strands in the hybridization process.

Corresponding examination of the alkylation reaction consisted of two other peaks at 526 and 538 amu. The initial samples examined by electrospray MS indicated that the daunomycin species was present in the precipitate. These results agree with those obtained by Koch and co-workers who reported the formation of the daunomycin/formaldehyde adduct (daunoform) with a $(M-1)^{1-}$ mass of 538 amu.[49, 55, 56] The absence of DNA peaks from the latter mass spectra can be explained in the differences of our synthesis steps. Other groups attempted the synthesis steps with higher DNA concentrations (mM) while the state of materials used in our studies only allowed this step to be carried out at concentrations of about 10^{-5} M. This, combined with the limitation of potential

alkylation sites, leads to a greater potential for excess in the reactants needed for the reaction and in turn a prominence of the daunoform species. Observation of formation of the daunoform adduct does however indicate favorable circumstances for the complete alkylation reactions to occur.

Electrochemical Characterization

Initial examinations of the redox behavior of daunomycin yielded a typical broad peak behavior similar to a quinone-like two-electron reduction. Results were consistent with those seen before in studies by Kertesz et.al indicating a uniform well-defined monolayer applied to the electrode surface.[57] The potentials and widths of peaks obtained changed little compared to results obtained in previous studies. This behavior also was maintained in the chemisorbed DM alkylated DNA species.

Preliminary studies utilizing the 20mer sequences from chapter 2 indicated some promise in these studies. Characterization of the tagged 20mer DNA used for the mass spectroscopic measurements was attempted with a monolayer formed on a mercury electrode. CV measurements were taken during various stages of the probe construction to determine the suitability of DM for these studies. Data shown in Figure 3.4 illustrates measurements taken on the mercury electrode. The first measurement is of DM alone in the buffered solution. The second measurement taken shows a decrease in the peak size due to a displacement effect with the interaction with of DNA. Two small effects in peak potential could be seen at this point. Cathodic and anodic peak separation for the free DM solution appears to be negligible. This number increases in the presence of DNA to about 30 mV. The overall peak potential shifts 30 mV as well. Both are most likely due to a more complex nature inherent with the electrode environment.

At this point, experimentation was switched to the thiol modified stem and loop immobilized on gold electrodes in an attempt to detect a signal difference between the two conformations of our probe, the stem-and-loop and its

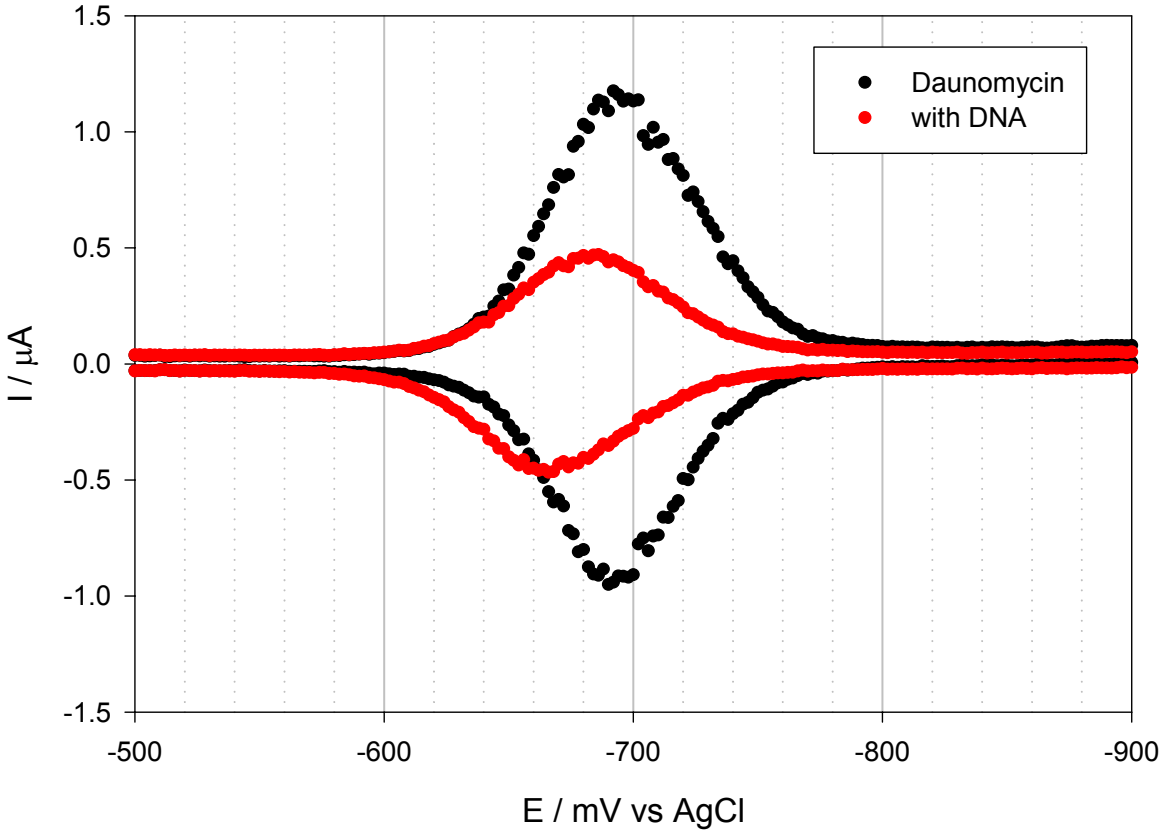


Figure 3.4 CV measurements of daunomycin on mercury electrodes before and after the addition of DNA

hybridized double helix counterpart. Signals such as those seen in Figure 3.5 were typical for these studies. In the initial stem-and-loop configuration, CV measurements detected a large well defined peak with typical peak characteristics seen in previous measurements. This electrode was then soaked in a buffered solution containing the 18mer complementary sequence for a period of no less than 30 minutes before being measured again. The second measurements show a drastic attenuation in the signal detected.

This disappearance is likely explained upon consideration of the relative position of the DM tag with respect to the electrode diffusion layer. The stem-and-loop conformation situates the probe's tagged end in a closer proximity the electrode surface where it is more suited for redox reactions within the electrode diffusion layer. Upon hybridization, the DNA in effect lengthens placing the DM tag further (roughly 15 base pairs) from the electrode. Similar data reported by Barton and co-workers illustrated greater difficulty in reducing DM by placing the site of alkylation at various points along a DNA 15mer.[2, 3] This greater distance makes the DM reduction kinetically harder to accomplish hence the attenuation of the signal. These results compare with those obtained in other studies from at least two other groups.

Studies presented by Heeger and co-workers achieved similar results with what they describe as a "signal on" and "signal off" device detection of the hybridization event.[52] The Heeger system utilized a 28mer modified with a 3'-thiol group and a 5'-ferrocene tag. Upon exposure to a complementary sequence their results illustrated a CV peak disappearance in the transition from stem-and-loop to the double helix states as seen in the results presented herein. This is explained through the effect of increased distance between the electrode surface and the ferrocene tag. Work presented by the Ouyang group worked using a similar system.[53] This system used a thionine electroactive group attached to the hairpin DNA molecule's 3'-end using 1,4-phenylene diisothiocyanate (PDC) linker. Their work was primarily interested in the thermal stability of the double helix formed and its corresponding effects on the current

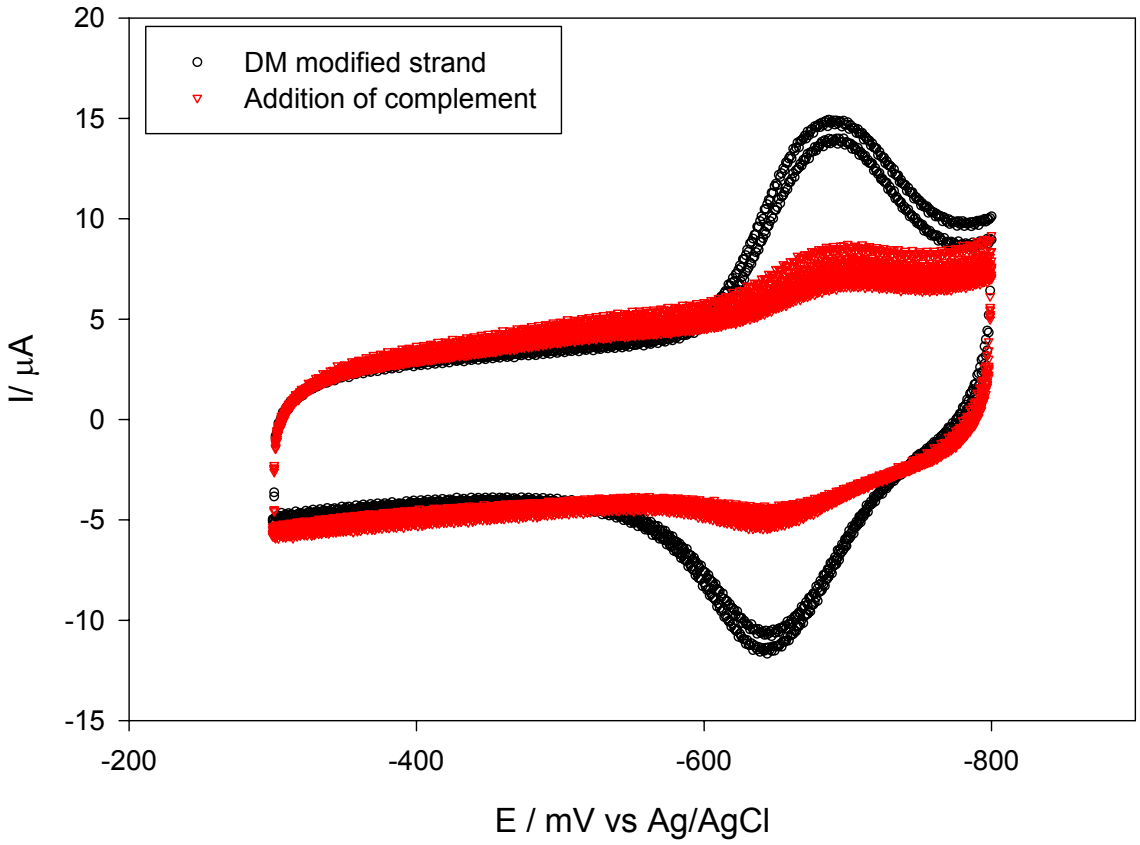


Figure 3.5 CV response of DM-modified DNA before and after addition of complementary sequence

measured. Their results do agree with those mentioned above in that a transition from the stem-and-loop conformation to the double helix slows, if not completely stops, the current flow for faradaic reaction of the redox tag.

Further characterization of our sensor examined the potential for regeneration and re-utilization described in the Heeger and Ouyang papers.[52, 53] Attempts to regenerate the sensor began with soaking the hybridized electrode in a 80 degree buffer to facilitate melting of the DNA double helix. The electrode was soaked for a period of five to ten minutes before being rinsed with a fresh buffer solution followed by a rinse in ultrapure water. Attempts to again detect the daunomycin electrochemical sensor were unsuccessful. Explanations for this rely mostly on descriptions in others work of a degree of thermal instability in the bond form during the alkylation reaction. Results described by Phillips and co-workers indicated that the bond could be temperature sensitive releasing DM tag at temperatures of 40 degrees and higher. [50] This would in turn make it difficult, if not impossible to reform the original interface configuration

Conclusions

The study presented here represent a preliminary examination of the use of tagged stem-and-loop DNA structures as electrochemical sensors. Results indicate a promising possible method for detection of the hybridization event for a stem-and-loop sensor immobilized on a gold electrode. An advantage this system would offer would be the ability for its use in *in-situ* remote operations. These conditions offer greater difficulty for spectroscopic measurements due to the unfavorable nature of transmitting a light beam in and out of such a sample. The most obvious advantage with this method lies in the cost associated with it. Typical sensor systems of this model can generate numerous costs associated in sample preparation alone. This method offers a simpler approach for modification of the DNA. The previous deep background from the electrochemical and binding studies of daunomycin offer a somewhat well defined system for characterization and study. Further work could consist of

using this system to adapt an array of electrodes, each with individual sequences, in order to determine an unknown DNA sequence faster. Carrying this one step further, the tags could be various redox couples for specific sequences and determining the sequence from the potential of the peak reduced in an array on one electrode. Each offer the benefits mentioned above with greater degrees of application.

CHAPTER 4
AQ-MODIFIED GOLD ELECTRODES

Introduction

Electroanalytical sensor designs for DNA fall into two basic groups: (1) modification of the electrode or (2) modification of the DNA molecule itself. Work described in previous chapters has relied primarily upon modification of the DNA molecule through chemical attachment of an electroactive group for detection. This chapter describes a system in which the electrode surface itself is modified for detection of the DNA double helix. The modification was carried out on gold electrodes by an AQ group modified with a thiol linker arm for attachment to gold electrode surface (Figure 4.1).

An important consideration in the design of any sensor system lies in the kinetics associated with the mechanism of the sensor itself. A good sensor requires kinetics that yield a measurable signal and at the same time is sensitive to the desired object of detection. AQ moieties have been shown by others to be apt DNA intercalator. The question addressed in this chapter is "does that the intercalation event have enough of an effect upon the attached AQ moieties to yield a measurable change in this system's electron transfer kinetics?"

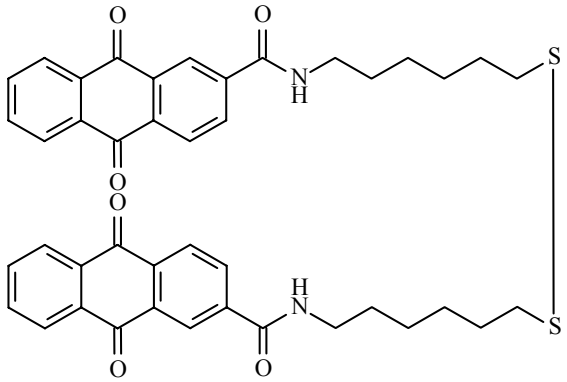


Figure 4.1 AQ used to modify gold electrodes

The work present herein employed two electroanalytical techniques to characterize the electron transfer kinetics of a self-assembled AQ monolayer in the presence and absence of a calf thymus DNA solution. Initial studies were conducted using chronoamperommetry (CA), in which a simple potential step was applied to the electrode. The ensuing current response and decay was measured and then mathematically simulated to extract the desired rate constants. The second approach utilized AC voltammetry where a more complex waveform is applied to the electrochemical cell. Variations in the frequencies associated with the waveform produced variations in the current that could be simulated with a different model system. While differences in the two methodologies present a difficulty in direct comparison of the rate constants extracted from their respective data sets, the rate constants are closely related and provide appropriate comparison of the response of the AQ-SAM in the presence and absence of DNA.

SAM Formation

Self-assembled monolayer (SAM) formation has been examined by many. SAMs can divided into two classes: (1) physical adsorption of molecules onto an electrode surface from a homogenous solution, and (2) chemisorption of thiols and related moieties onto precious metal electrodes like gold and platinum. The basic premise involves the adsorption of a molecule or set of molecules to the electrode surface due to weak molecular attraction and binding forces. These molecules then self orient in relation to the given surface in such a manor as to form the most stable arrangement for a given set of conditions.

Formation of SAMs via thiol chemisorption to gold electrodes has been employed. These ideas saw their initial use in studies by Allara and Nuzzo and quickly caught on.[58] In the usual design, an electroactive couple is attached to an electrode with a thiol modified linker arm. The kinetics of these studied systems are usually determined for a given system. One of the most observable effects a thiol system has is the reduction of the electrode double layer

capacitance. This arises from the deceased dielectric constant, relative to an aqueous double layer, of the ordered hydrocarbon layer of the SAM. A detailed description of thiol characteristics and history is provided by Finklea.[59]

Some of the most interesting uses of thiol groups in electrochemical studies involves the attachment of DNA n–mers to gold electrodes. This has enhanced the ability to design specific sequence probes and their use. The ability to control the orientation of such systems was demonstrated by Barton and co-workers.[33] In their system, the orientation the DNA helix attached to a gold electrode was controlled by the response of the negative phosphate backbone to the applied electrode potential. Their study measured the thickness of the thiol attached DNA layer as a function of electrode potential. The DNA shifted from an upright thicker layer to a thinner horizontal one as electrode potential became more negative. Each of the above mentioned characteristics make a thiol based SAM an ideal candidate in the monolayer formation of sensors.

AQ Kinetics

Anthraquinones and related compounds are one of the most studied electrochemically active species that interact with DNA. The planar structure resulting from the π-bonding of the rings make the compound suitable for intercalation between base pairs of the double helix. The number of electrochemical studies using AQs also provides a large background for comparison of any results obtained.

The general model for AQ electrochemistry involves a two-electron, two-proton reversible reduction from the quinone to hydroquinone state. However, most kinetic studies refer to the more complex nine-membered square scheme in Figure 4.2 described by Laviron and others.[60, 61] This scheme provides a basis to account for the effects of pH upon the quinone reduction pathway. The complexity of this model makes for varied discussion and arguments in this area.

A simpler model for the examination of the AQ modified surface of interest here is provided by the Randle's equivalent circuit (Figure 4.3). This circuit, in a

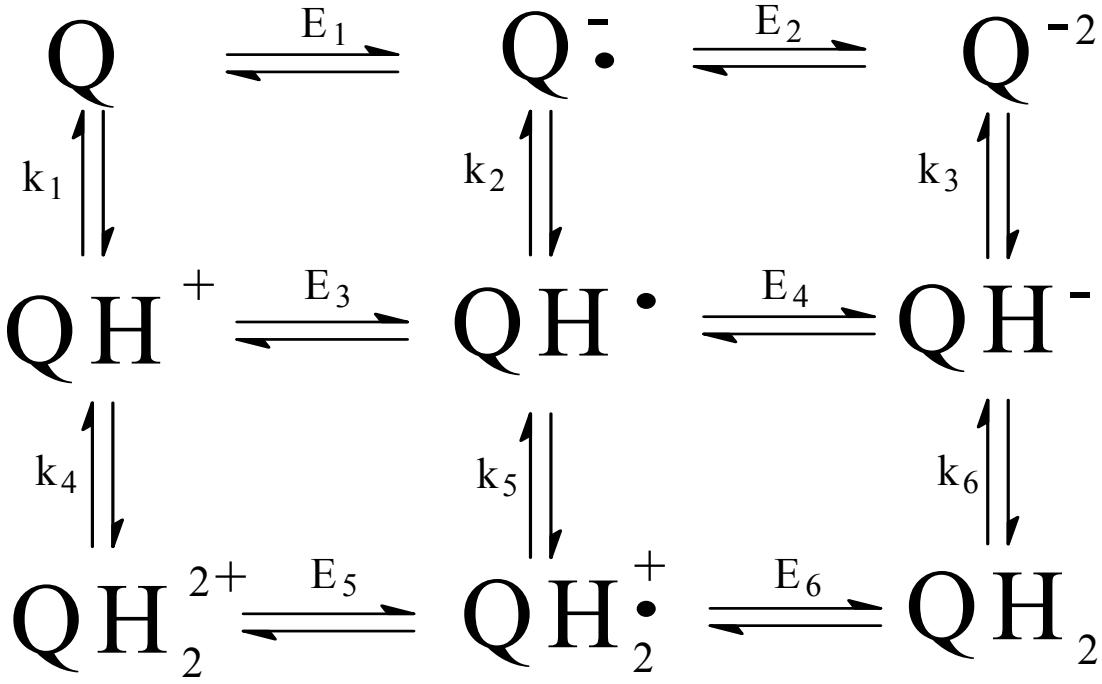


Figure 4.2 Typical nine-membered square scheme

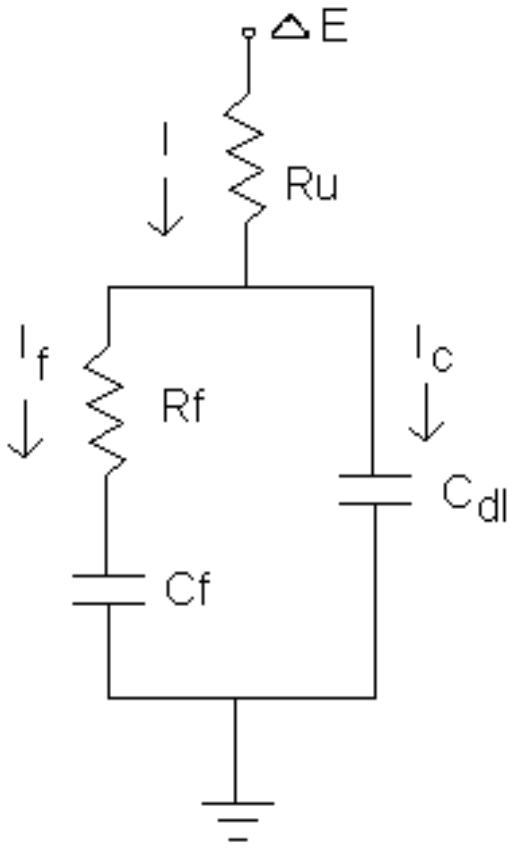


Figure 4.3 Randle's circuit

straightforward way, allows for separation of the faradaic and non-faradaic components of any current measured in this system. The faradaic components can be separated from experimental data and studied in greater detail for characterization.

Both methods employed herein, chronoamperommetry and alternating current voltammetry (CA and ACV), can be modeled with the Randle's circuit example. In this approach, a given current flow is divided into the faradaic and nonfaradaic parts. The uncompensated resisted (R_u) is inherent to any given system. On the non-faradaic (I_c) side, the background current relates to the double layer capacitance (C_{dl}). The faradaic side (I_f) of the circuit is controlled by the faradaic resistance (R_f) that depends on the system and on the fardaic capacitance (C_f) which is related to the amount of material on the electrode surface.

CA Theory

Chronoamperommetry is a widely utilized method for the determination of the electron transfer kinetics of various systems. The basic experimental procedure involves an applied overpotential step past the standard redox potential of a system under study. The overpotential minimizes any reverse reaction and the resulting current decay is related to the electron transfer kinetics of the system being examined. The decay of the current measured for a simple one-step mechanism is related to the kinetics of the system with the equation for a simple logarithmic decay:

$$I = I_0 e^{(-kt)} \qquad (4.1)$$

However, real situations generally call for analysis using the more complex EE and ECE models embedded in the nine-membered square scheme above. These pathways consist of successive two-electron (EE) transfer steps or electron transfers interspersed with proton transfer steps (ECE). Simulations of the multiple step mechanisms is possible using equations from the model derived

by Kertesz et. al.[62] The Kertesz model assumes the faradaic currents, as in the Randle's circuit, are additive for the total current measured. Using data, in which the background current has been subtracted out, makes the faradaic component of the system ready for simulation. A demonstration of these models was achieved using daunomycin adsorbed on mercury electrodes.

The basic procedure of the data analysis separates the current into two components. Equations for the separate currents of each step, noted as I_1 and I_2, were derived to a form usable in data fitting programs. In the EE mechanism the equations were:

$$I_1 = FA\Gamma_T k_1 e^{-k_1 t} \qquad (4.2)$$

and

$$I_2 = FA\Gamma_T \frac{k_1 k_2}{k_2 - k_1}(e^{-k_1 t} - e^{-k_2 t}) \qquad (4.3)$$

$A\Gamma_T$ accounts for the surface coverage, and F is Faraday's constant, and k_1 and k_2 are the rate constants of the individual steps.

Further CA data analysis varying the overpotential step allows for interpolation of the standard rate constant data (k_o) at the system redox potential. A plot and linear fit of the simulated rate constant versus the applied overpotential allows for calculation of k_o from the equation:

$$\ln k_i^c = \ln k_{oi}^c - \alpha f \eta \qquad (4.4)$$

where f is the combined constants F/RT, η is the overpotential, and i indicates the first or second step of the mechanism. In this equation the superscript c refers to cathodic current. Analogous equations relate to the anodic process.

ACV Theory

In AC voltammetry a potential waveform similar to that used in standard linear voltammetry is applied to the electrochemical cell. The potential step applies a voltage step pattern that has been modified with a small AC sine wave perturbation on the order of 10 millivolts. Based on work presented by Laviron , the amplitude of the current measured using AC voltammetry is given by the equations[63] :

$$\frac{I_{pk}}{\omega\varepsilon} = \frac{F^2}{4RT} n^2 A\Gamma_T \sin\phi \qquad (4.5)$$

and

$$\phi = \tan^{-1}\left(\frac{1}{\omega R_{ct} C_{ads}}\right) \qquad (4.6)$$

where I_{pk} is the AC current measured, ω is $2\pi f$, f the AC frequency in Hz, ε is the magnitude of the applied AC potential (ΔE), $A\Gamma_T$ relates to the electrode surface coverage, R_{ct} is the resistance to charge transfer, and C_{ads} is the capacitance due to adsorption.

The background current in this model is linearly proportional to the C_{dl}. This allows for the background to be accounted for in these measurements as a proportional amount. Combining these equations yields a much simpler one:

$$I_{ratio} = n^2 \frac{C_{ads}}{C_{dl}} \sin\phi \qquad (4.7)$$

Calculations of a similar manner presented by Creager and Worster also show the capability for determining an electron transfer rate constant, k_{et}, with this method.[64] Their model determines the equation:

$$k_{et} = \frac{1}{2R_{ct} C_{ads}} \qquad (4.8)$$

Applying this to equation 4.6 for ϕ, it can be seen that the current ratio measured for simulation is related to the k_{et} term:

$$\phi = \tan^{-1}\left(\frac{2k_{et}}{\omega}\right) \qquad (4.9)$$

Our system for AC voltammetry offers the advantage of only having two fitting parameters for the data obtained: the standard electron rate constant and the ratio of double layer capacitance and the pseudo-capacitance of the adsorption mechanism. This compares to data fitting for four parameters offered by many other methods of analyses. The rate constant controls the point of inflection with regard to the x-axis for the plot (Figure 4.4). The capacitance ratio is measured from the separation of the plateaus of the plot. This also offers the advantage of small peaks with very little dependence upon the phase of the signal measured.

Experimental

Materials

2-Mercaptoethanol (2ME) was purchased from Fisher. Stock solutions were diluted with water to prepare soaking solutions. 6-Mercaptohexanol (6MH) and calf thymus DNA were purchased from Sigma-Aldrich. 6MH was diluted with an ethanol water mixture for soaking solutions.

The 6AQ disulfide was synthesized before in house in work previously described.[65] Suspensions of 6AQ were prepared with 1 to 2 mg of solid material in 10 mL of a 50/50 mixture ethanol and hexane solvent.

Calf thymus DNA arrived from Sigma-Aldrich in pre-prepared 2-mg amounts. Each was diluted with water for use.

All other compounds for buffering and electrolyte control were used as received from Fisher Scientific Co.

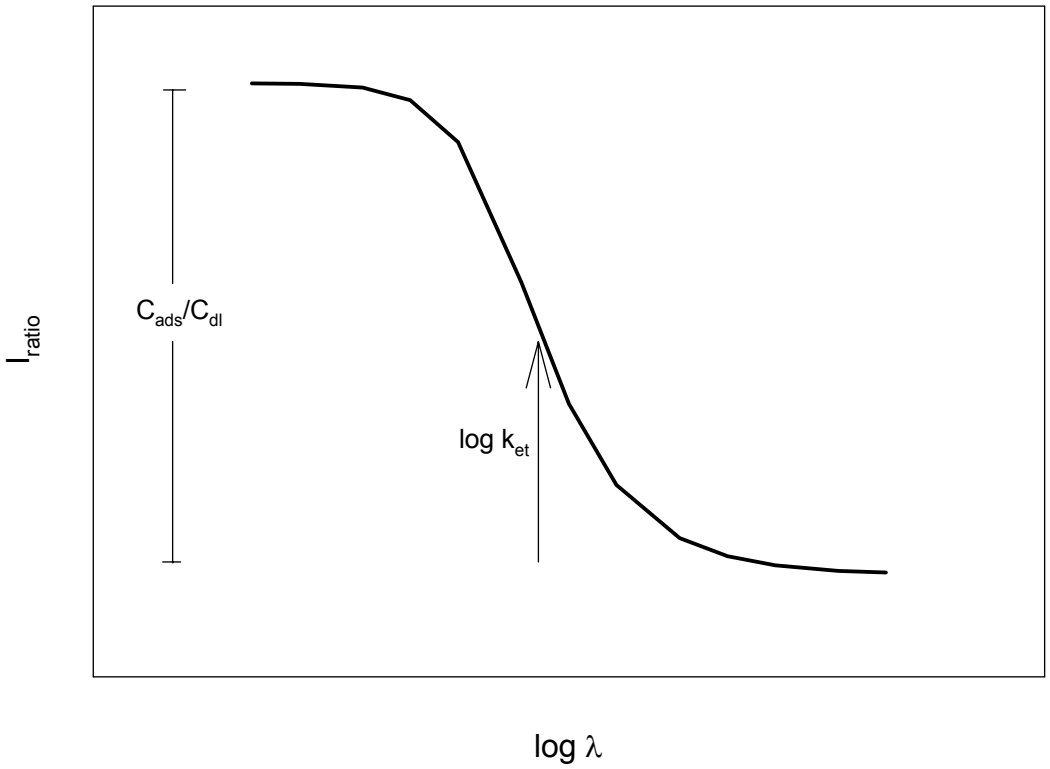


Figure 4.4 Typical ACV frequency response curve

Electrode Preparation

Gold disk electrodes of 3 mm diameter were cleaned by alumina polishing and piranha solution (3:1 H_2SO_4:H_2O_2) followed by repeated cyclic voltammetry (CV) scans in 1 M sulfuric acid for cleansing. Surface area measurement were carried out through integration of the oxide reduction peak of the gold electrode in sulfuric acid.[54] The electrodes were rinsed with water followed by ethanol before being soaked in AQ suspensions. Electrodes were soaked in the stirred suspensions for no less than 12 hrs with periodic CV scans in 0.1 M phosphate, 0.5 M ionic strength (NaCl) pH 7 buffer to "set" the monolayer as it formed. Once finished, the electrodes were rinsed with ethanol and water and stored under refrigeration were they could be kept without losing the CV 6AQ response. A stainless steel cell and a Ag/AgCl electrode were used for the counter and reference electrodes respectively.

Electrochemical Experimental

Electrochemical measurements were conducted using a CH Instruments model 650A potentiostat. Phosphate buffer (0.1 M) from pH 3 to pH 9, and made to a constant ionic strength of 0.5 M using NaCl, were purged with nitrogen gas that had been passed through a manganese/vermiculite column for oxygen removal. The cells were purged for 15-20 minutes before measurements were taken and a nitrogen blanket was kept over the system during measurements. A 50 mV/s cyclic voltammogram was first obtained. From this, the monolayer surface coverage was determined from the anodic sweep peak areas assuming a two electron process.

AC voltammetry experiments were conducted through an instrumental software macro command feature that allowed for instrument pre-programming for a series of measurements. Each series collected AC voltammograms at various AC frequencies from 1 to 1000 Hz with a amplitude of 10 mV and a sampling period of 2 seconds. All AC voltammograms were measured in a potential window of about 500 mV centered upon the $E_{1/2}$ value at the given pH of

the buffer system. Following each set of ACV measurements, chronoamperometric measurements were obtained as well as another cyclic voltammogram as a check on the monolayer stability.

Chronoamperometric measurements were taken by applying an initial potential ensuring the electrodes in an oxidized state. Potential steps were then applied in approximately 50 mV increments with the initial step to the peak potential determined in the CV measurement. Each step was repeated for three cycles before changing to the next potential. The system was then reversed choosing an initial potential such that the electrode was in a reduced state and potential steps were applied in the reverse direction. The data sets were then background corrected with chronoamperometric data obtained on the same electrode modified with a 6MH monolayer. Background corrected data were simulated using the model described above and a data fitting program included in the SigmaPlot™ software.

Results and Discussion

Effect of Electrode Modification

The effects thiol modified layers have on electrochemical measurements are well documented.[59] The decrease in the dielectric constant for a modified electrode can significantly impact many measurements. With this in mind a study was conducted comparing various electrode modifications to determine one suitable for use as a “blank” electrode in the CA measurements to be conducted. This study in Figure 4.5 compared the CA results for a clean gold electrode to that obtained for a 2ME-, a 6MH-, and a 6AQ-modified electrode.

As expected the 6AQ layer showed the expected increase in measurable current, versus that obtained for its blank counterpart, due to the reduction of the AQ moiety . The 2ME and the 6MH layers also behaved as expected showing a decrease in the measurable background current. This effect was more enhanced with the ordering provided by the longer 6MH layer. With these results, it was decided to utilize measurements of a 6MH-modified electrode as a

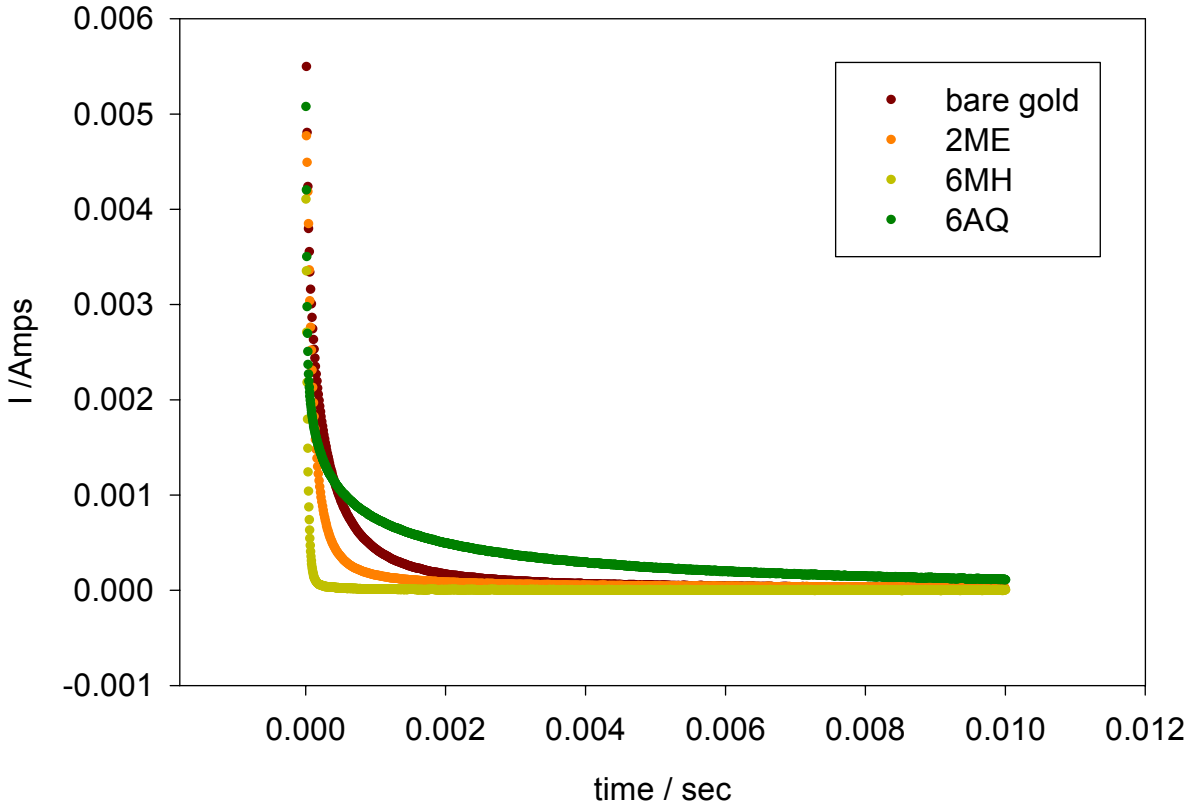


Figure 4.5 Overlayed measurements of various gold modifications. Measurements were taken in pH 7.1 phosphate buffer with a potential step from -0.2 to -0.75 V vs Ag/AgCl reference

blank for subtraction in most CA measurements of the 6AQ modified electrodes. A typical 6MH background subtracted CA data set is shown in Figure 4.6.

Effects of pH

Examination of the kinetics of electron transfer for a 6AQ modified electrode included the effects of pH upon the redox potential of the peaks measured. Slow sweep studies took CV measurements at sweep rates of 50 μV/s. The slow sweep rate minimized the peak separation allowing for a more precise measurement of the potentials. As seen in Figure 4.7, the slow sweep studies illustrated a double peak behavior. Each peak was taken for individual redox potential and the data was collected versus pH in Table 4.1 . The data in Table 4.1 are $E_{1/2}$ values calculated in the usual fashion ($E1/2 = (E_{pk}^{a} + E_{pk}^{c})/2$). The potentials collected from these measurements were used for fitting the data obtained in subsequent CA studies.

The two-stepped nature of the 6AQ response was evident in both the CV and the CA data. However, the complexity of the nine-membered square scheme renders an exact kinetic analysis of the CA data impractical. The use of the $E_{1/2}$ values in Table 4.1 represents a compromise in the data analysis. Accordingly, The “standard rate constants” (k_{o1} and k_{o2}) extracted from the CA data are to be viewed as “global” constants in the sense used by Laviron in related systems.[60, 66]

CA measurements were taken under various pH systems to examine any effects upon a 6AQ-modified electrode. As seen in Figure 4.8 surface coverage data for these same measurements remained constant. Data referred to in later tables lists the standard rate constants obtained by fitting the experimental data using equation 4.4 as described earlier in SigmaPlot™ graphing software. This set shows some possible kinetic variation related the pH of the system. It can be noted that there is a theoretical precedent for the existence of minima in plots of ln (rate constant) versus pH for complex redox equilibria involving coupled proton transfer steps.[60] These changes could arise from any of a set of

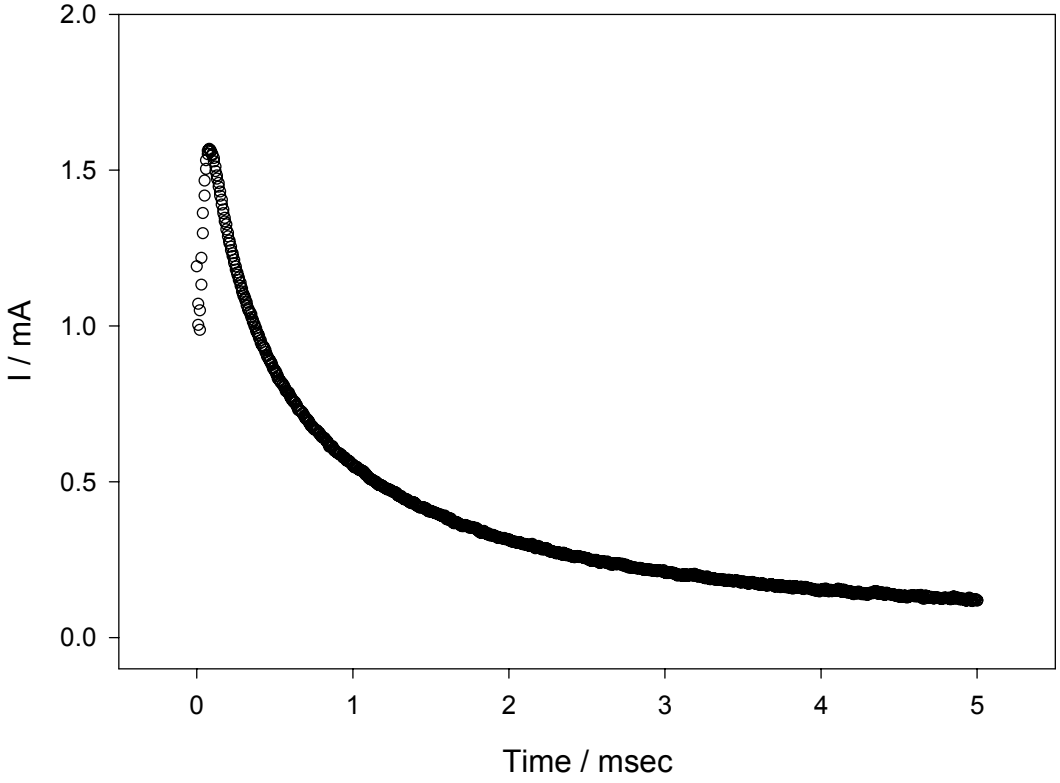


Figure 4.6 Background subtracted chronoamperometric measurement

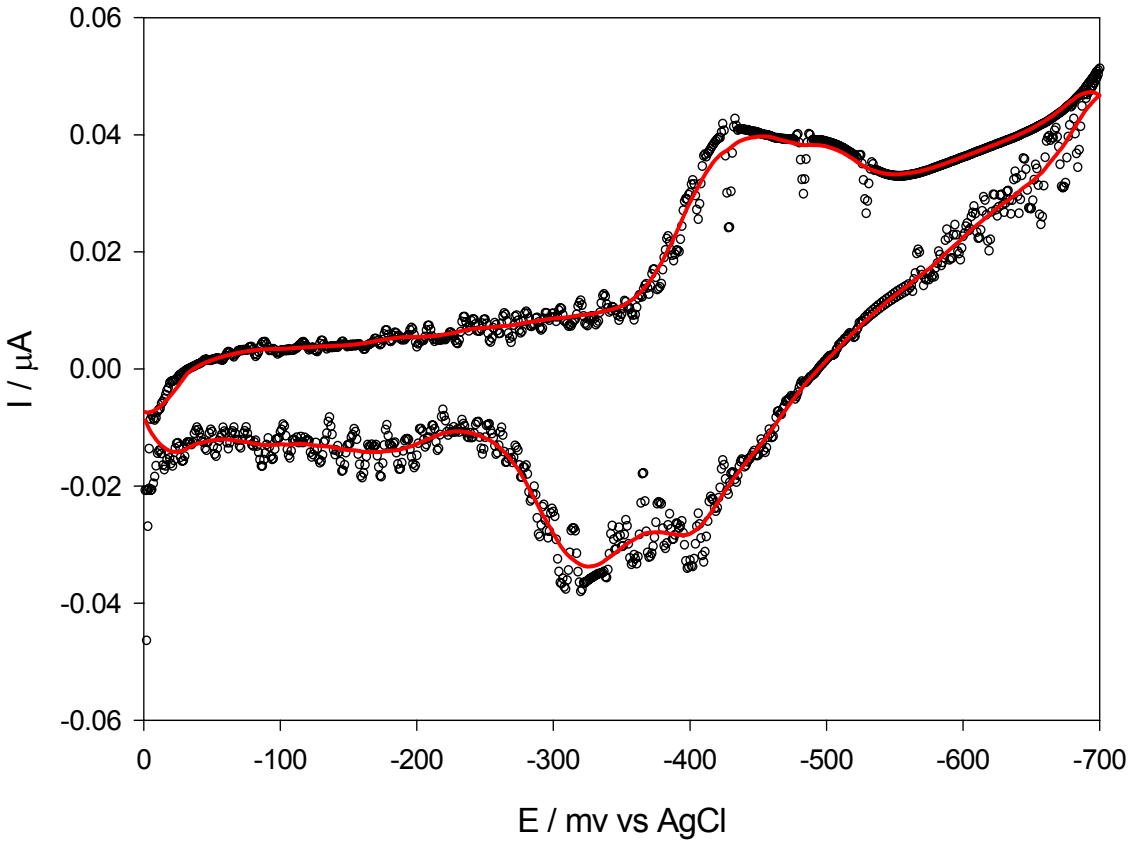


Figure 4.7 CV measurement of 6AQ layer at 50 μV/sec in pH 5.2 buffer. The red line represent the data after smoothing for easier reading of the peak potentials.

Table 4.1 Effects of pH on individual $E_{1/2}$ potentials

pH / potential	$E^1_{1/2}$ (mV vs Ag/AgCl)	$E^2_{1/2}$ (mV vs Ag/AgCl)
2.8	-272	-325
3.8	-335	-400
4.3	-340	-420
5.2	-390	-445
5.7	-445	-485
6.3	-473	-533
7.1	-525	-555

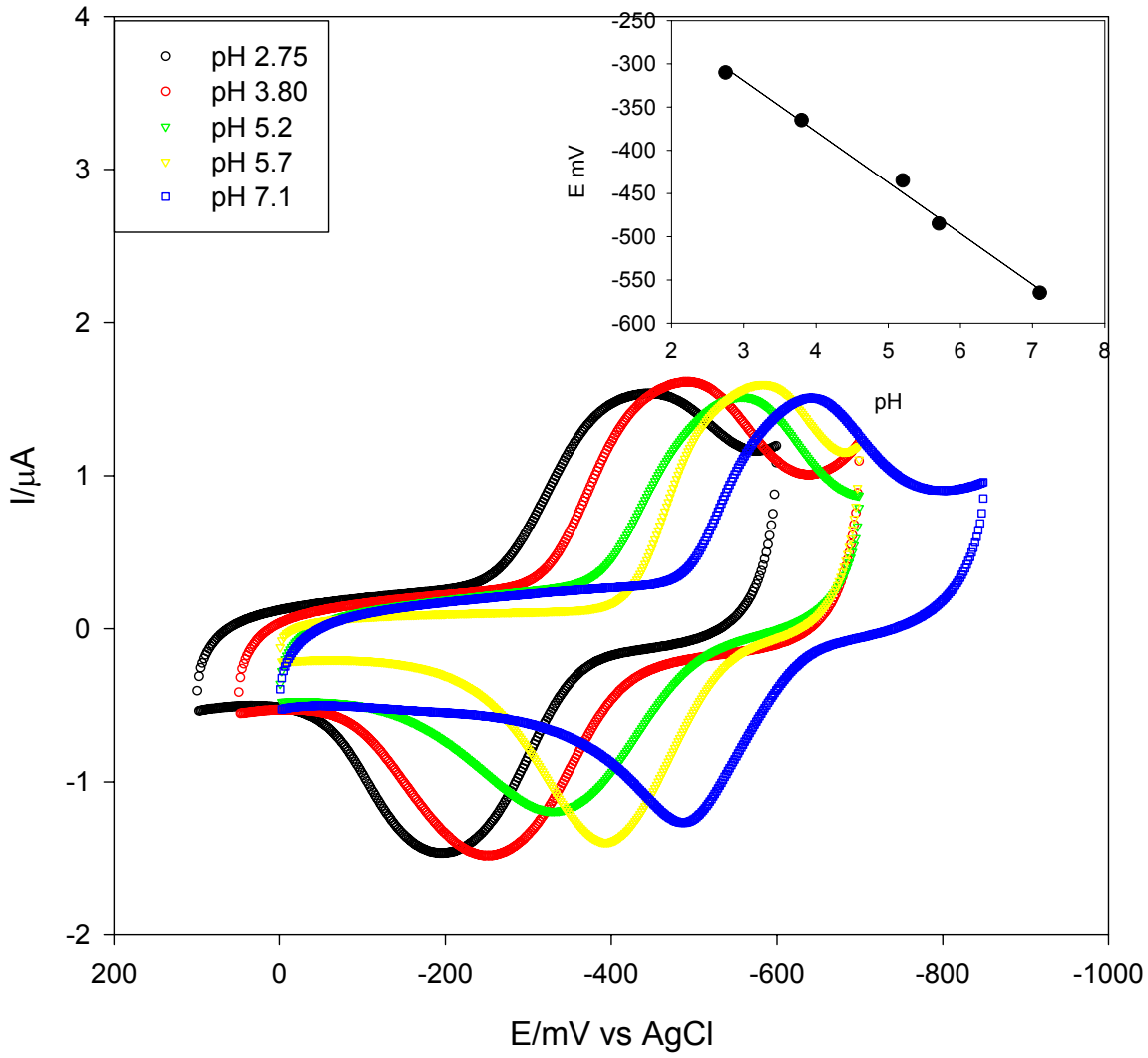


Figure 4.8 CV measurements taken in various phosphate buffers at 100 mV/s. Inset plots rough peak potential versus pH. Slope of this line was 58.9 mV/pH compared to the theoretical 59.5 mV/pH.

possibilities including AQ orientation on the electrode surface and changes related to the change of pathways in the nine-membered EE scheme in Figure 4.2.

DNA Sensor System

Studies of the effects of DNA were carried out in the same buffer systems used in measuring the rate constants. Calf thymus DNA was added to a concentration of 10 ppm and the measurements were repeated as above. Standard rate constants and α-values are collected in Tables 4.2 through 4.5. Data for a pH of 5.7 was unattainable due to unforseen circumstances.

The data in Tables 4.2 and 4.3 indicate a possible perturbation of the anodic CA data. This slowing effect would likely would arise from interactions between the AQ moiety and the DNA making the AQ not as free for reduction/oxidation reactions having such an effect. These interactions could possibly be explained using the results presented by Barton and co-workers discussed before. The Barton results indicated a change in orientation of a thiol attached ODN as a result of applied electrode potential. The effect could also explain why the perturbation in the data is not seen in the cathodic measurements. The more negative starting potential of the anodic CA measurement steps could cause a more upright DNA orientation allowing for a more direct DNA/probe interaction, making the results more observable.

Further attempts to examine this interaction in more detail followed the model described earlier with a 6AQ-modified electrode. The system approach described here consists of the 6AQ thiol and 2ME immobilized on a gold electrode, illustrated in Figure 4.9. The 2ME serves as spacer and attempts to block the AQ moiety from any electrode surface interactions. Other thiols, such as 6MH, were considered, but the similarity in linker arm length was thought to described here consists of the 6AQ thiol and 2ME immobilized on a gold electrode, illustrated in Figure 4.9.

Table 4.2 Standard rate constants (s^{-1}) for 6AQ-modified electrodes at various pH's

	Cathodic		Anodic	
pH	**k_{o1} (+/- 12 %)**	**k_{o2} (+/- 50 %)**	**k_{o1} (+/- 17 %)**	**k_{o2} (+/- 45 %)**
2.8	55	0.7	85	1
3.8	45	0.5	10	<1
4.3	220	3	60	0.5
5.2	23	2	45	1
5.7	160	1	150	5
6.3	330	8	100	3
7.1	120	1	140	3

Table 4.3 Standard rate constants (s^{-1}) for 6AQ-modified electrodes in the presence of 10 ppm calf thymus DNA at various pH's

	Cathodic		Anodic	
pH	**k_{o1} (+/- 11 %)**	**k_{o2} (+/- 35 %)**	**k_{o1} (+/- 28 %)**	**k_{o2} (+/- 35 %)**
2.8	80	2	34	1
3.8	130	3	6	1
4.3	105	1	9	<1
5.2	32	<1	90	2
5.7	-	-	-	-
6.3	200	1	55	<1
7.1	160	1	100	1

Table 4.4 Transfer coefficients for 6AQ-modified electrodes at various pH's

	Cathodic		Anodic	
pH	**α_1 (+/- 17 %)**	**α_2 (+/- 8 %)**	**α_1 (+/- 20 %)**	**α_2 (+/- 11 %)**
2.8	0.17	0.41	0.15	0.42
3.8	0.21	0.47	0.28	0.53
4.3	0.14	0.41	0.19	0.47
5.2	0.26	0.46	0.19	0.37
5.7	0.17	0.45	0.13	0.29
6.3	0.14	0.39	0.16	0.30
7.1	0.18	0.47	0.12	0.25

Table 4.5 Transfer coefficients for 6AQ-modified electrodes in the presence of 10 ppm calf thymus DNA at various pH's

	Cathodic		Anodic	
pH	**α_1 (+/- 10 %)**	**α_2 (+/- 18 %)**	**α_1 (+/- 18 %)**	**α_2 (+/- 10 %)**
2.8	0.17	0.29	0.19	0.36
3.8	0.14	0.27	0.30	0.37
4.3	0.16	0.41	0.26	0.44
5.2	0.24	0.39	0.15	0.32
5.7	-	-	-	-
6.3	0.16	0.44	0.19	0.27
7.1	0.21	0.49	0.14	0.28

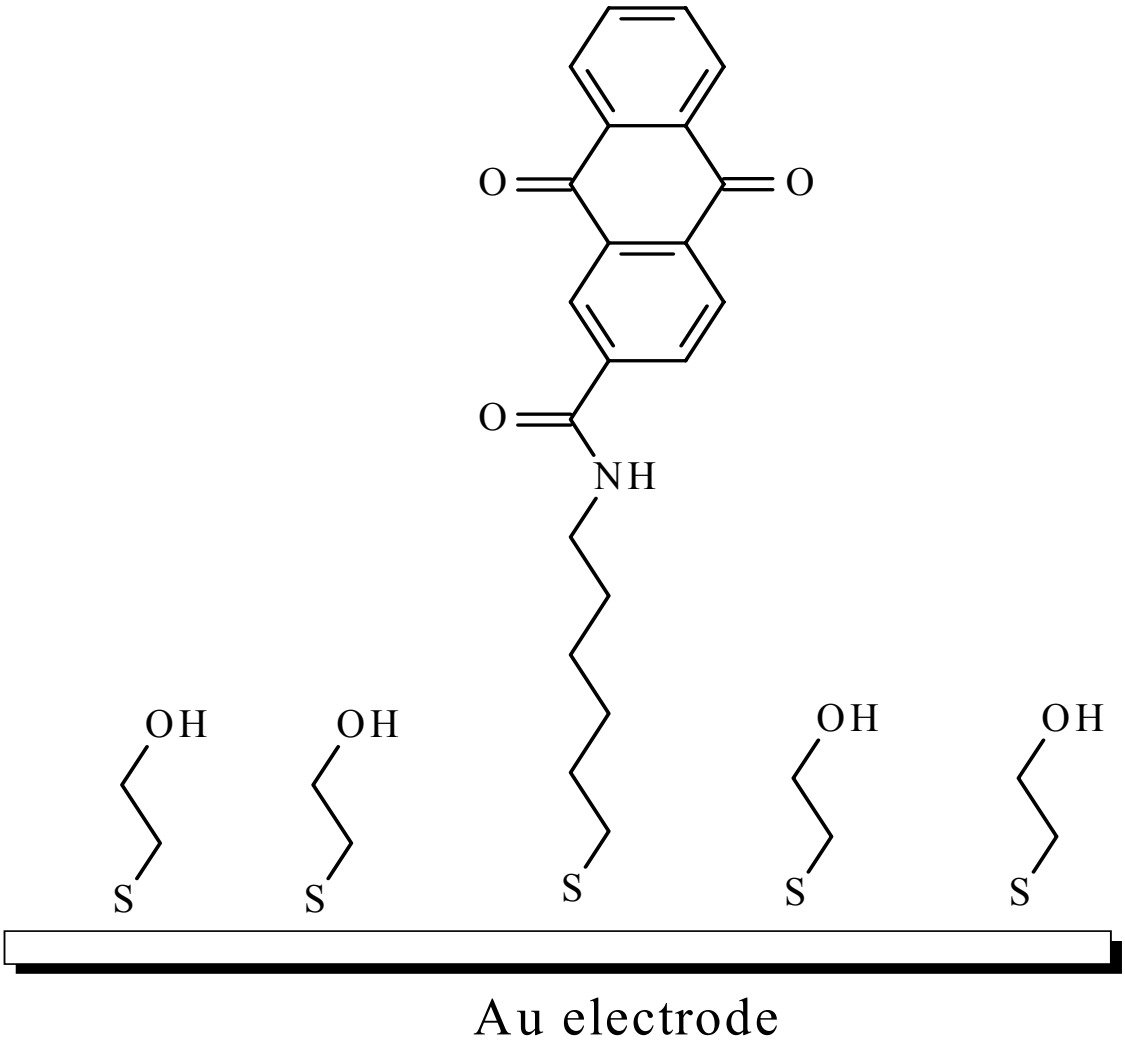


Figure 4.9 Typical modifications to gold electrode by thiol-modified 6AQ

Studies were conducted in pH 7.1 buffer in order to minimize any effects not arising from the DNA hybridization event. The α-values collected in Tables 4.4 and 4.5 show little effect due to the presence of DNA solution. It can also be noted that they are less than 0.5, which is the value expected for a simple one-electron transfer step unaffected by coupled chemical reactions or concerted bond formation.

At this point an alternative method to obtain kinetic data was also employed in order to achieve a degree of data confirmation. AC voltammetry methods described by Creager and Worster[64] to study were employed to study this electrode system. ACV measurements were taken concurrently with CA, and the data was fitted to equations 4.7, 4.8, and 4.9 above. Figure 4.10 shows a typical ACV measurement taken at a frequency of 1 Hz. This frequency was varied for subsequent measurements, and the corresponding data obtained in these experiments were plotted and simulated as described earlier.

CA data were measured as before taking sets of data extending the potential window with each ensuing measurement. Rate constants obtained for each step were then plotted similar to Figure 4.11. A linear fit program was then applied to this data for the determination of standard k_o values in Table 4.6. Virtually all such measurements provided excellent fits with correlations of 99% or greater. ACV simulations as Figure 4.12 determining the k_{et} value were taken for each set of conditions. Fits of the ACV data also appeared to maintain a good correlation considering its non-linear nature. As seen in Table 4.6, little effect could be seen measured by either method on the electron transfer kinetics. This is could be due to the length of the AQ-thiol linker arm. The six-carbon chain most likely does not allow enough free movement or free movement of the AQ moiety for proper interaction with the DNA double helix to see a greater effect upon the kinetics. A thiol arm of a minimum of twelve to fifteen carbons could offer the greater freedom in movement and the interaction needed in order see a significant effect.

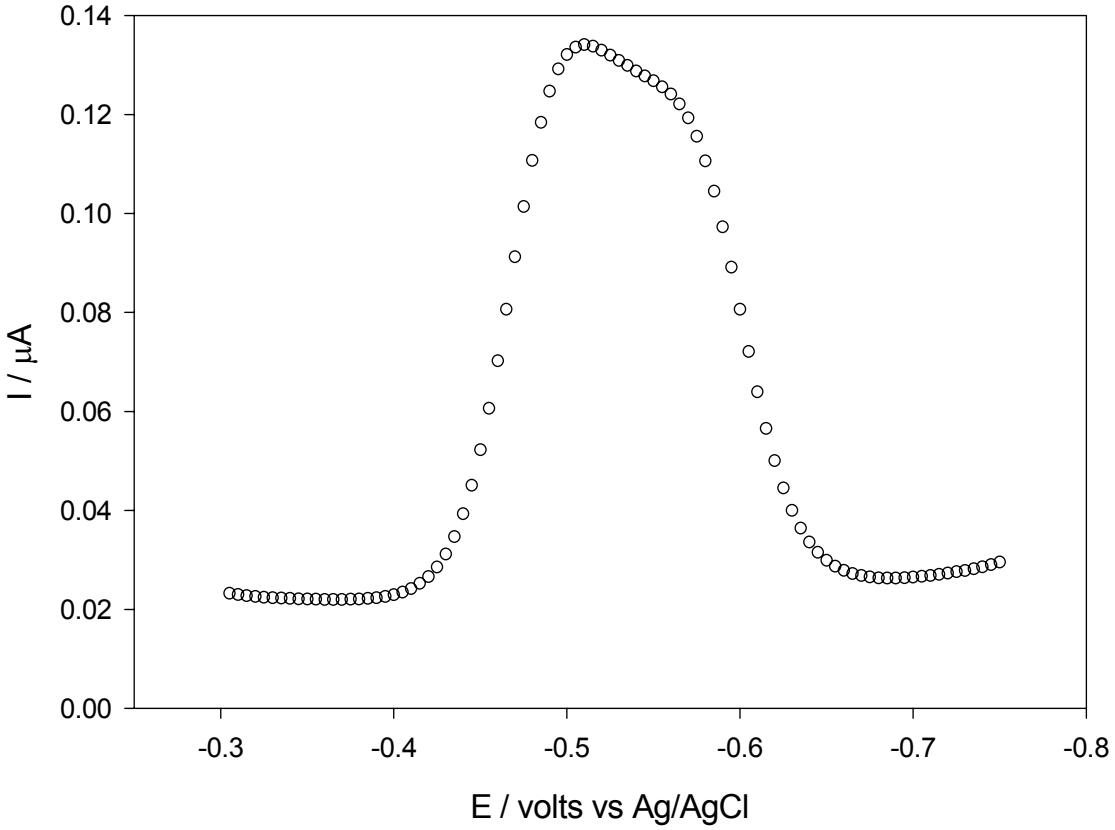


Figure 4.10 Typical ACV measurement of a 6AQ-modified electrode measured at a frequency of 1 Hz

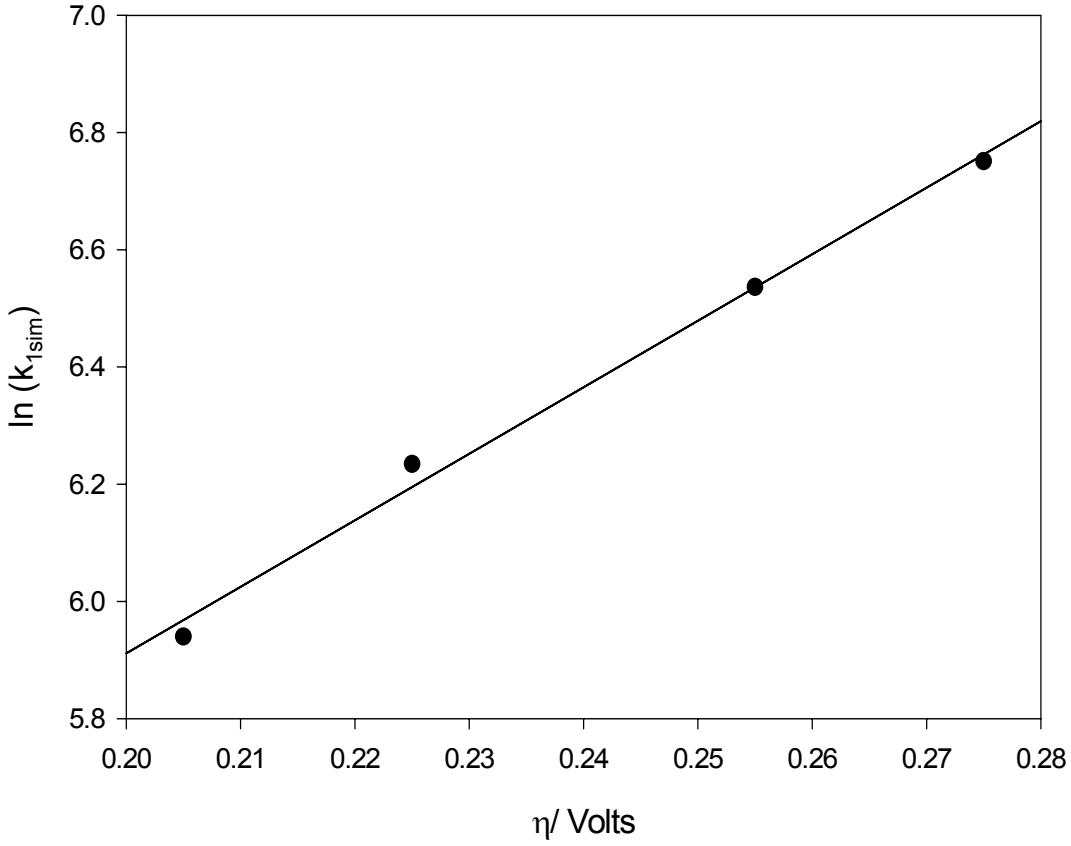


Figure 4.11 Rate constant versus overpotential for typical 6AQ electrode. Equation for linear fit was y=1.4x +3.6 with an r^2 value of 0.993

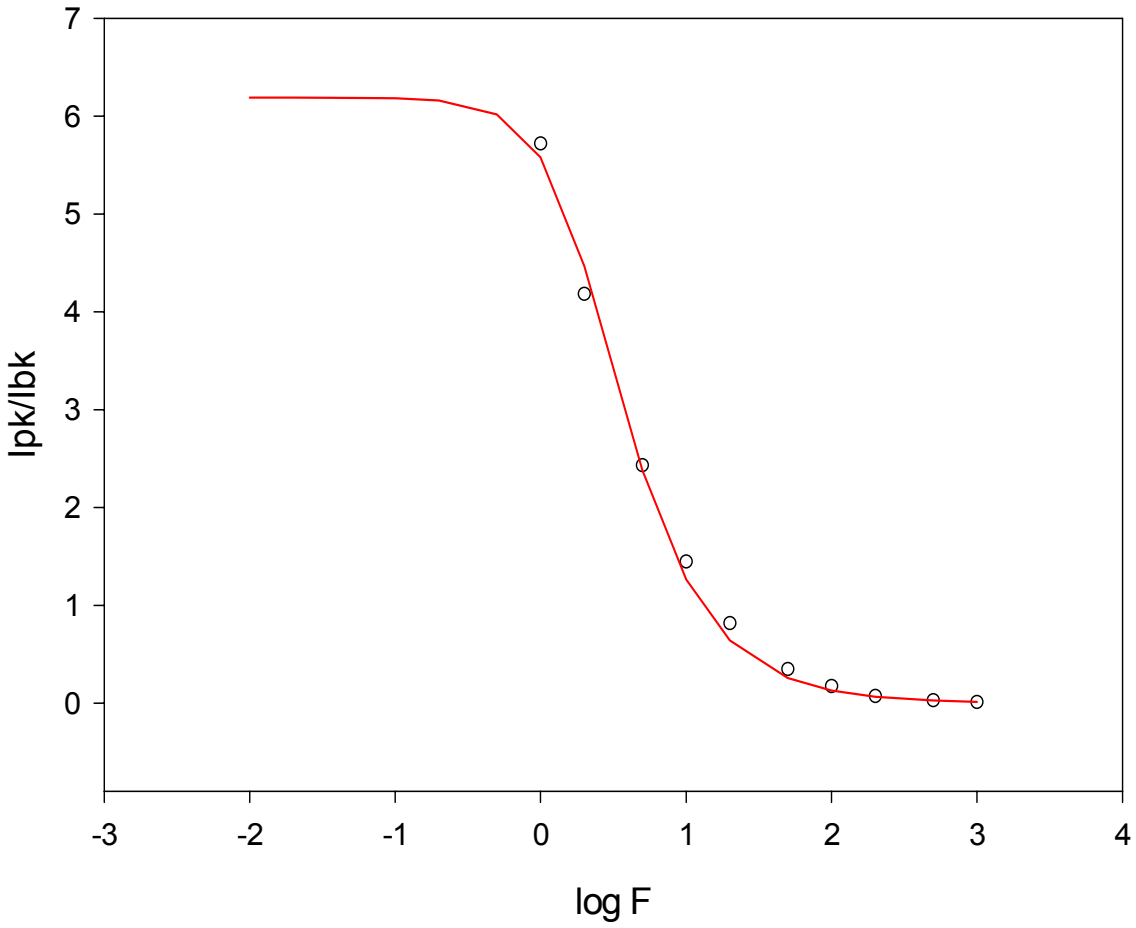


Figure 4.12 Plot of ACV current ratio data used for determination of k_{et} value. Red line shows fitted data versus experimental.

Table 4.6 Kinetic data for the 6AQ electrode and the 6AQ- and 2ME-modified electrode in pH 7.1 phosphate buffer measured by CA and ACV

	Cathodic CA		Anodic CA		ACV
	k_{o1} (+/- 11%)	k_{o2} (+/- 50%)	k_{o1} (+/- 0.4%)	k_{o2} (+/- 25%)	k_{et} (+/- 6%)
6AQ	150 s^{-1}	<2 s^{-1}	110 s^{-1}	<5 s^{-1}	8.7 s^{-1}
6AQ + 2ME	220 s^{-1}	<5 s^{-1}	170 s^{-1}	<10 s^{-1}	9.8 s^{-1}
6AQ + 2ME + DNA	110 s^{-1}	<2 s^{-1}	110 s^{-1}	<2 s^{-1}	8.8 s^{-1}

Conclusions

In this study, two electroanalytical methods were used for extracting kinetic information from an AQ-SAM in aqueous solution. While an exact correlation could not be made between the respective rate data, the results were in qualitative agreement. The two-step nature of the AQ/AQH_2 system was evident in both the CV and the CA data analysis.

Except for a possible effect on the anodic process, a significant perturbation of the AQ kinetics in the presence of DNA was not observed. The rate data in Table 4.3 suggest that there is a slowing down of the anodic redox reaction in the presence of DNA. This is perhaps related to the negative potential employed to set the SAM in a reduced state prior to the application of the CA excitation steps. Following Barton et al. model, this procedure should extend the orientation of the DNA AQ complex from the electrode surface.

CHAPTER 5
SPECULATIONS FOR FURTHER WORK

The experiments discussed in the previous chapters have illustrated a basis for examination of DNA hybridization using electrochemical techniques. The AQ based systems described here have some potential for use on a routine basis. As discussed before, the AQ moiety offers a perfect example of the type of compound for use in the development of such systems. The AQ group is known to have interactions in the DNA double helix and at the same time offers the possibility of dual detection using electroanalytical and molecular fluorescence techniques. The work described utilized these interactions to electrochemically examine various sensor styles to monitor any effect the hybridization event may have upon the electron transfer kinetics of the AQ moiety. Results reported are promising for the potential use of the modifications. Each system requires its own degree of “fine tuning” for future work.

The AQ-modified nucleotides discussed in chapter 2 can serve as a model for other similar systems using different electrochemical tags. One of the greatest concerns for the study described is the use of a mercury electrode. The HDME is not readily applicable to analysis requiring a massive amount of repetitive measurements. Modification for the use of AQ 20mers in a thiol-based system as described in the other chapters is more suitable for multiple measurements. An added problem with the AQ-modified 20mers system is the synthesis of the modified ODNs. The steps for synthesis of these compounds require greater attention. Use of PNAs might provide for a greater ease in the synthesis of the probes that would work similar to their ODN counterpart.

The AQ-modified 20mers might benefit from a molecular beacon model in future studies. Modifications like the 2AQ 20mer places an electron acceptor at the 5' end of a double helix. Further studies to modify the 3' end with a suitable electron donor could serve to examine the conductivity possibilities in the DNA helix. Work presented by the Barton group, utilized a thiol modified ODN cross-

linked with daunomycin to examine the electron transfer capabilities of the DNA helix. Their results indicated a hindrance to the kinetics of such a system with one base pair mismatch in a 15mer ODN.[3]

The daunomycin modified stem-and-loop system experiments described in chapter 3 were intended as a preliminary study examining the potential of an immobilized molecular beacon system. The use of MB based DNA analysis has grown over time to the extent that fluorescent modified ODNs are readily available from DNA synthesizing corporations. Since these systems are limited by the spectrophotometric interference, the investigation of an electrochemical based system becomes attractive.

The stem-and-loop approach relies on the covalent attachment of the daunomycin tag to the DNA strand. Results reported here and by others indicated a thermal instability in the cross-linked bond. This prevents the thermal cycling for reclamation of the sensor. Other means of "melting" the double helix (pH, ionic strength, etc.), which as the same time leave the sensor chemically bonded to the ODN, should be investigated.

An obvious place for the future work of thiol modified AQ systems, as well as others, is the expansion of the simulation mechanisms. Initial work presenting the EE model for simulation also included a mathematical model for simulation of the more complicated ECE mechanism.[62] The extra chemical step in this model greatly increases the complexity such simulations. Further work in the examination of these systems though could offer as great a degree of CA simulation as there is available in the commercial CV simulation generators.

The results obtained using a thiol modified AQ group show limited response as carried out using CA and ACV. This is most likely due to a lack of interaction between the AQ moiety and the DNA being detected. The slight variation detected in the case of the anodic potential step data can mostly likely be explained due to a reorientation of the AQ group due to the more negative initial potential applied before stepping of the potential. These results parallel those from Baton and co-workers where they examined the orientation of a thiol

based ODN as a function of the potential applied to the electrode base.[33] More detailed studies utilizing AFM and other scanning probe techniques would provide a greater understanding of this behavior of the layer.

A different means of utilizing the orientation dependence upon potential could be examined by applying a potential during the monolayer application to the gold electrode. The effect of this potential would be expected to alter the density of thiol groups applied to the gold surface. Similar studies have been carried out by Finklea et al. where they described a “shock” effect due to slight stripping octadecanethiols that were loosely packed on the electrode surface.[67] Their tightly pack film were left intact in these stripping measurements. This density could play a large role in the tag’s ability to interact with DNA in solution. Enhancing these interactions might generate greater detectable differences between the signal in the presence and absence of the DNA analyte.

Another approach for enhancing the 6AQ sensor system could come from manipulation of the thiol linker arm length. Increasing the length of our six carbon chain to one of 12 to 15 carbons could offer a greater freedom for the development of any interactions that could create detectable signal differences. Care for such work would also need be taken not to make the linker arm too long extending the tag too far from the electrode diffusion layer to achieve a measurable signal.

Each of the thiol based systems described also offers the potential for applicability to microscale detection methods. The simplicity in the direct preparation of the electrode sensors make them open to modification in order to form arrays of electrodes for the simultaneous analyses of various sequences. These electrode arrays could offer a great time saving advantage for ODN sequence determination. Inherent in these systems is also the possibility of designing a multiple tag detection scheme where various electroactive groups are used to modify individual sequences similar to a “redox spectrum”. This would again save on time for bulk analyses and could offer simultaneous measurements of multiple sequences.

WORKS CITED

(1) Watson, J. D.; Crick, F. H. *Nature* **1953**, *171*, 737-738.

(2) Kelley, S. O.; Boon, E. M.; Barton, J. K.; Jackson, N. M.; Hill, M. G. *Nucl. Acids Res.* **1999**, *27*, 4830-4837.

(3) Kelley, S. O.; Jackson, N. M.; Hill, M. G.; Barton, J. K. *Angew. Chem. Int. Ed.* **1999**, *38*, 941-945.

(4) Gasper, S. M.; Schuster, G. G. *J. Am. Chem. Soc.* **1997**, *119*, 12762-12771.

(5) Gasper, S. M.; Armitage, B.; Shui, X.; Hu, G. G.; Yu, C.; Schuster, G. B.; Williams, L. D. *J. Am. Chem. Soc* **1998**, *120*, 12402-12409.

(6) Okahata, Y.; Kawase, M.; Niikura, K.; Ohtake, F.; Furusawa, H.; Ebara, Y. *Anal. Chem.* **1998**, *70*, 1288-1296.

(7) Bardea, A.; Dagan, A.; Ben-Dov, I.; Amit, B.; Willner, I. *Chem. Commun.* **1998**, 839-840.

(8) Herne, T. M.; Tarlov, M. J. *J. Am. Chem. Soc.* **1997**, *119*, 8916-8920.

(9) Remeta, D. P.; Mudd, C. P.; Berger, R. L.; Breslauer, K. J. *Biochemistry* **1993**, *32*, 5064-5073.

(10) Roche, C. J.; Thomson, J. A.; Crothers, D. M. *Biochemistry* **1994**, *33*, 926-935.

(11) Bonnet, G.; Tyagi, S.; Libchaber, A.; Kramer, R. *Proc. Natl. Acad. Sci. USA* **1999**, *96*, 6171-6176.

(12) Bayer, E.; Bauer, T.; Schmeer, K.; Bleicher, K.; Maier, M.; Gaus, H.-J. *Anal. Chem.* **1994**, *66*, 3858-3863.

(13) Ganem, B.; Li, Y.-t.; Henion, J. D. *Tet. Lett* **1993**, *34*, 1445-1448.

(14) Light-Wahl, K. J.; Springer, D. L.; Winger, B. E.; Edmonds, C. G.; Camp, D. G.; Thrall, B. D.; Smith, R. D. *J. Am. Chem. Soc* **1993**, *115*, 804-805.

(15) Thiel, A. J.; Frutos, A. G.; Jordan, C. E.; Corn, R. M.; Smith, L. M. *Anal. Chem.* **1997**, *69*, 4948-4956.

(16) Burgener, M.; Sanger, M.; Candrian, U. *Bioconj. Chem.* **2000**, *11*, 749-754.

(17) Palacek, E. *Nature* **1960**, *188*, 656-657.

(18) Wang, J.; Bard, A. J. *Anal. Chem.* **2001**, *73*.

(19) Millan, K. M.; Mikkelsen, S. R. *Anal. Chem.* **1993**, *65*, 2317-2323.

(20) Steel, A. B.; Herne, T. M.; Tarlov, M. J. *Anal. Chem.* **1998**, *70*, 4670-4677.

(21) Patolsky, F.; Lichtenstein, A.; Willner, I. *J. Am. Chem. Soc.* **2000**, *122*, 418-419.

(22) Armistead, P. M.; Thorp, H. H. *Anal. Chem.* **2001**, *73*, 558-564.

(23) Napier, M. E.; Thorp, H. H. *Langmuir* **1997**, *13*, 6342.

(24) Wang, J.; Palacek, E.; Nielsen, P. E.; Rivas, G.; Cai, X.; Haruki, S.; Dontha, N.; Luo, D.; Farias, P. A. M. *J. Am. Chem. Soc.* **1996**, *118*, 7667-7670.

(25) Wang, J.; Jiang, M.; Fortes, A.; Mukherjee, B. *Anal. Chim. Acta* **1999**, *402*, 7-12.

(26) Korri-Youssoufi, H.; Garnier, F.; Srivastava, P.; Dodillot, P.; Yassar, A. *J. Am. Chem. Soc.* **1997**, *119*, 7388-7389.

(27) Campbell, C. N.; Gal, D.; Cristler, N.; Banditrat, C.; Heller, A. *Anal. Chem.* **2002**, *74*, 158-162.

(28) Caruana, D. J.; Heller, A. *J. Am. Chem. Soc* **1999**, *121*, 769-774.

(29) Brazill, S. A.; Kim, P. H.; Kuhr, W. G. *Anal. Chem.* **2001**, *73*, 4882-4890.

(30) Anne, A.; Bouchardon, A.; Moiroux, J. *J. Am. Chem. Soc* **2003**, *125*, 1112-1113.

(31) Murphy, C. J.; Arkin, M. R.; Jenkins, Y.; Ghatlia, N. D.; Bossmann, S. H.; Turro, N. J.; Barton, J. K. *Science* **1993**, *262*, 1025-1029.

(32) Kelley, S. O.; Barton, J. K. *Science* **1999**, *283*, 375-381.

(33) Kelley, S. O.; Barton, J. K.; Jackson, N. M.; McPherson, L. D.; Potter, A. D.; Spain, E. M.; Allen, M. J.; Hill, M. G. *Langmuir* **1998**, *14*, 6781-6784.

(34) Leng, F.; Savkur, R.; Fokt, I.; Przewloka, T.; Priebe, W.; Chaires, J. B. *J. Am. Chem. Soc* **1996**, *118*, 4731-4738.

(35) Whittemore, N. A.; Mullenix, A. N.; Inamati, G. B.; Manoharan, M.; Cook,

P. D.; Tuinman, A. A.; Baker, D. C.; Chambers, J. Q. *Bioconj. Chem.* **1999**, *10*, 261-270.

(36) Hodgson, A., Adsorption, Desorption and Bonding at Surfaces, http://www.ssci.liv.ac.uk/~andrewh/SectionB.pdf (accessed July 2004).

(37) Bard, A. J.; Faulkner, L. R. *Electrochemical Methods: Fundamentals and Applications*; John Wiley & Sons: New York, 1980.

(38) Guiochon, G.; Shirazi, S. G.; Katti., A. M. *Fundamentals of Preparative and Nonlinear Chromatography*; Academic Press: Boston, 1994.

(39) Fasman, G. D., Ed. *Handbook of Biochemistry and Molecular Biology: Nucleic Acids*, 2nd ed.; CRC Press: Cleveland, OH, 1985.

(40) Dean, J. A., Ed. *Lange's Handbook of Chemistry*, 13th ed.; McGraw-Hill: New York, 1985.

(41) Forster, R. J. *Anal. Chem.* **1996**, *68*, 3143.

(42) Kertesz, V.; Whittemore, N. A.; Inamati, G. B.; Manoharan, M.; Cook, P.; Baker, D. C.; Chambers, J. Q. *Electroanalysis* **2000**, *12*, 889-894.

(43) Palacek, E. *Bioelectrochem Bioenergetics* **1988**, *20*, 179-194.

(44) Yamana, K.; Kumamoto, S.; Nakano, H.; Matsuo, Y.; Sugie, Y. *Chem. Lett.* **2001**, *30*, 1132-1133.

(45) Yamana, K.; Kumamoto, S.; Hasegawa, T.; Nakano, H.; Sugie, Y. *Chem. Lett.* **2002**, *31*, 506-507.

(46) Tayagi, S.; Kramer, R. *Nature Biotechnology* **1996**, *14*, 303-308.

(47) Palanti, S.; Marrazza, G.; Mascini, M. *Anal. Lett.* **1996**, *29*, 2309-2331.

(48) Wang, A. H.-J.; Gao, Y.-G.; Liaw, Y.-C.; Li, Y.-k. *Biochemistry* **1991**, *30*, 3812-3815.

(49) Luce, R. A.; Sigurdsson, S. T.; Hopkins, P. B. *Biochemistry* **1999**, *38*, 8682-8690.

(50) van Rosmalen, A.; Cullinane, C.; Cutts, S. M.; Phillips, D. R. *Nucl. Acids Res.* **1995**, *23*, 42-50.

(51) Cullinane, C.; Cutts, S. M.; van Rosmalen, A.; Phillips, D. R. *Nucl. Acids Res.* **1994**, *22*, 2296-2303.

(52) Fan, C.; Plaxco, K. W.; Heeger, A. J. *Proc. Natl. Acad. Sci. USA* **2003**, *100*, 9134-9137.

(53) Mao, Y.; Luo, C.; Ouyang, Q. *Nucl. Acids Res.* **2003**, *31*, e108.

(54) Trasatti, S.; Petrii, O. A. *Pure & Appl. Chem* **1991**, *63*, 711-734.

(55) Taatjes, D. J.; Guadiano, G.; Resing, K.; Koch, T. H. *J. Med. Chem.* **1996**, *39*, 4135-4138.

(56) Taatjes, D. J.; Fenick, D. J.; Guadiano, G.; Koch, T. H. *Curr. Pharm. Design* **1998**, *4*, 203-218.

(57) Kertesz, V.; Chambers, J. Q.; Mullenix, A. N. *Electrochim. Acta* **1999**, *45*, 1095-1104.

(58) Nuzzo, R. G.; Allara, D. L. *J. Am. Chem. Soc.* **1983**, *105*, 4481-4483.

(59) Finklea, H. O. In *Electroanal. Chem.*; Bard, A. J., Rubinstein, I., Eds.; Marcel Dekker, Inc.: New York, 1996; Vol. 19, pp 109-335.

(60) Laviron, E. *J. Electroanal. Chem.* **1983**, *146*, 15-36.

(61) Meunier-Prest, R.; Laviron, E. *J. Electroanal. Chem.* **1992**, *328*, 33-46.

(62) Kertesz, V.; Chambers, J. Q.; Mullenix, A. N. *Anal. Chem.* **1999**, *71*, 3905-3909.

(63) Laviron, E. *J. Electroanal. Chem.* **1979**, *105*, 35-42.

(64) Creager, S. E.; Wooster, T. T. *Anal. Chem.* **1998**, *70*, 4257-4263.

(65) Kertesz, V.; Whittemore, N. A.; Chambers , J. Q.; McKinney , M. S.; Baker, D. C. *J. Electroanal. Chem.* **2000**, *493*, 29-36.

(66) Laviron, E. *J. Electroanal. Chem.* **1984**, *169*, 29-46.

(67) Finklea, H. O.; Snider, D. A.; Fedyk, J.; Sabatani, E.; Gafni, Y.; Rubinstein, I. *Langmuir* **1993**, *9*, 3660-3667.

VITA

Adam Nathanial Mullenix was born in Kingsport, TN in 1974. He attend Temple Star Elementary and Sullivan Middle School before starting at Sullivan South High School in 1987. Adam was active in the school music program before graduating in 1992. From here he attending Tennessee Technological University in Cookeville, TN active in the scientific disciplines. Upon graduation with a B.S. in chemistry in 1996, Adam began graduate school in chemistry at The University of Tennessee, Knoxville and completed a PhD in chemistry in 2004.